WELCOME…

Metal Fatigue Part 2

Raymond Patin, JSC

Ivatury Raju
ivatury.s.raju@nasa.gov

NESC ACADEMY WEBCAST

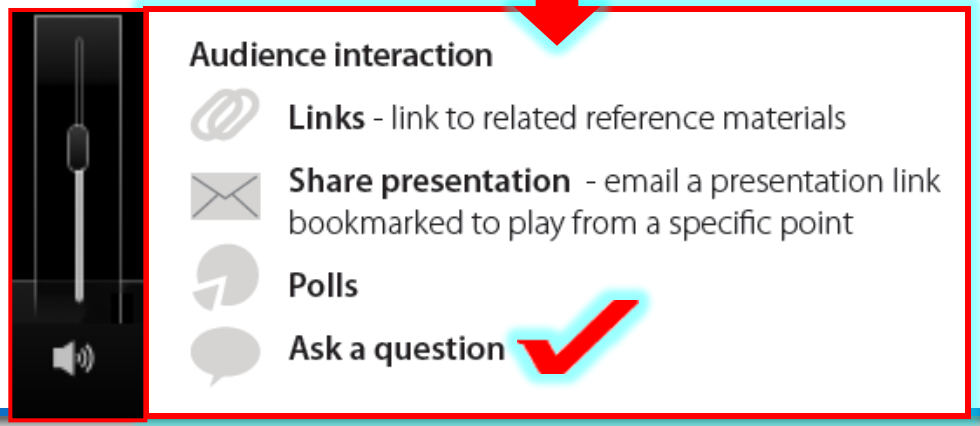

Metal Fatigue

a cursory overview

Part II

by

Raymond Patin

NASA/JSC

Subject Outline

- Introduction – Definition & Historical Overview
- The S-N Curve
- The S-N Endurance Limit
- S-N Fatigue Scatter
- Torsion Fatigue
- Mechanics of Fatigue Damage Accumulation
- Fatigue Failure Fracture Surface Features
- **Strain-Life**
- **Linear Elastic Fracture Mechanics**
- **Fatigue Life Example Problem**

S-N Fatigue Summary

What is metal fatigue?

The definition of "fatigue" according to ASTM* Standard E 1150 reads as follows: "***The process of progressive localized permanent structural damage occurring in a material subjected to conditions that produce fluctuating stresses and strains at some point or points and that may culminate in cracks or complete fracture after a sufficient number of fluctuations***."

***ASTM** – American Society for Testing and Materials

Flow chart description of the metal fatigue process

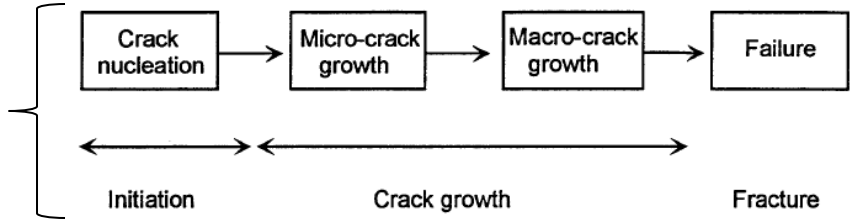

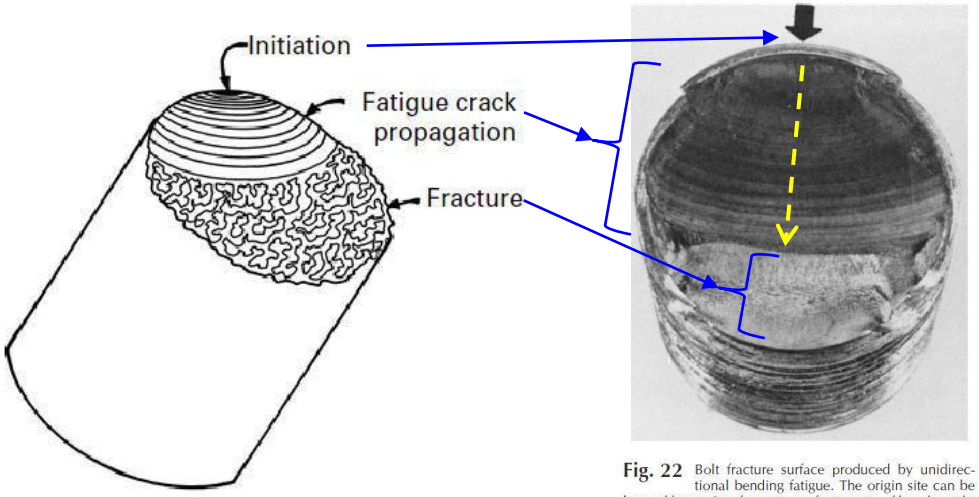

Fig. 22 Bolt fracture surface produced by unidirectional bending fatigue. The origin site can be located by tracing the centers of curvature of beach marks back to the thread root at the arrow. Source: Ref 4

Fatigue Damage Accumulation Process

A schematic representation of the fatigue crack nucleation, initiation, and propagation phases is provided below.

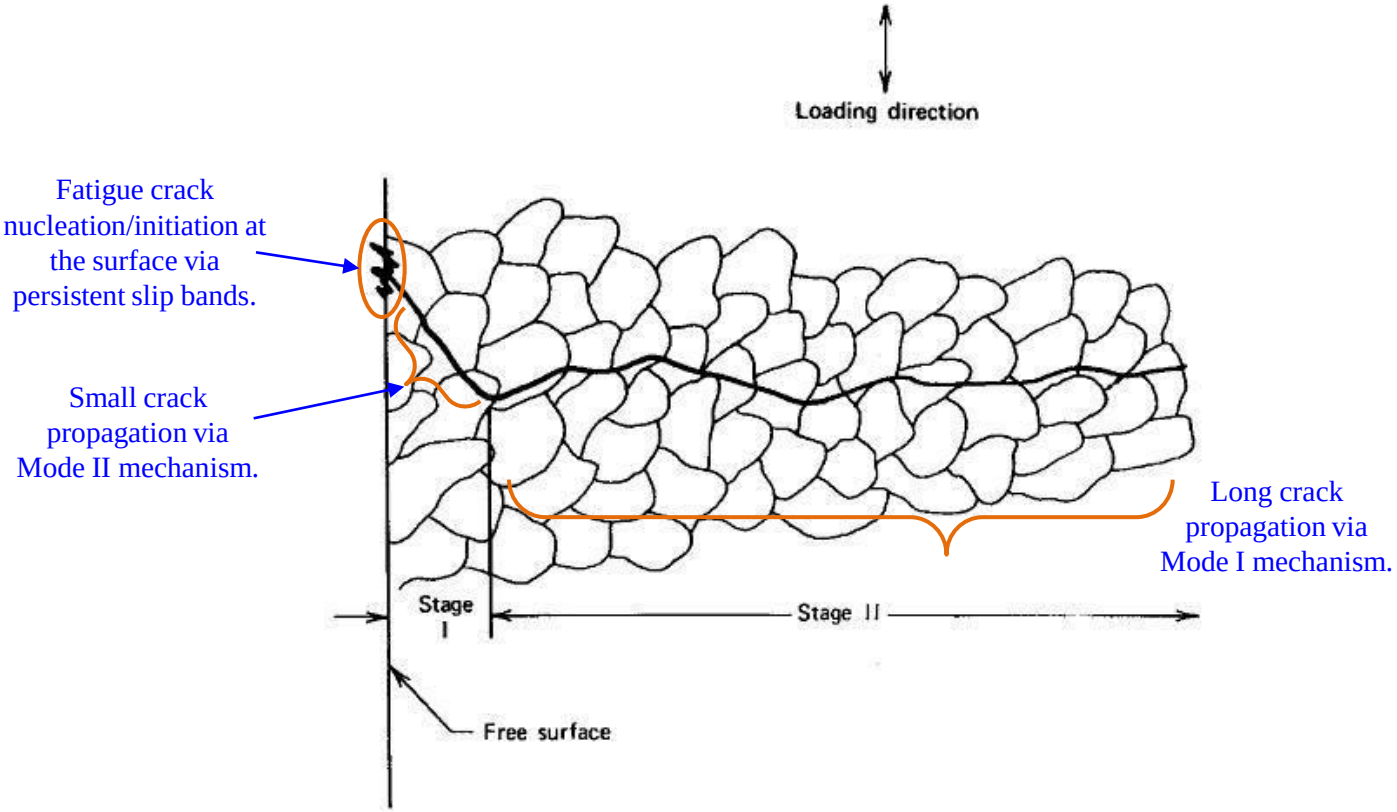

Figure 3.13 Schematic of stages I (shear mode) and II (tensile mode) transcrystalline microscopic fatigue crack growth.

Ref.: R. I. Stephens, A. Fatemi, R. R. Stephens, H. Fuchs, "**Metal Fatigue in Engineering, 2nd ed.,"** John Wiley & Sons**,** 2000, pp. 51**.**

S-N curve ; Fatigue Damage Accumulation

The cyclic time required to nucleate and initiate a fatigue crack consumes the majority of the overall fatigue life.

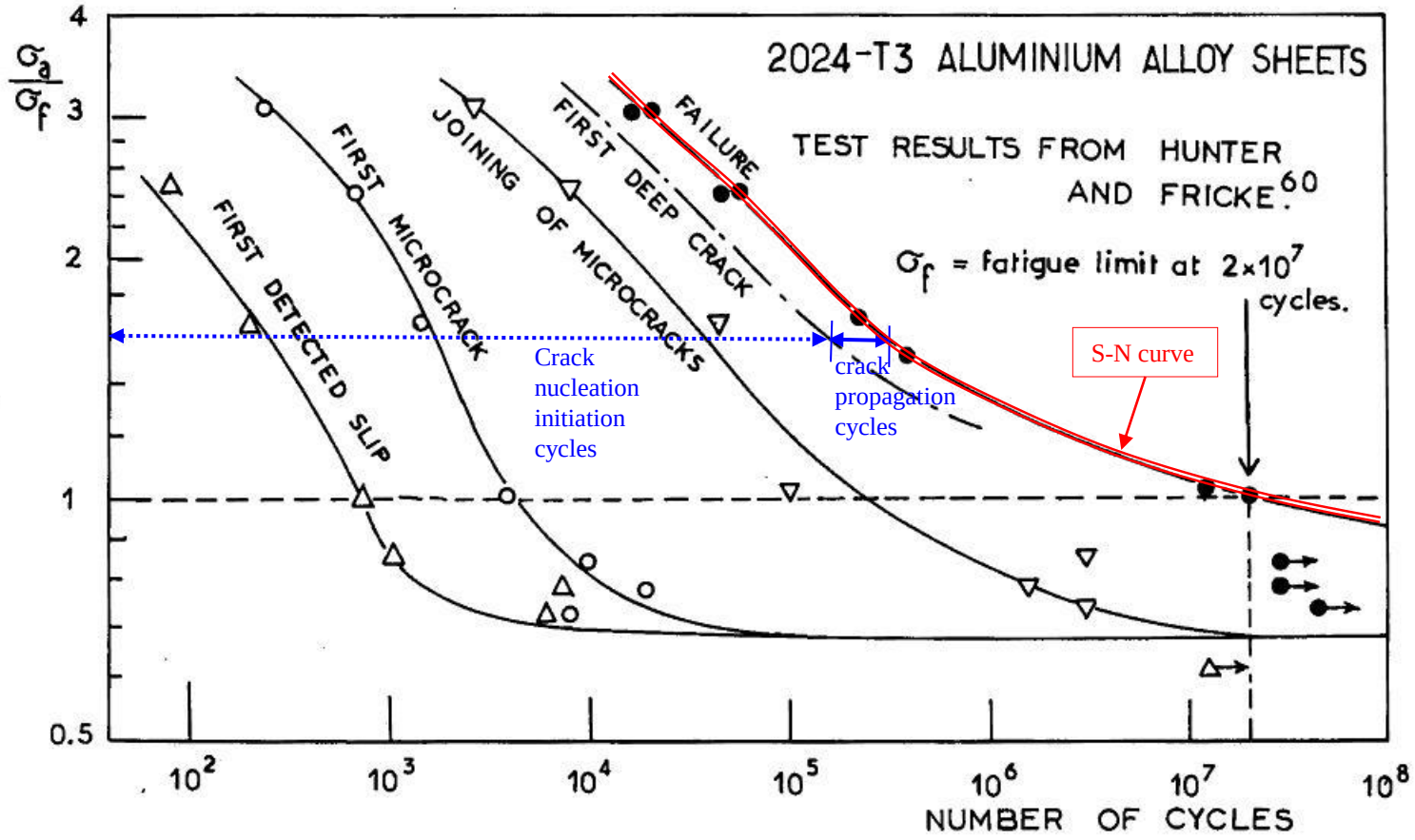

Fig. 5.42 Curves of stress versus number of cycles for first plastic slip, first microcrack, first joining of microcracks, first deep crack and failure

Ref. :W.G. Barrois, **Manual of Fatigue of Structures ; Fundamental and Physical Aspects**, AGARD-MAN-8-70, June 1970, pg 227.

Strain Life Analysis

Stress & Strain Concentration Factors

The stress and strain linear elastic concentration factors are equal and constant. As the local response becomes nonlinear (beyond material yield) the strain concentration increases while the stress concentration decreases (as per the material response). Thus for locally nonlinear responses the material total strain (which can be measured directly) is an ideal analytical parameter.

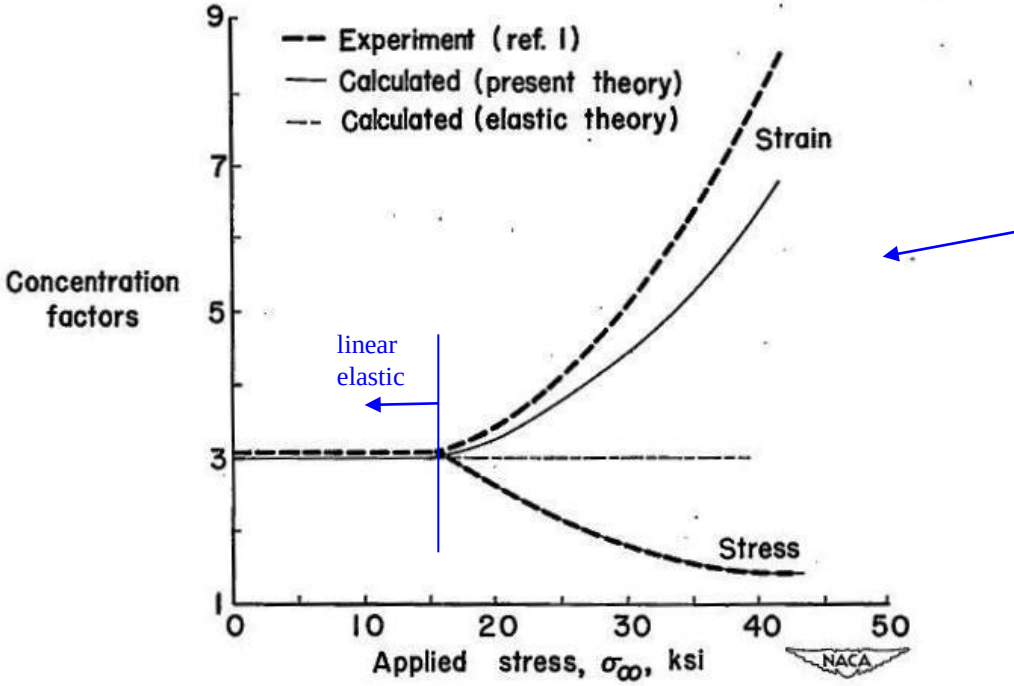

Figure 2.- Comparison between calculated stress and strain concentration factors and tests of reference 1.

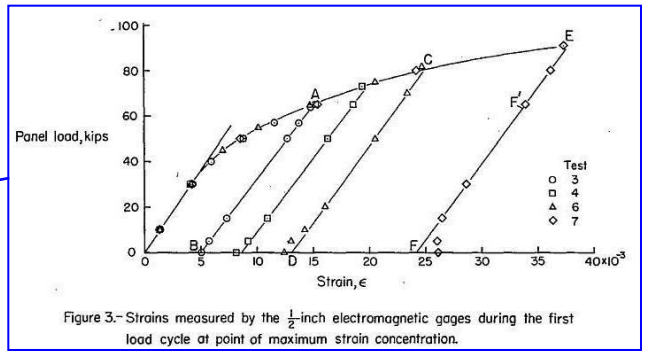

Figure 3.- Strains measured by the $\frac{1}{2}$-inch electromagnetic gages during the first load cycle at point of maximum strain concentration.

Ref.:R.E. Stowell, **Stress and Strain Concentration at a Circular Hole**, NACA TN 2073, 1950, pg 11.

Stress-Strain Curves – Monotonic & Cyclic

The elements of a monotonic (zero to max loading) and a cyclic (fully reversed) stress-strain response are provided below. In both cases the total strain can be separated into the elastic and plastic components.

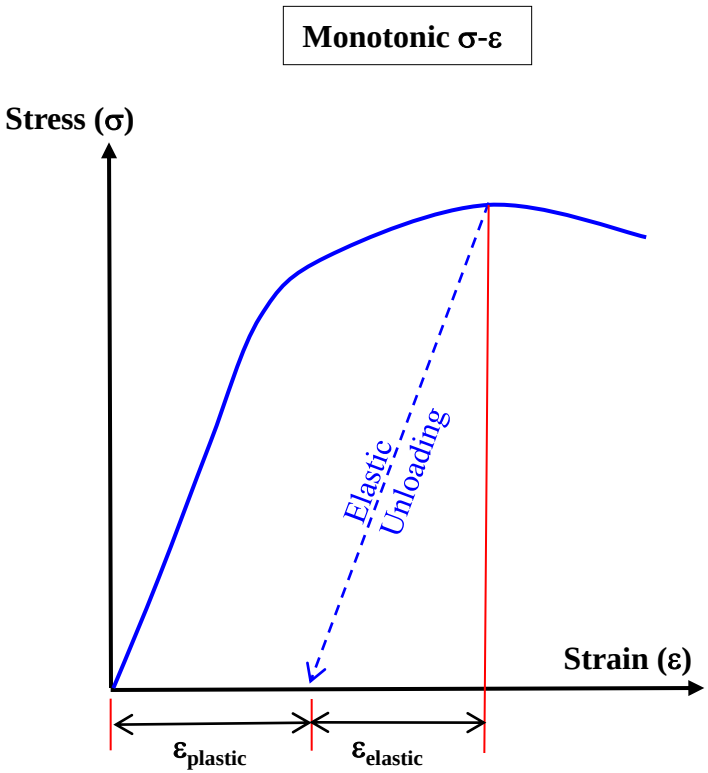

$$\varepsilon_{total} = \varepsilon_{elastic} + \varepsilon_{plastic}$$

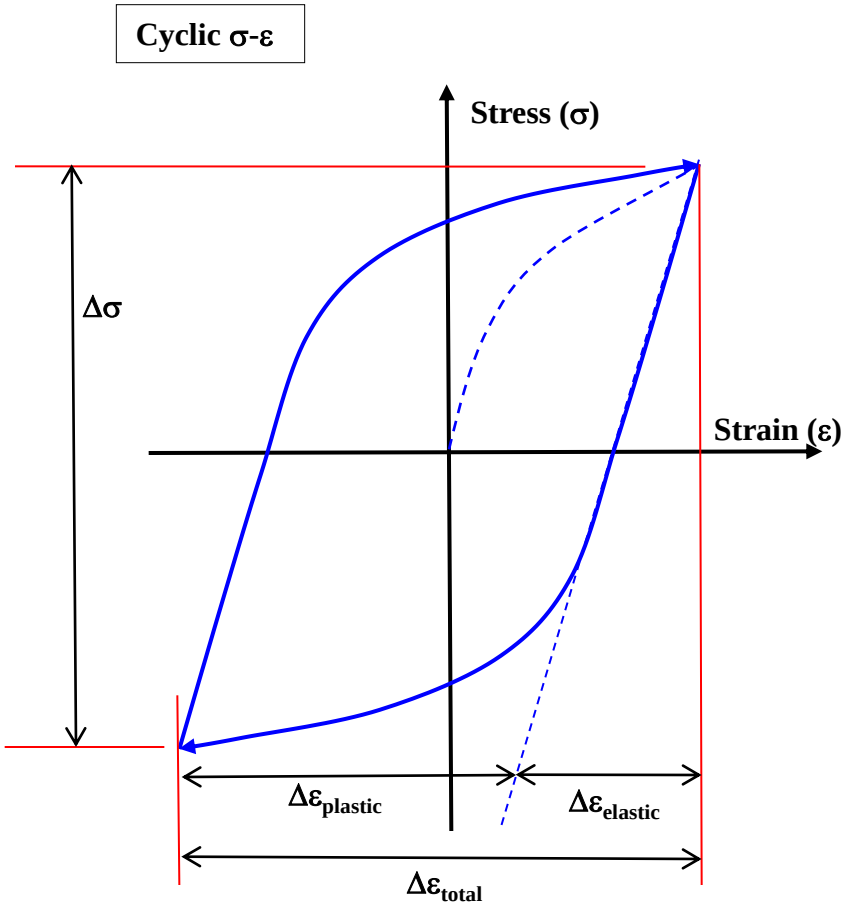

$$\Delta\varepsilon_{total} = \Delta\varepsilon_{elastic} + \Delta\varepsilon_{plastic}$$

Manson-Coffin Relation

Research into metal formability (late 1940's) quantified the remaining ductility after a finite number of loading reversals to failure (very low cycle fatigue). S.S. Manson and C.L. Coffin independently formulated a relationship between applied plastic strain-range and cycles to failure (early 1950's) ;

$\Delta\varepsilon_{plastic} = C(N)^d$

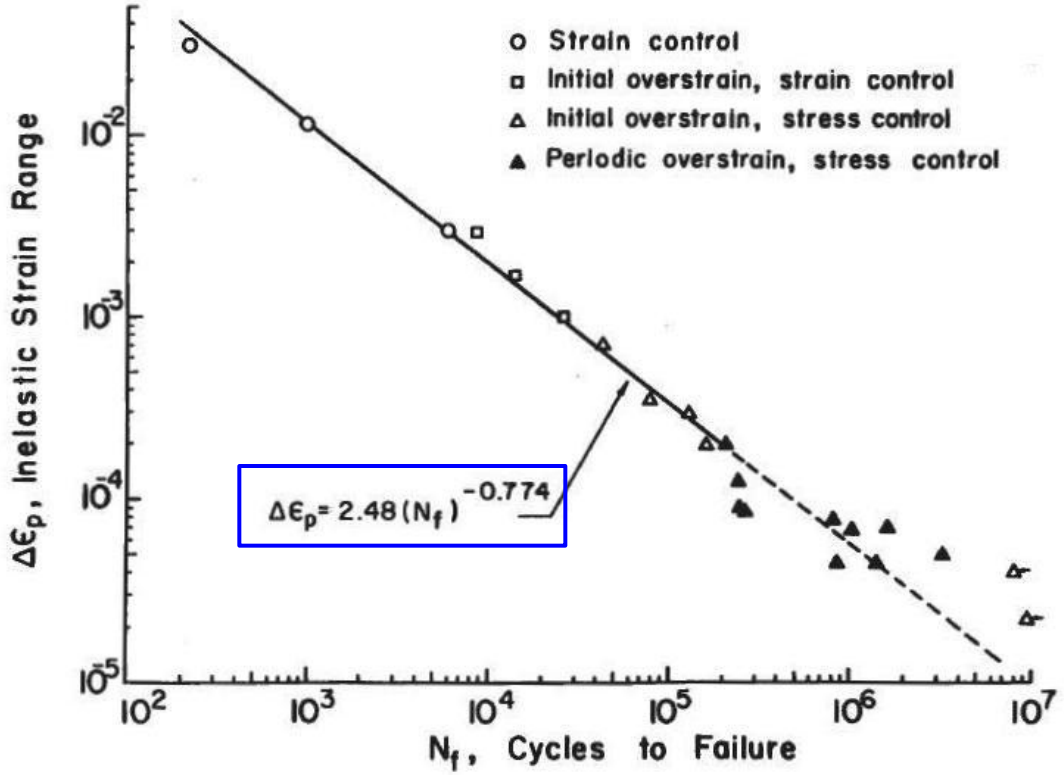

Fig. 15 Inelastic Strain versus Life for SAE 4340 Steel (14)

Ref.: JoDean Morrow, J.F. Martin, N.E. Dowling, **Local Stress-Strain Approach to Cumulative Fatigue Damage Analysis**, UILU-ENG 74 6001, T.&A.M. Report No. 379, 1974, pg 47.

Strain-Life ; the Manson-Coffin-Basquin Relation

Basquin defined cyclic life as power law relation of the applied stress range. Combining the Mason-Coffin relation with the Basquin relation results in the strain-life formulation ; cycles to failure defined as a function of applied elastic and plastic strain ranges.

Strain–Life Relationship

$$\frac{\Delta\epsilon}{2} = \underbrace{\frac{\sigma_f'}{E}(2N_f)^b}_{\text{elastic}} + \underbrace{\epsilon_f'(2N_f)^c}_{\text{plastic}}$$

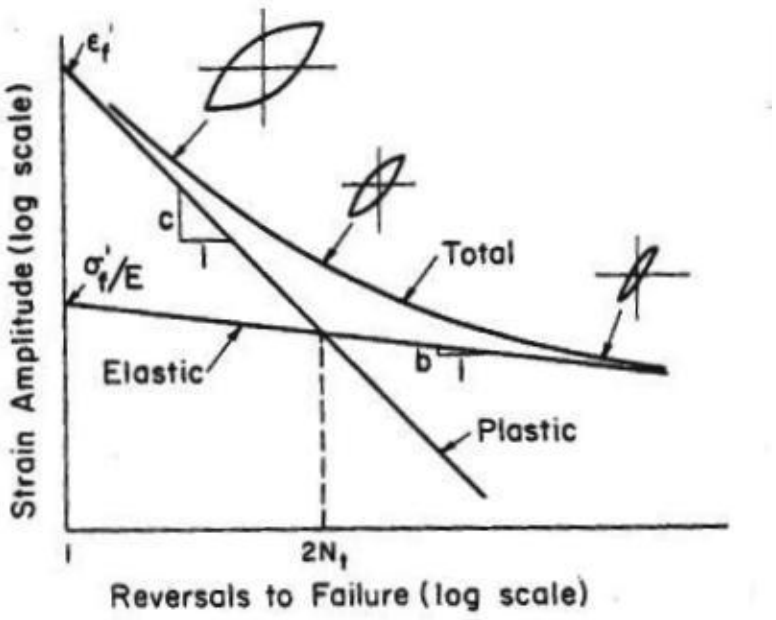

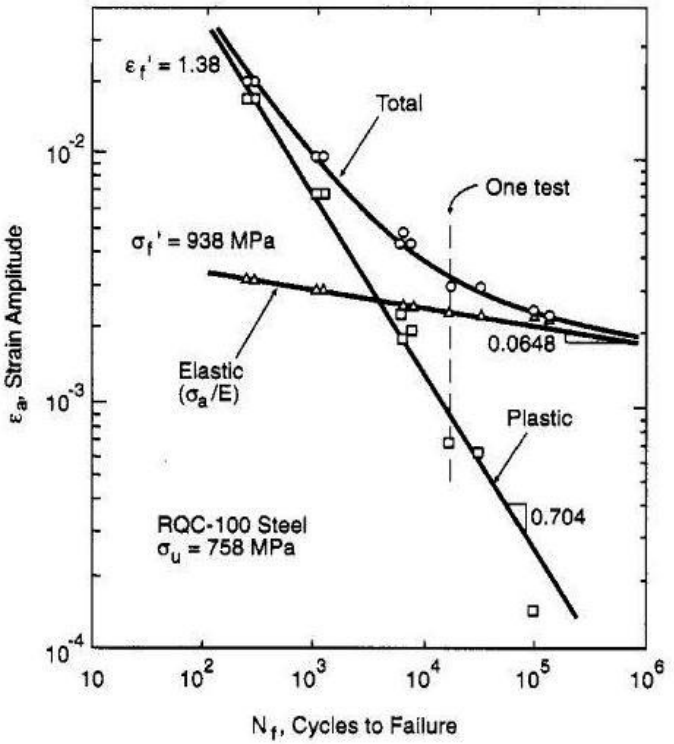

Figure 6 Elastic, plastic, and total strain vs. life curves for RQC-100 steel (reproduced by permission of Pearson Education, Inc., Upper Saddle River, NJ, from Dowling, © 1999, "Mechanical Behavior of Materials," 2nd edn., p. 653).

Strain-Life Methodology (constant amplitude)

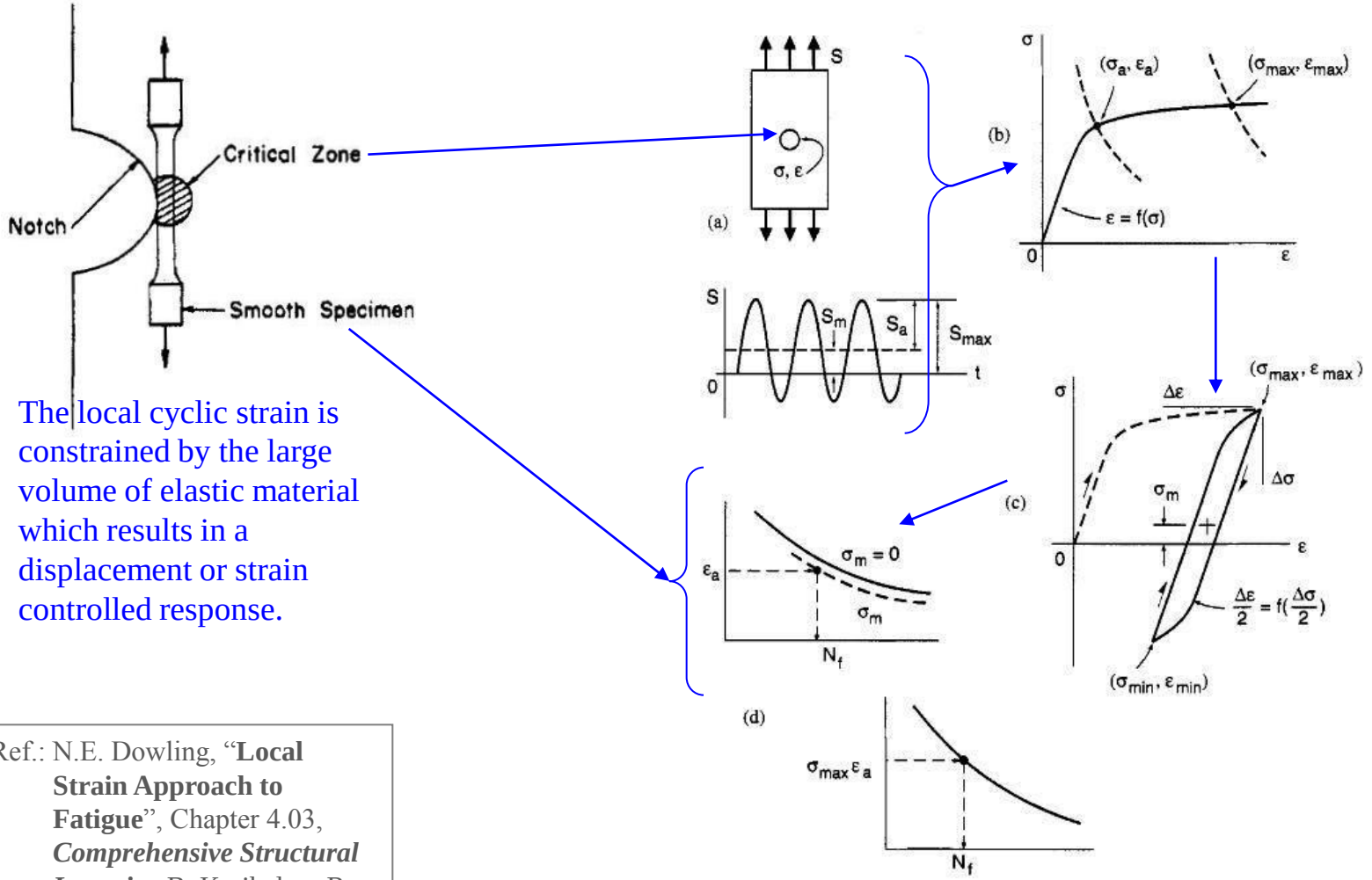

The local cyclic strain is constrained by the large volume of elastic material which results in a displacement or strain controlled response.

Figure 8 Procedure for strain-based life prediction for a notched member under constant-amplitude loading (reproduced by permission of Pearson Education, Inc., Upper Saddle River, NJ, after Dowling, © 1999, "Mechanical Behavior of Materials," 2nd edn., p. 675).

Ref.: N.E. Dowling, "**Local Strain Approach to Fatigue**", Chapter 4.03, ***Comprehensive Structural Integrity***, B. Karihaloo, R. O. Ritchie, and I. Milne, overall editors, Elsevier Science Ltd. Oxford, England, 2003.

Linear Elastic Fracture Mechanics

LEFM Historical Overview

1913 – C.E. Inglis publishes "Stresses in Plate due to Presence of Cracks and Sharp Corners" which defines the stress field for 2-D elliptical openings.

1920 – A.A. Griffith, "The Phenomena of Rupture and Flow in Solids", proposes that fracture will occur when the strain energy released during crack extension exceeds the rate of increase in the material resistance to fracture (surface energy in Griffith's formulation).

1948 - G.R. Irwin and E. Orowan independently modify Griffith's criterion to include the work done in plastic deformation such that it could be applied to ductile materials/metals.

1956 – G.R. Irwin equates the strain energy release rate to the stress and displacement field in the vicinity of the crack tip (fracture process zone) as opposed to the energy balance for the entire elastic solid.

1957 – Irwin's "Analysis of Stresses and Strains Near the End of a Crack Traversing a Plate" shows that the crack tip stress field can be characterized by the stress intensity factor **K** and that the stress representation is equivalent to strain energy methodology.

1961 – P.C. Paris et al. demonstrate that the stress intensity factor **K** is a viable parameter to characterize fatigue crack propagation rates.

Ref.: **Fracture Mechanics Retrospective : Early Classic Papers (1913-1965)**, John M. Barson, editor, American Society for Testing and Materials, 1987, pp 1-10.

Stress Intensity Factor

In 2-dimensional linear elasticity the equilibrium equations (sum forces & moments = 0), constitutive relations [$\sigma(\varepsilon)$], and the compatibility relations (ensures continuity between the 3 strain components and the 2 displacement variables) must be satisfied for a solution to be attained. The introduction of a function (Airy's stress function) allows for the 2-D elastostatic problem to be transformed into a fourth order partial differential equation. Thus for a linear elastic isotropic material with constant body forces the equation to be solved (independent of material properties) is given below:

$$\nabla^2(\nabla^2\Phi) = \nabla^2\left(\frac{\partial^2\Phi}{\partial x^2} + \frac{\partial^2\Phi}{\partial y^2}\right) = \nabla^2(\sigma_{yy} + \sigma_{xx}) = 0$$

An abbreviated derivation of the Griffith problem (2D crack in biaxial tension field) is provided below :

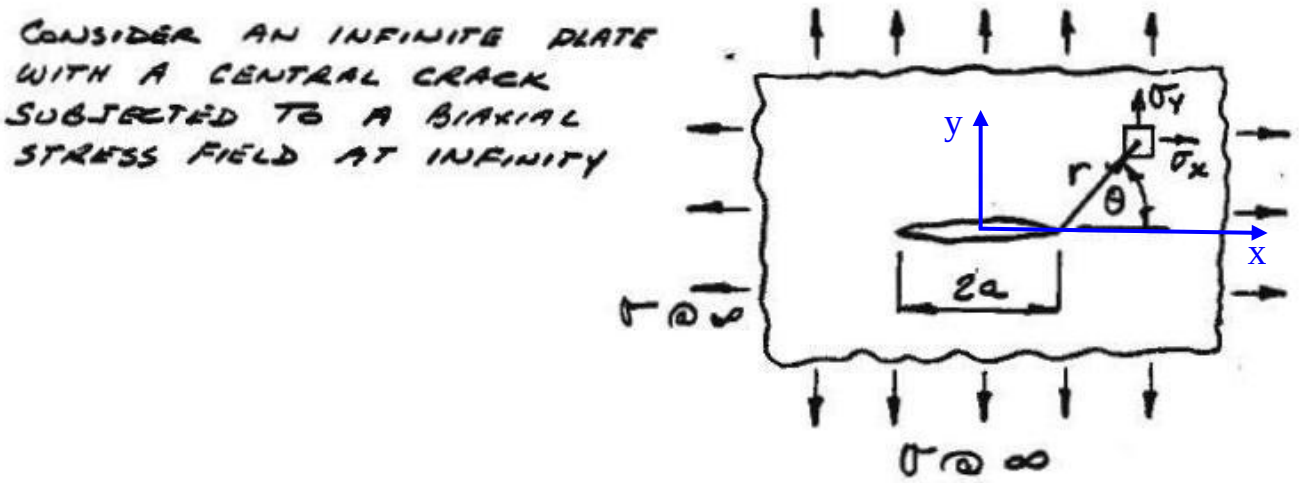

Ref.: T. Swift, **Damage Tolerance Technology Short Course**, FAA, 1985.

Stress Intensity Factor ; (cont.)

The Westergaard stress function (complex variables) with the origin shifted to the crack tip is provided below:

MOVING THE ORIGIN OF COORDINATES TO THE RIGHT HAND END OF THE CRACK AND REPLACING Z BY Z+a IN Z WILL GIVE

$$Z = \frac{\sigma(z+a)}{\sqrt{(z+a)^2-a^2}} = \frac{\sigma(z+a)}{(z^2+2az+a^2-a^2)^{1/2}}$$

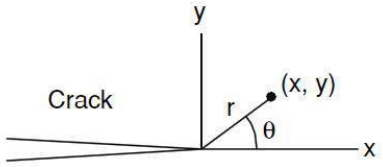

The stress normal to the crack plane (σ_y) is given as : $\sigma_y = Re\,Z + y\,Im\,Z'$

Going through the calculations (with r<<a) yields the following result for σ_y :

$$\therefore \sigma_y = \frac{\sigma\sqrt{a}}{(2r)^{1/2}} \cos\frac{\theta}{2}\left(1+\sin\frac{\theta}{2}\sin\frac{3\theta}{2}\right)$$

IF THIS EQUATION IS COMPARED TO EQUATION 8 IT WILL BE NOTICED THAT A $\sqrt{\pi}$ IS MISSING FROM THE BOTTOM LINE. IT IS NOT MATHEMATICALLY NECESSARY TO INCLUDE THIS TERM. HOWEVER IN ORDER TO BE EQUIVALENT TO THE ENERGY APPROACH EVOLVING FROM THE WORK OF GRIFFITH THE FRACTURE MECHANICS COMMUNITY DECIDED TO INCLUDE THIS TERM. THEREFORE MULTIPLYING THE ABOVE EQUATION BY $\sqrt{\pi}/\sqrt{\pi}$ (WHICH DOES NOT CHANGE IT MATHEMATICALLY) GIVES

$$\sigma_y = \frac{\sigma\sqrt{\pi a}}{(2\pi r)^{1/2}} \cos\frac{\theta}{2}\left(1+\sin\frac{\theta}{2}\sin\frac{3\theta}{2}\right)$$

The term ($\sigma\sqrt{\pi a}$) defines the magnitude/intensity of the crack tip stress field and is labeled the (crack tip) stress intensity factor (SIF) with units ksi$\sqrt{in}$.

The other terms in the solution $f(r,\theta)$ define the stress field distribution.

Ref.: T. Swift, **Damage Tolerance Technology Short Course**, FAA, 1985.

Stress Intensity Factor ; (cont.)

The Mode I stress and displacement field LEFM results are provided below.

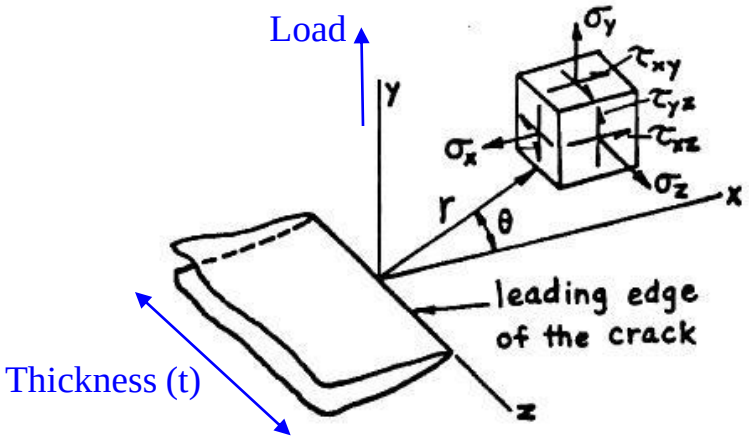

Fig. 2-Coordinates Measured from the Leading Edge of a Crack and the Stress Components in the Crack Tip Stress Field.

Mode I:

$$\sigma_x = \frac{K_I}{(2\pi r)^{1/2}}\cos\frac{\theta}{2}\left[1-\sin\frac{\theta}{2}\sin\frac{3\theta}{2}\right] + \sigma_{x_0} + O(r^{1/2})$$

$$\sigma_y = \frac{K_I}{(2\pi r)^{1/2}}\cos\frac{\theta}{2}\left[1+\sin\frac{\theta}{2}\sin\frac{3\theta}{2}\right] + O(r^{1/2})$$

$$\tau_{xy} = \frac{K_I}{(2\pi r)^{1/2}}\sin\frac{\theta}{2}\cos\frac{\theta}{2}\cos\frac{3\theta}{2} + O(r^{1/2})$$

} (1)

and for plane strain (with higher order terms omitted)

$$\sigma_z = \nu(\sigma_x+\sigma_y), \quad \tau_{xz} = \tau_{yz} = 0$$

$$u = \frac{K_I}{G}\left[r/(2\pi)\right]^{1/2}\cos\frac{\theta}{2}\left[1-2\nu+\sin^2\frac{\theta}{2}\right]$$

$$v = \frac{K_I}{G}\left[r/(2\pi)\right]^{1/2}\sin\frac{\theta}{2}\left[2-2\nu-\cos^2\frac{\theta}{2}\right]$$

$$w = 0$$

Ref.: H. Tada, P. Paris, G. Irwin, **The Stress Analysis of Cracks, 2nd Ed.**, Del Research Cor., pg. 1.3, 1985.

Crack Tip Stress Field

The stress field response for an elastic body with a notch (finite radius) and a crack (radius $\rightarrow 0$) differs in terms of the stress magnitudes and distribution. The section thickness also affords stress state changes (plane stress vs. plane strain) which influences the local yielding response.

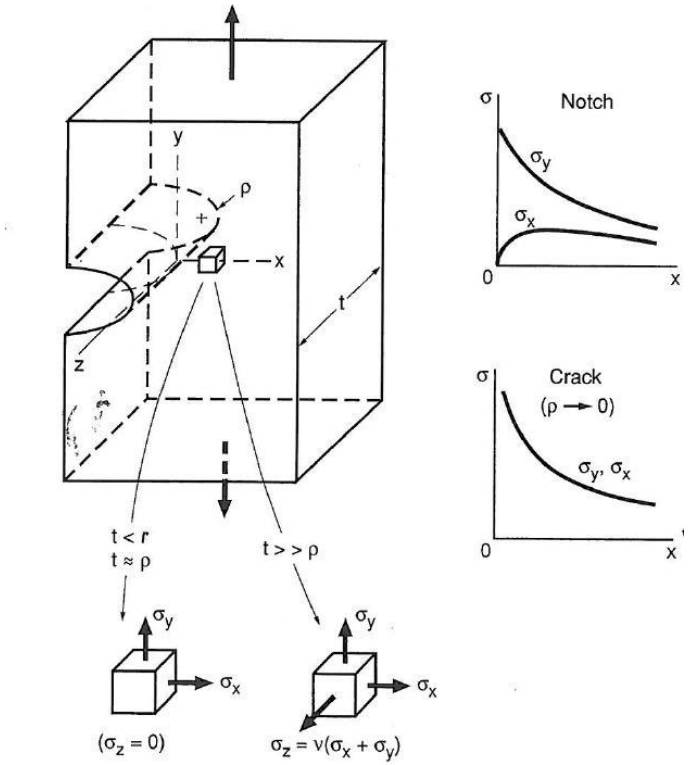

Ref.: N.E. Dowling, **Mechanical Behavior of Materials, 2nd Ed.**, Prentice Hall, pg. 277, 1999.

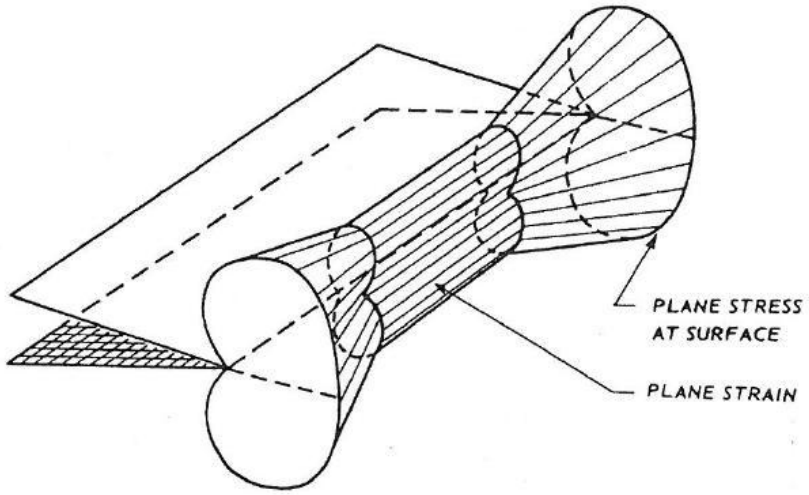

Ref.: H.L. Ewalds, R.J.H. Wanhill, **Fracture Mechanics**, Edward Arnold, pg. 67, 1984.

Crack Tip Stress Field – Fracture Toughness Influence

The stress intensity factor for the defined failure load (stress) and crack size is the material fracture toughness. Beyond a certain thickness the fracture toughness reaches a limiting value; plane strain fracture toughness (K_{Ic}).

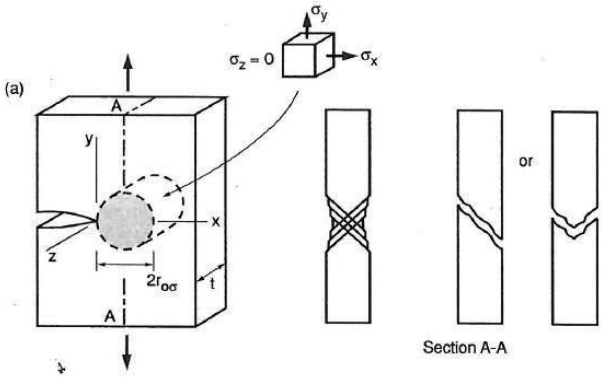

Plane Stress [$\sigma_z = 0$; $\varepsilon_z = -\upsilon/E(\sigma_x+\sigma_y)$]

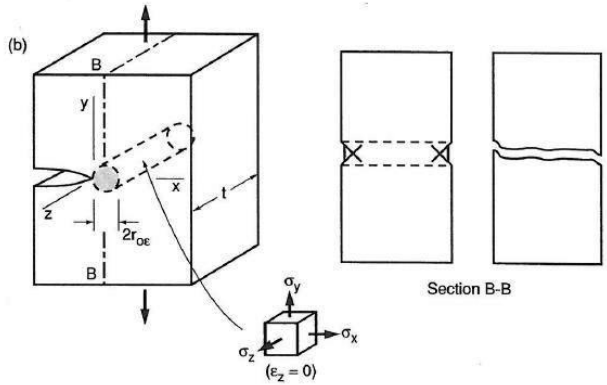

Plane Strain [$\varepsilon_z = 0$; $\sigma_z = \upsilon(\sigma_x+\sigma_y)$]

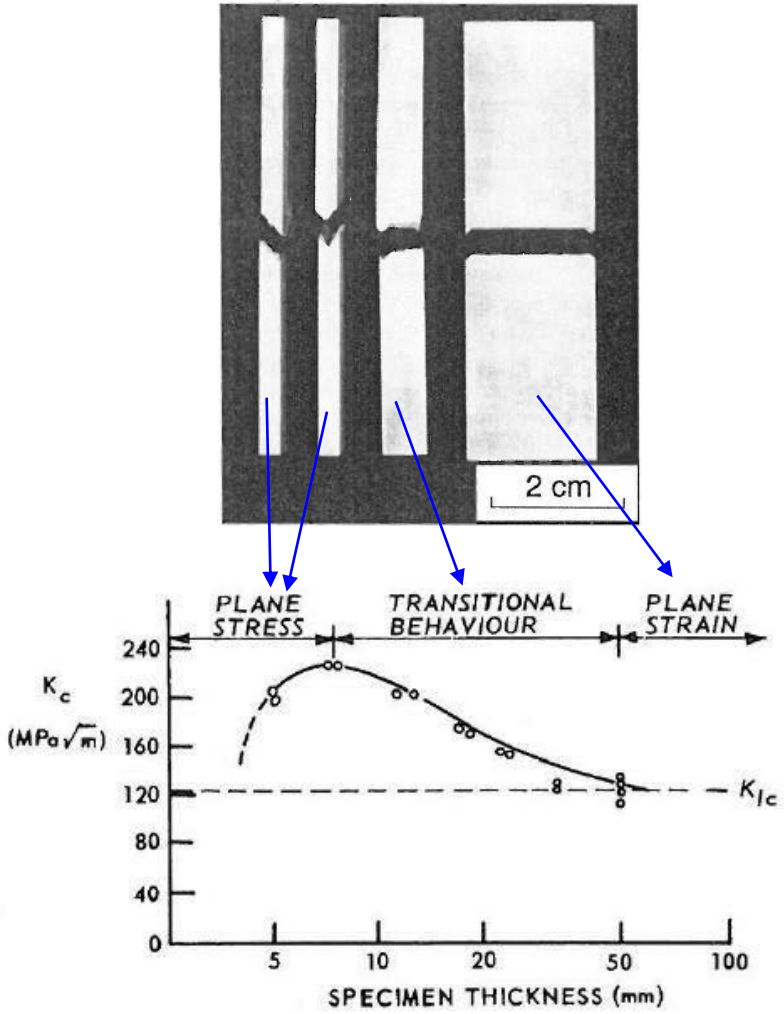

Fatigue Crack Growth/Propagation Rate

The application of cyclic loading to a structure with a crack-like defect can result in fatigue crack propagation. The fatigue crack increment on a per cycle basis is very small. The crack propagation rate is defined as the differential **da/dN** where '**a**' represents the crack size/length and '**N**' represents the number of applied cycles.

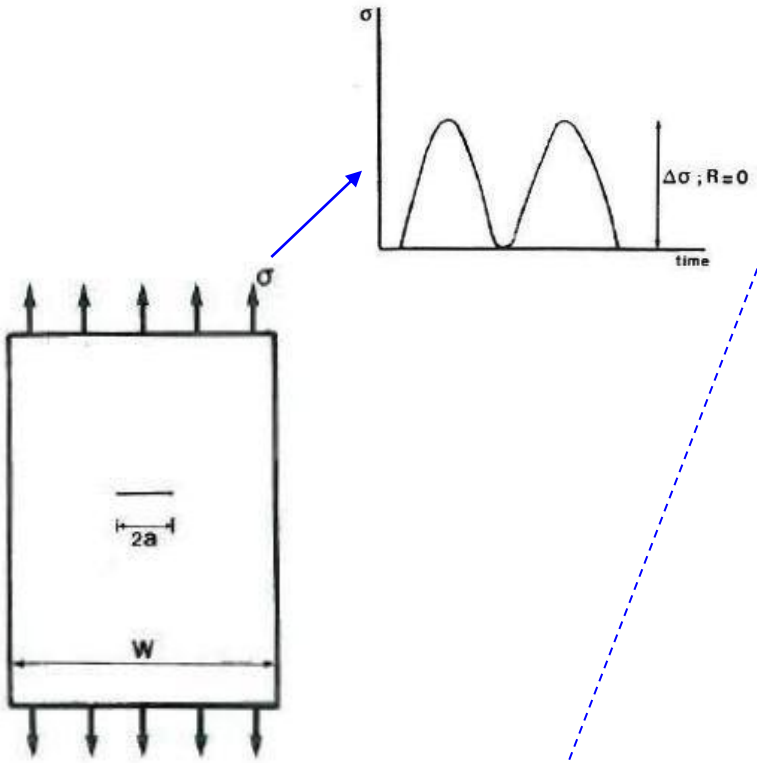

$\Delta\sigma\uparrow \rightarrow da/dN\uparrow$
$(a+\Delta a)\uparrow \rightarrow da/dN\uparrow$ (typically)

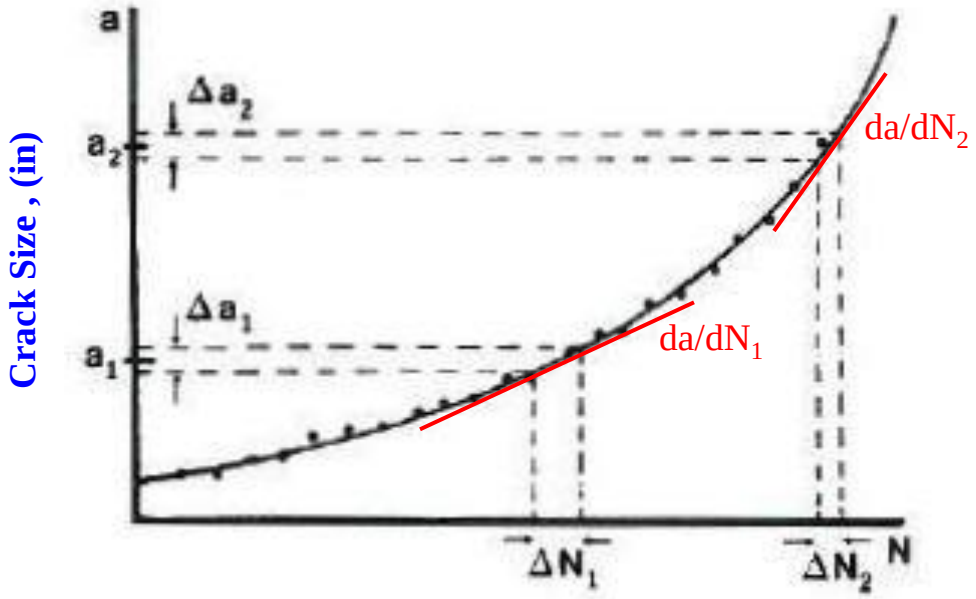

Ref.: David Broek, **The Practical Use of Fracture Mechanics**, Kluwer Academic Publishers, 1989, pg. 127.

Fatigue Crack Growth/Propagation Rate ; da/dN = f(ΔK)

George Irwin correlated cracked body failure load with crack tip stress intensity factor ($K=\sigma\sqrt{(\pi a)}\cdot\beta_{geom}$) ; Paul Paris extended the stress intensity factor to fatigue crack propagation correlation ($\Delta K=\Delta\sigma\sqrt{(\pi a)}\cdot\beta_{geom}$).

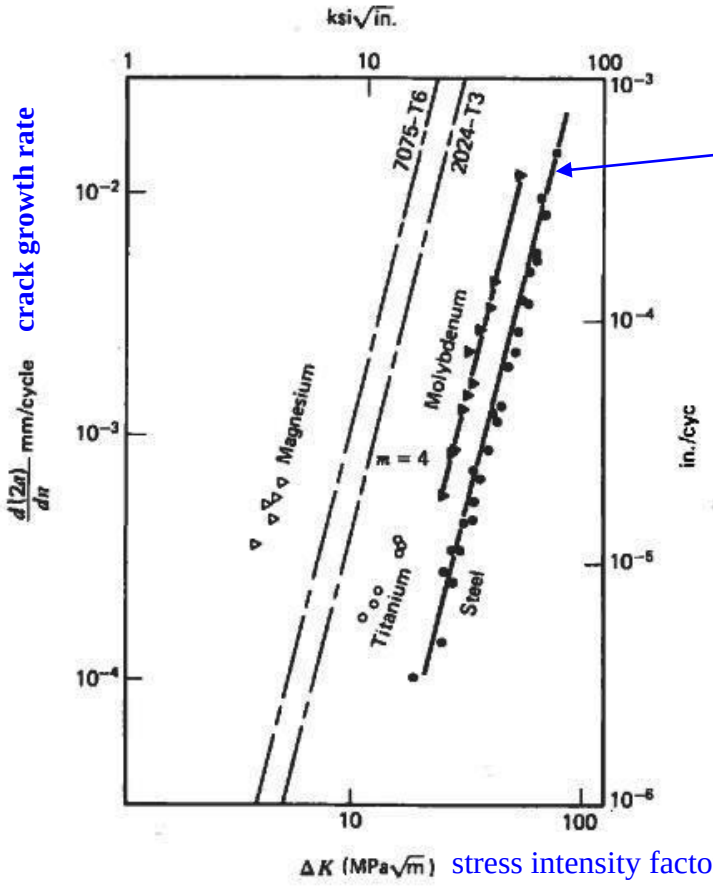

$$\frac{da}{dN}=A\Delta K^m \qquad (13\text{-}3)$$

where $\frac{da}{dN}$ = fatigue crack growth rate

ΔK = stress intensity factor range ($\Delta K = K_{max} - K_{min}$)

A, m = f (material variables, environment, frequency, temperature, stress ratio)

Ref.: R.W. Hertzberg, **Deformation and Fracture Mechanics of Engineering Materials, 3rd ed.**, John Wiley & Sons, 1989, pp. 519-520.

FIGURE 13.3 Fatigue crack propagation for various FCC, BCC, and HCP metals. Data verify power relation between ΔK and da/dN.[4] (With permission of Syracuse University Press.)

Fatigue Crack Growth/Propagation Rate ; da/dN = f(ΔK) – (cont.)

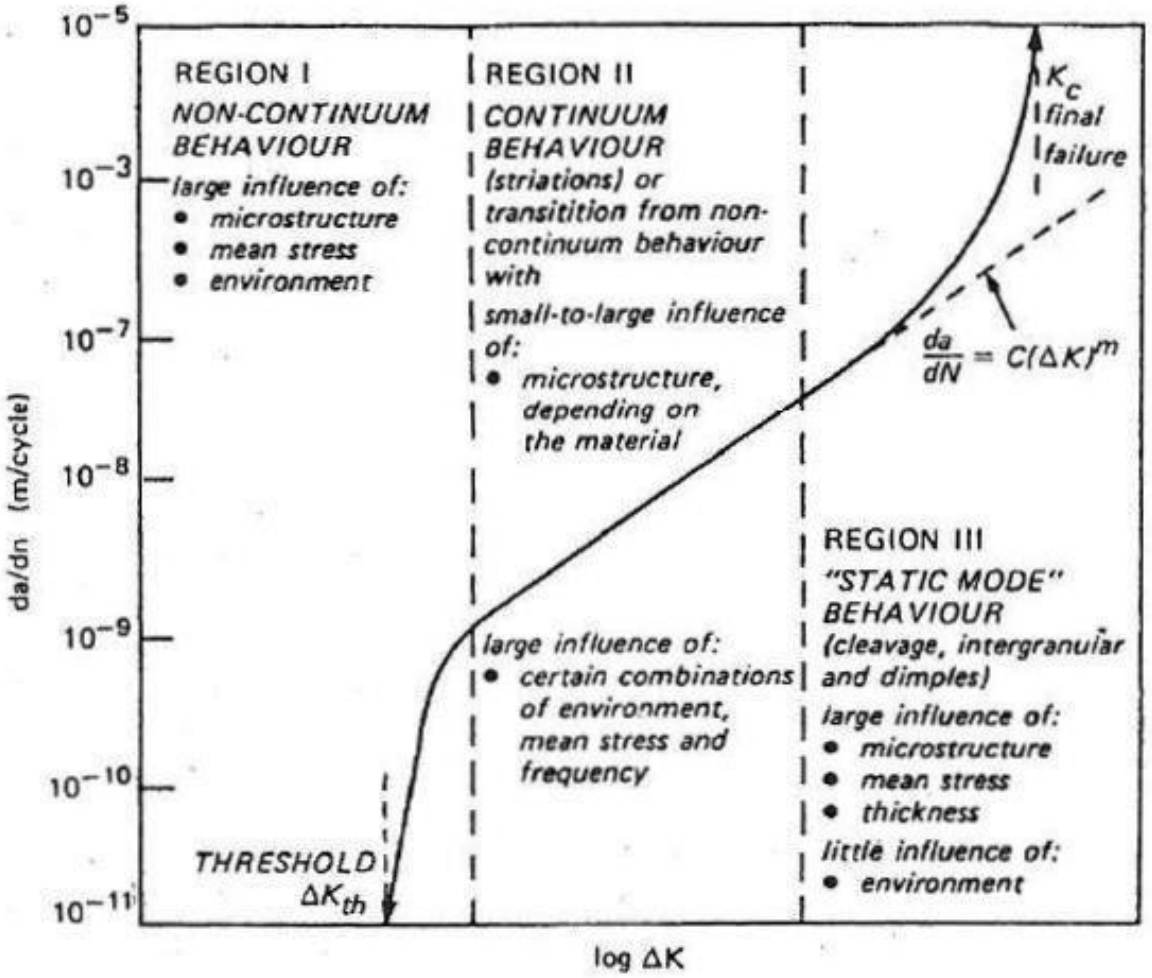

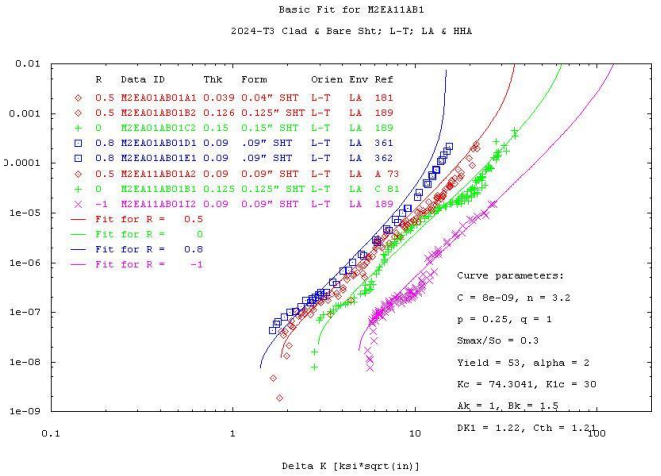

Ref.: R.O. Ritchie, W.W. Gerberich, J.H. Underwood, **Fatigue and Fracture**, Technical Report ARCCB-TR-88016, 1988, pg. 55.

Fatigue Crack Growth/Propagation Rate ; da/dN = f(ΔK) – (cont.)

Attempts at correlating fatigue crack growth rates as a function of applied stress, net section stress, etc. competed with stress intensity factor correlation in the early 1960's. A definitive test demonstration involved remotely loaded panel ($a\uparrow \rightarrow \Delta K\uparrow \rightarrow da/dN\uparrow$; $dK/da>0$) and a wedge loading cracked panel ($a\uparrow \rightarrow \Delta K\downarrow \rightarrow da/dN\downarrow$; $dK/da<0$) resulting in a single da/dN - ΔK curve.

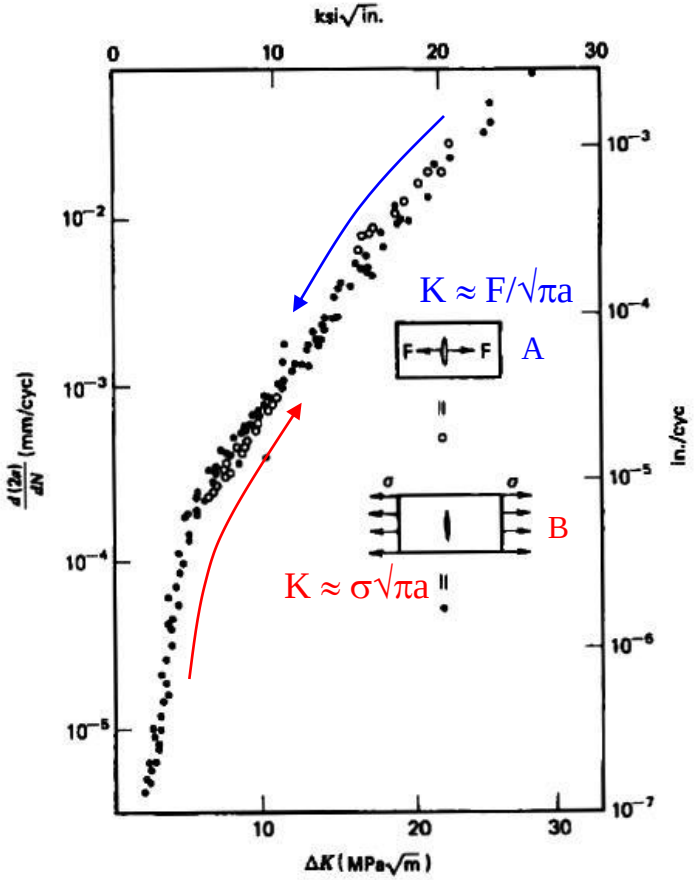

FIGURE 13.5 Fatigue crack propagation behavior in 7075-T6 for remote and crack line loading conditions.[4] (With permission of Syracuse University Press.)

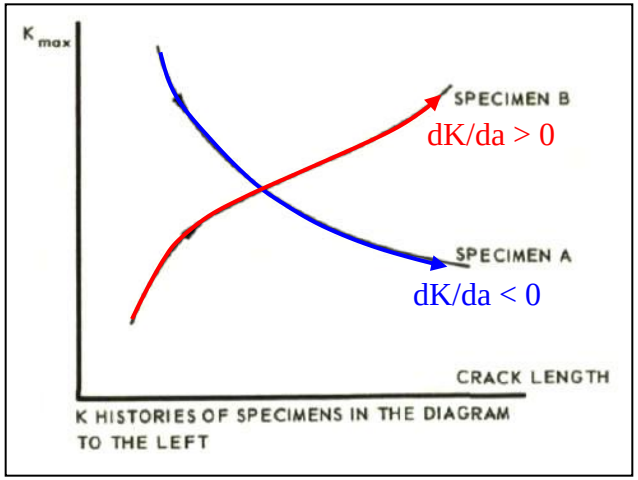

Test specimen crack driving force trend

Ref.: R.W. Hertzberg, **Deformation and Fracture Mechanics of Engineering Materials, 3rd ed.**, John Wiley & Sons, 1989, pg. 523.

Fatigue Crack Growth/Propagation Orientation

The material processing influences the resulting microstructure which in turn affects the fracture parameters (toughness and growth rate). Within the orientation designation the first letter represents the applied loading direction and the second letter represents the crack propagation direction (mode-I tension opening).

Long-Transverse properties are typically upper bound values in bar stock.

Short-Transverse properties are typically lower bound values in bar stock.

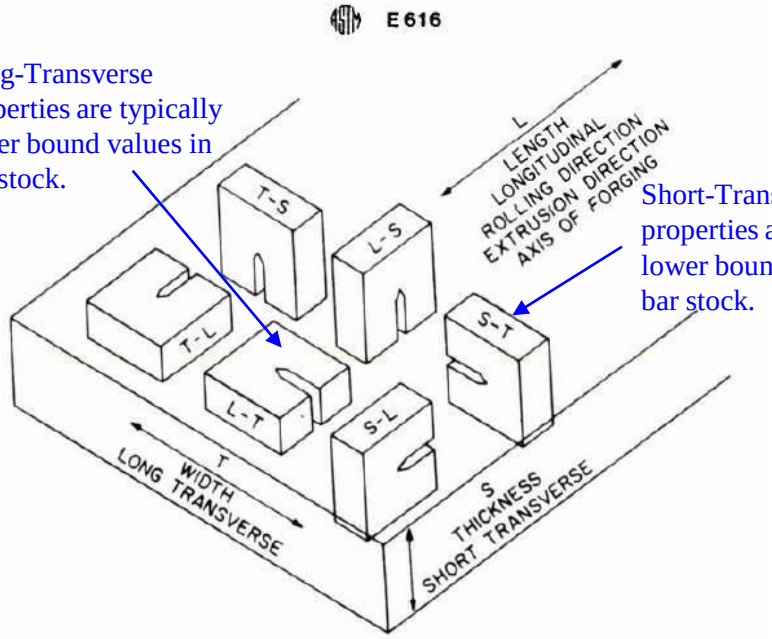

FIG. 3 Crack Plane Orientation Code for Rectangular Sections

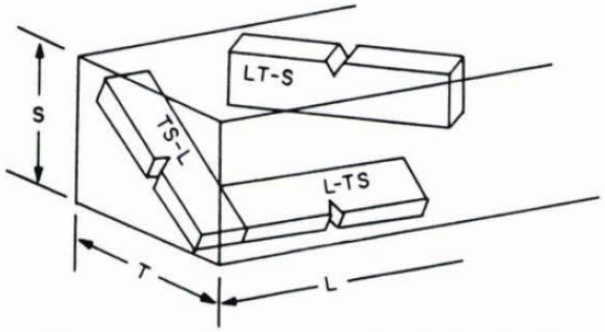

FIG. 4 Crack Plane Orientation Code for Rectangular Sections Where Specimens Are Tilted with Respect to the Reference Directions

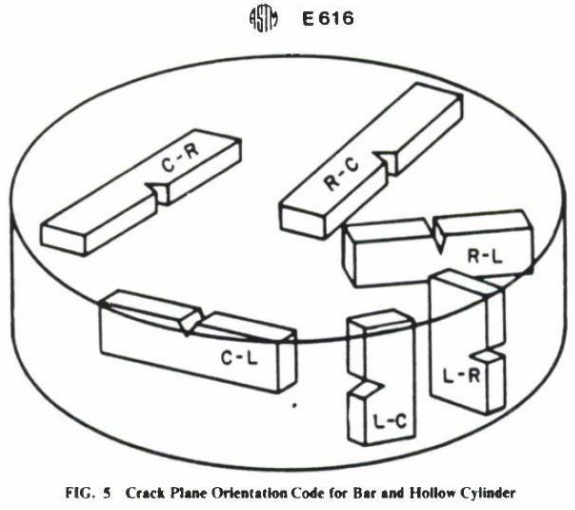

FIG. 5 Crack Plane Orientation Code for Bar and Hollow Cylinder

Ref.: Gallagher, Giessler, Berens, Engle, **USAF Damage Tolerant Design Handbook**, AFWAL-TR-82-3073, 1984, pp. B-21,22.

Fatigue Crack Growth Scatter - Batch/Lot Variations

There can measurable variation in fatigue crack growth between different material production lots/batches and also from different suppliers (as much as a factor of 2 difference). In fracture critical applications where fracture is dictating design parameters it is prudent to verify/account for material property lot/batch variations.

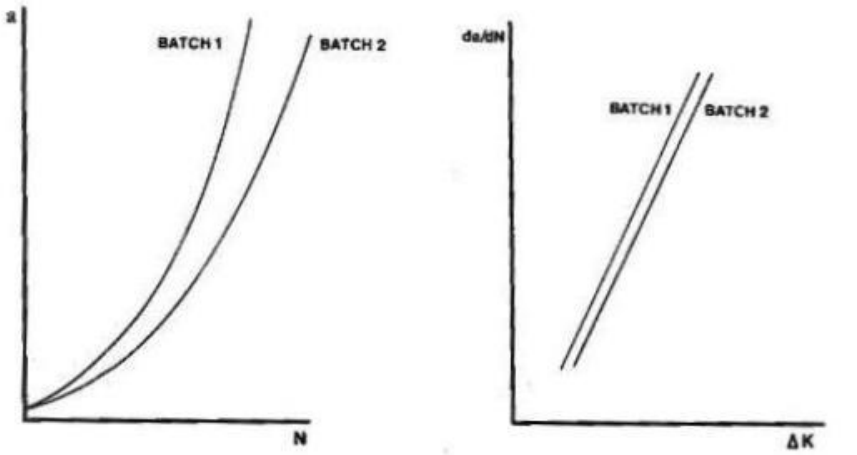

Figure 7.16. Typical scatter due to batch-to-batch and heat-to-heat variations.

Ref.: David Broek, **The Practical Use of Fracture Mechanics**, Kluwer Academic Publishers, 1989, pg. 233.

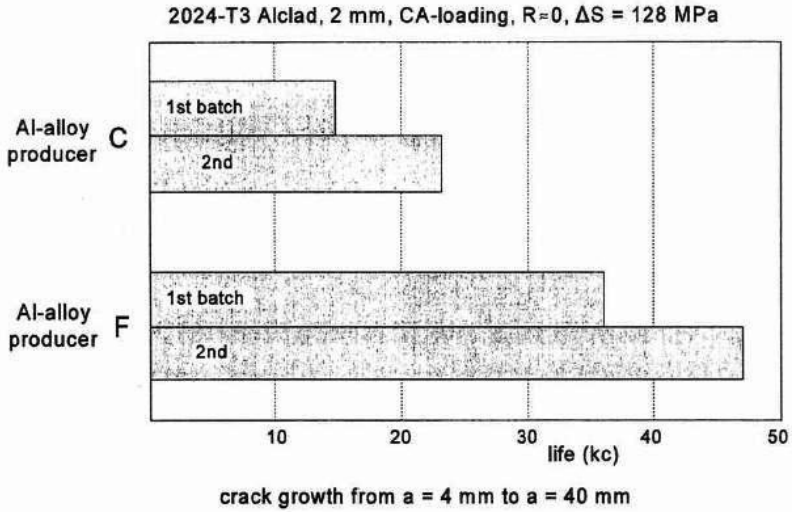

Fig.8.16: Comparison between crack growth lives of sheet specimens of different producers and different batches [27].

Ref.: Jaap Schijve, **Fatigue of Structures and Materials**, Kluwer Academic Publishers, 2001, pg. 199.

Fatigue Crack Growth Scatter

The scatter in fatigue crack growth was measured in 68 identical center cracked panels of 2024 aluminum (same lot of material, test fixtures, and measurement techniques. The scatter in the crack growth data is bounded by a deterministic factor of 2.

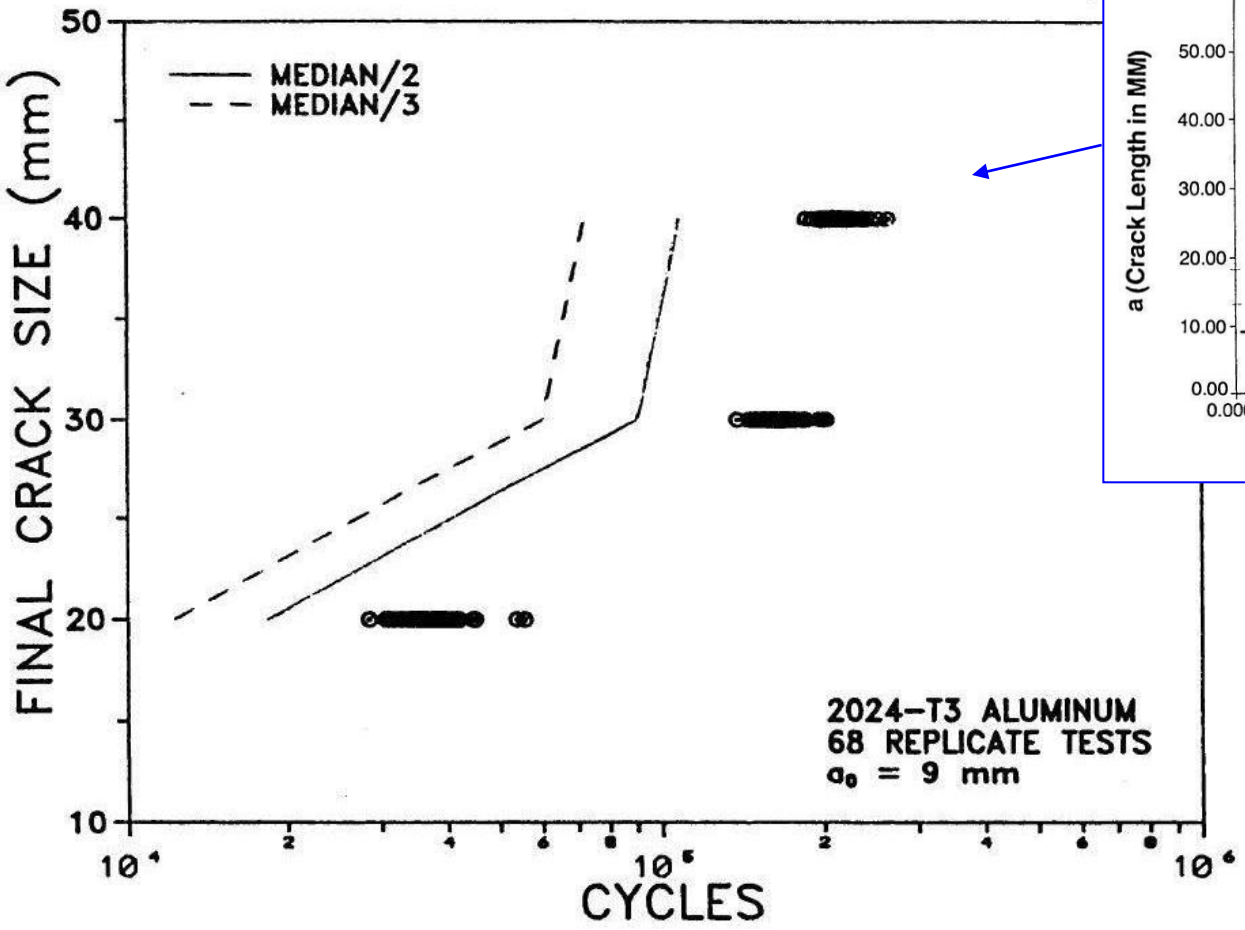

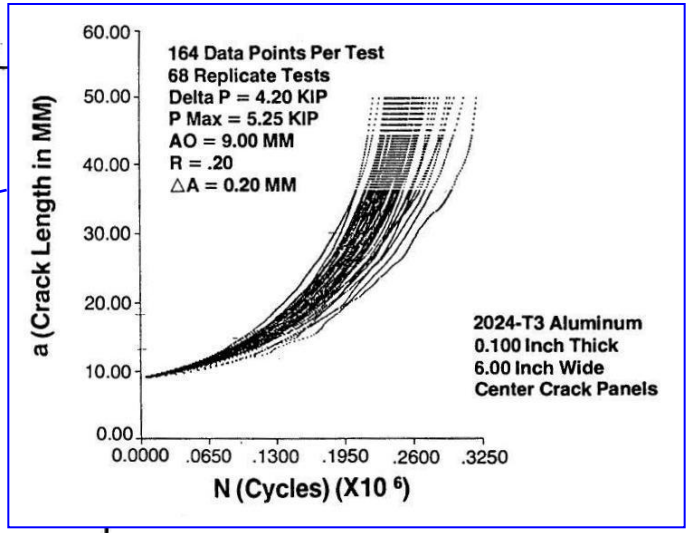

Ref.: A.P. Berens, **Fatigue Life Scatter Factors in Aircraft Applications**, UDR-TR-92-138, 1992.

Fatigue Crack Growth Scatter – Applicability Limits

As in S-N fatigue the scatter within the asymptotic regions of the fatigue crack growth rate curve are regimes wherein the deterministic scatter factor on life does not adequately bound the inherent material scatter.

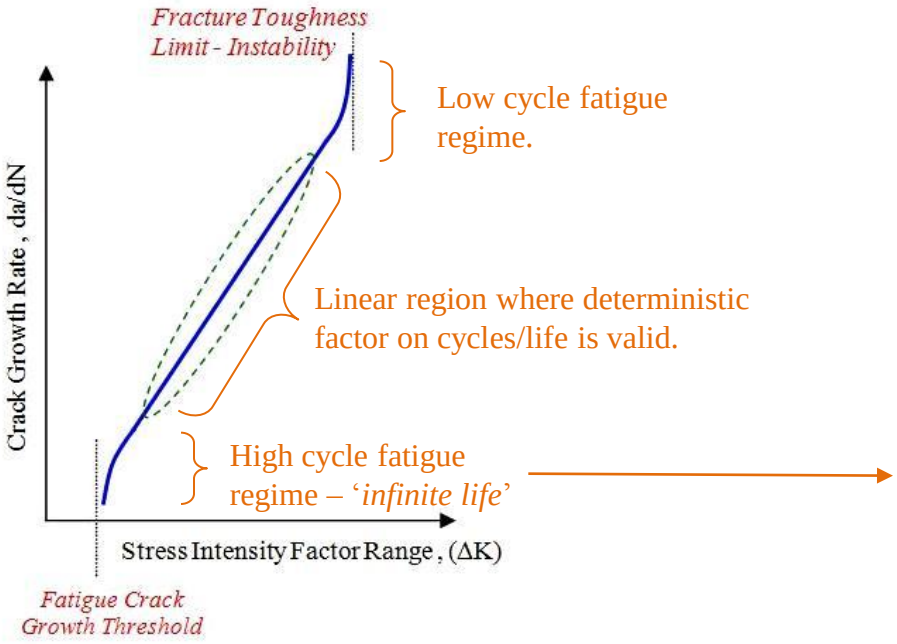

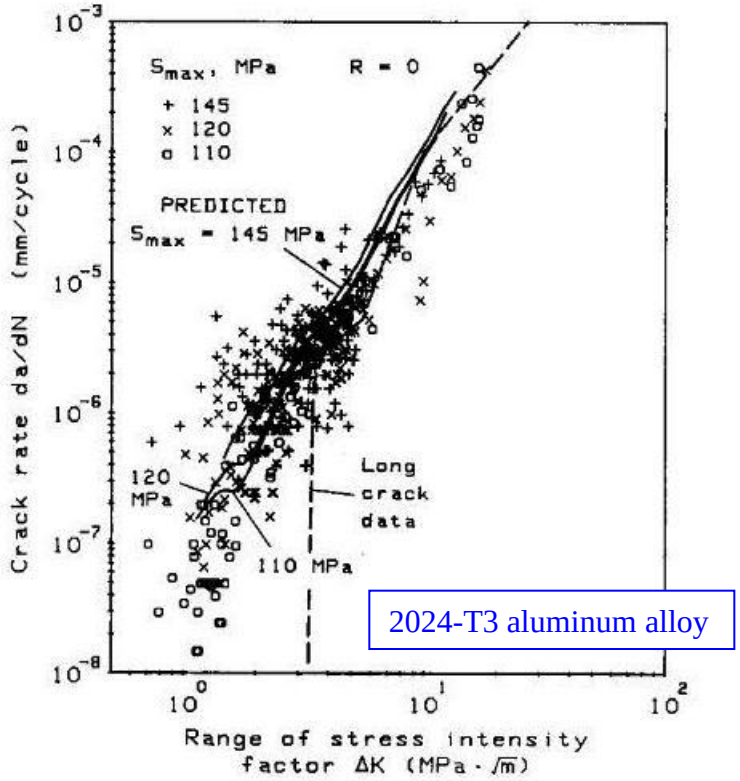

Figure 86.- Experimental and predicted crack-growth rates for short cracks under R = 0 loading.

Ref.:J.C. Newman, Jr., and P.R. Edwards, **Short-Crack Growth Behaviour in an Aluminum Alloy**, AGARD-R-732, June 1988, pg 57.

Fatigue Crack Growth & S-N Scatter

The validity of the deterministic scatter factor magnitudes for fatigue (fatigue crack initiation & propagation) and fracture (fatigue crack propagation) is substantiated by Zhang Fu-Ze. The results incorporate large test data sets and theoretical results for limited data. The deterministic scatter factor for S-N fatigue is >4 while the that for fatigue crack growth is <2.

Tab. 1 The values of different kinds of scatter factors for aeronautical structural components

The number of tested structural components, n		1	2	3	4	5
The scatter factors for testing, f_0. p=99.87% r=90%	The scatter factors for crack initiation life σ_s =0.18	5.9	5.0	4.7	4.5	4.4
	The scatter factors for crack growth life σ_s =0.0623	1.8	1.8	1.7	1.7	1.7
The scatter factors for theoretical computation, for p=99.87% *(Independent of number of specimens)*	The scatter factor for crack initiation life σ_s =0.224			4.7		
	The scatter factor for crack growth life σ_s =0.0623			1.6		

Note: p is the reliability level, and r, the confidence level.

S-N fatigue scatter factor

Crack Growth / Fracture Mechanics scatter factor

Ref.: Zhang Fu-Ze, **The Fatigue Scatter Factors and Reduction Factors in the Design of Aircraft and Helicopters Structural Lives**, SAE 911984, September 1991, pg 174.

LEFM Service Life Analysis Steps

A crack case solution that is representative of the local geometry and applied stress is combined with the fatigue spectrum to define the applied stress intensity factor range for a given number of cycles. The resulting crack growth increment is determined by integrating the crack growth rate equation for the material. The process is continued until analytical failure is achieved.

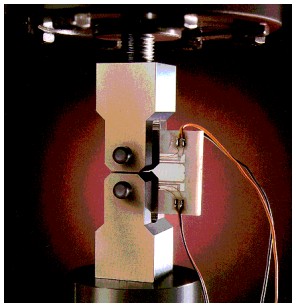

Material testing to define the fracture mechanics properties.

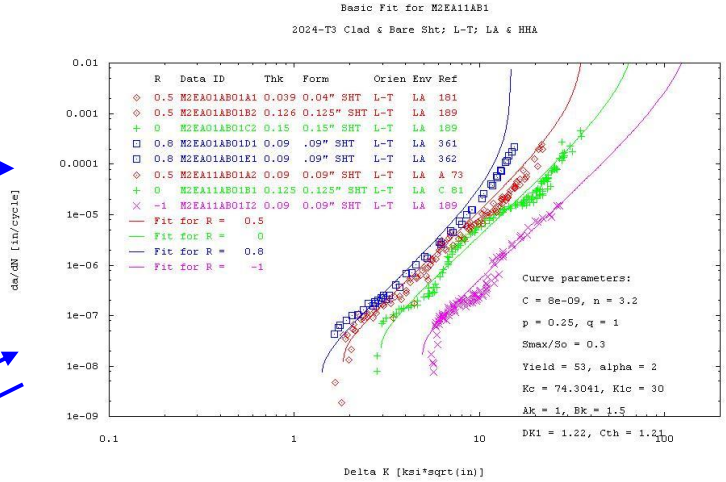

ΔK is combined with da/dN to compute Δa.

Crack size is incremented (Δa).

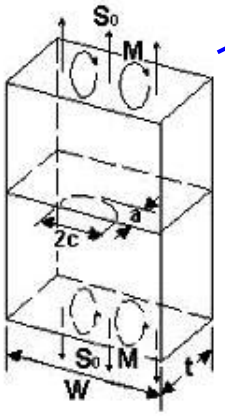

$$S_1 = \frac{6M}{Wt^2}$$

$$0 < \frac{2c}{W} \leq 1$$

$$0.1 \leq \frac{a}{c} \leq 1.2$$

Fatigue spectrum loading cycle (Δσ) defines (ΔK) for the crack case solution.

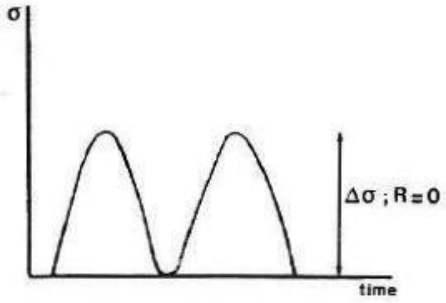

LEFM Service Life Analysis ; (cont.)

The service life analysis result maps the change in crack size as a function of usage (applied cycles). The established safe interval of operation allows for multiple inspection opportunities so as to mitigate a service related structural failure.

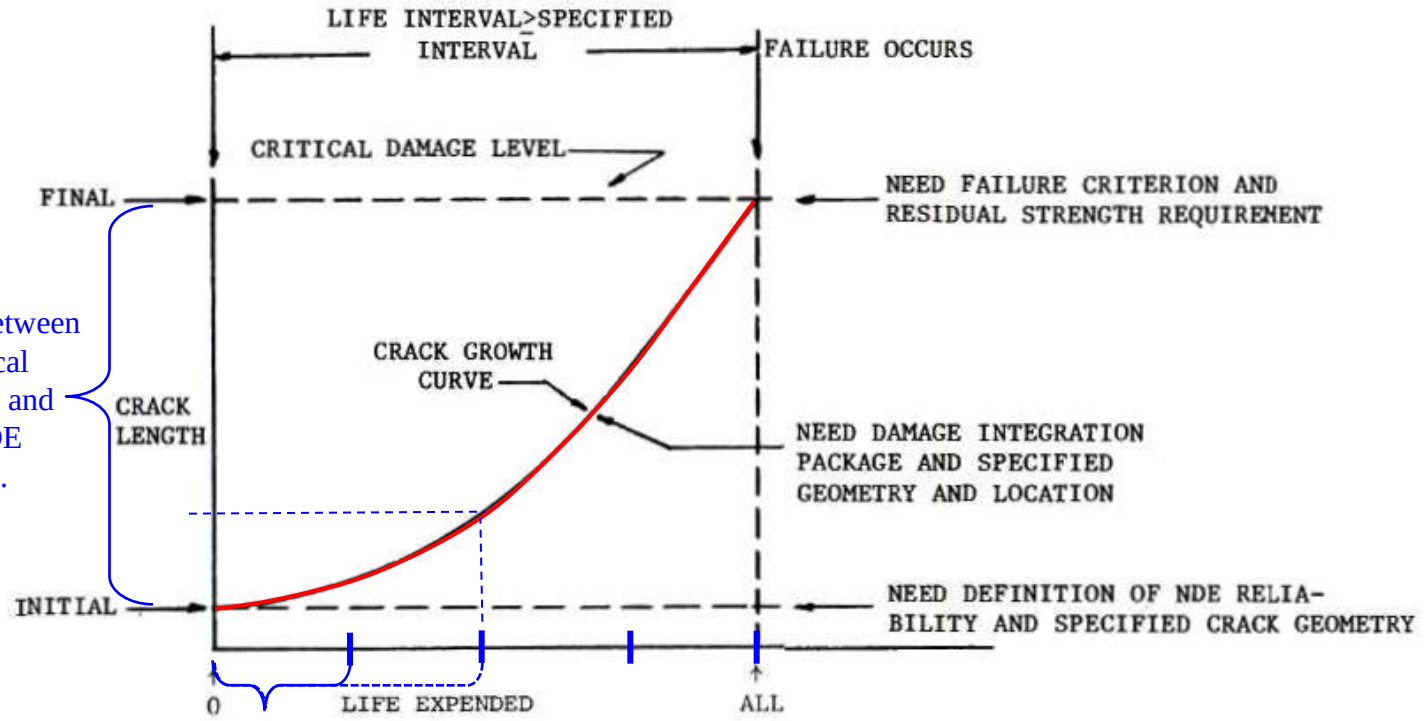

Ref.: Gallagher, Giessler, Berens, Engle, **USAF Damage Tolerant Design Handbook**, AFWAL-TR-82-3073, 1984, pp. 4.1.7.

NASGRO Demonstration of Part-Thru Crack SIF Solutions w/ Thru-Crack Data

Test demonstration of the NASGRO LEFM code for a surface crack in a flat plate (bending & tension) is provided below.

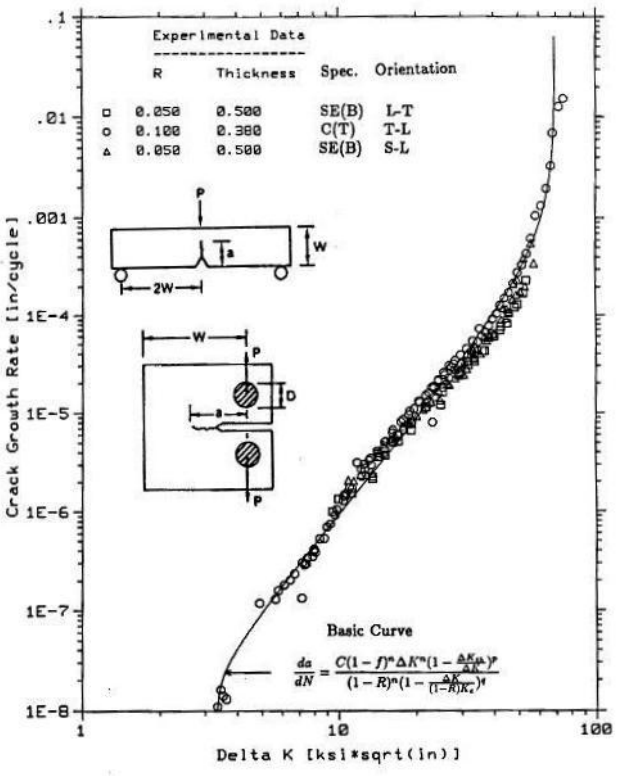

Baseline fatigue crack growth data for thru-thickness cracks in standard specimens.

Heat tinting of titanium as various crack growth increments leaves visible marker bands on the fracture surface.

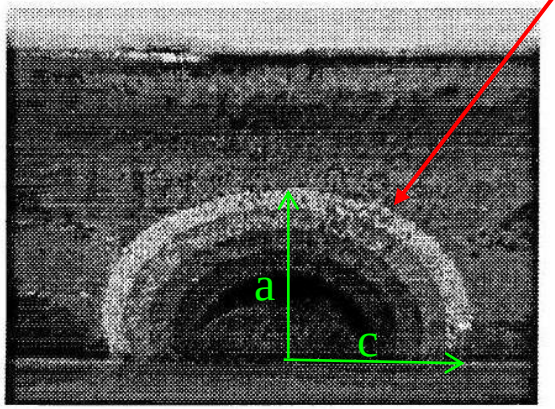

a/c ≈ 1.0

Surface Crack - Tension

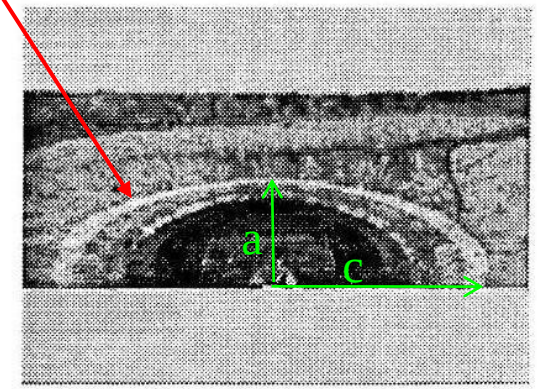

a/c < 1.0

Surface Crack - Bending

Due to thru-thickness stress gradient from unidirectional bending

Ref.: Royce G. Forman, Sambi R. Mettu, **Behavior of Surface and Corner Cracks Subjected to Tensile and Bending Loads in Ti-6A1-4V Alloy**, NASA-TM-102165, September 1990, pp. 27, 32.

NASGRO Demonstration of Part-Thru Crack SIF Solutions ; (cont.)

Test demonstration of the NASGRO LEFM code for a surface crack in a flat plate (bending & tension) is provided below.

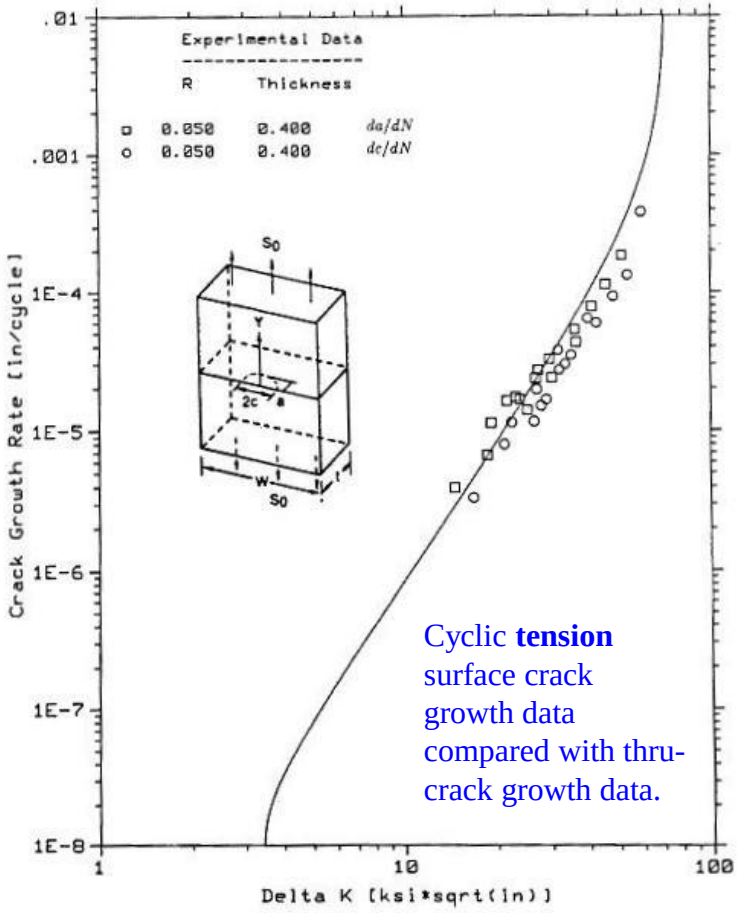

Cyclic **tension** surface crack growth data compared with thru-crack growth data.

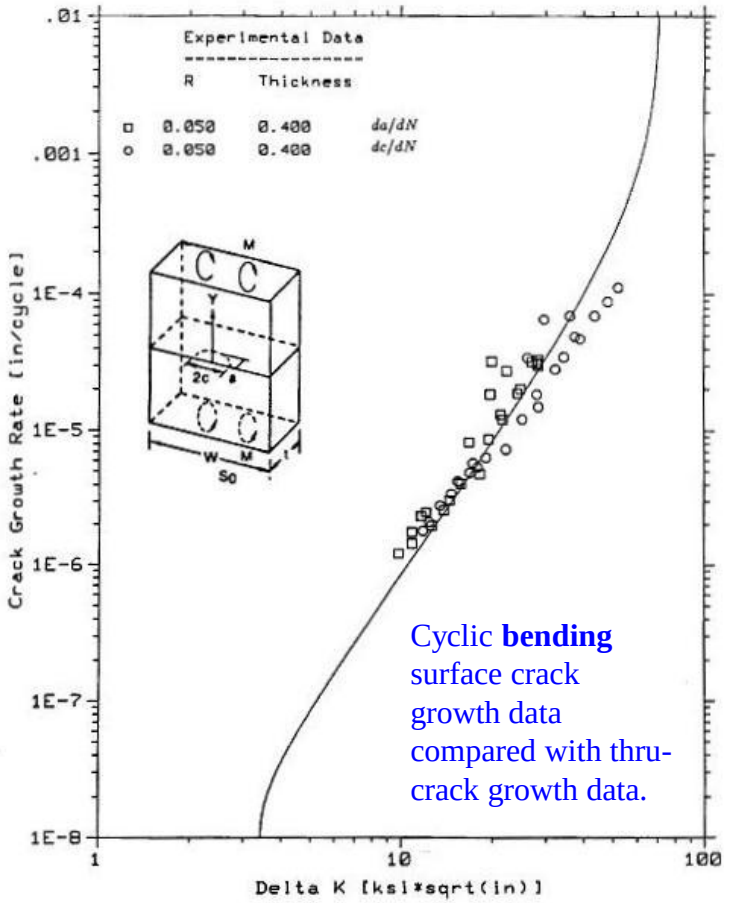

Cyclic **bending** surface crack growth data compared with thru-crack growth data.

Ref.: Royce G. Forman, Sambi R. Mettu, **Behavior of Surface and Corner Cracks Subjected to Tensile and Bending Loads in Ti-6A1-4V Alloy**, NASA-TM-102165, September 1990, pp. 33, 34.

Verification of Part-Thru Crack SIF Solutions w/ Test Data

The stress intensity factor solutions for part thru cracks are determined analytically. A sample verification of the Newman-Raju solution for a corner crack at an open hole is provided below.

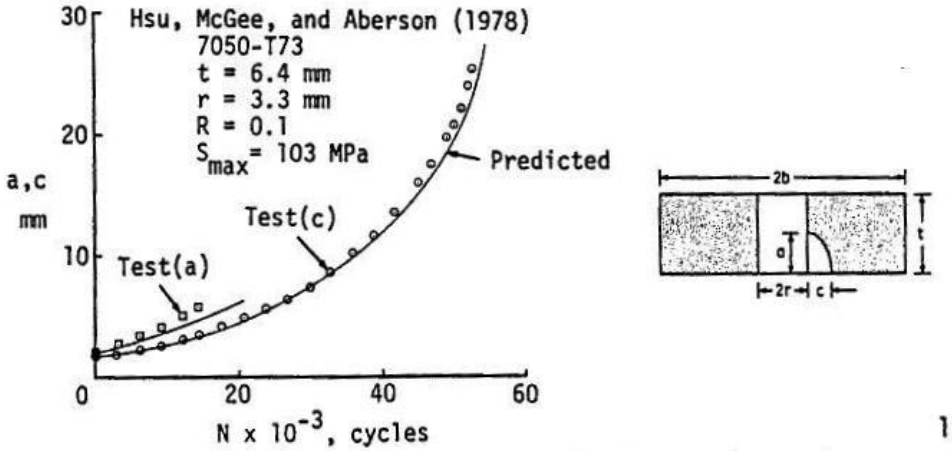

Fig. 12. Experimental and predicted fatigue crack growth for a corner crack at a hole under tension.

a/t > **c/t** due to near constant stress in bore of hole relative to decreasing stress gradient in direction ⊥ to hole axis.

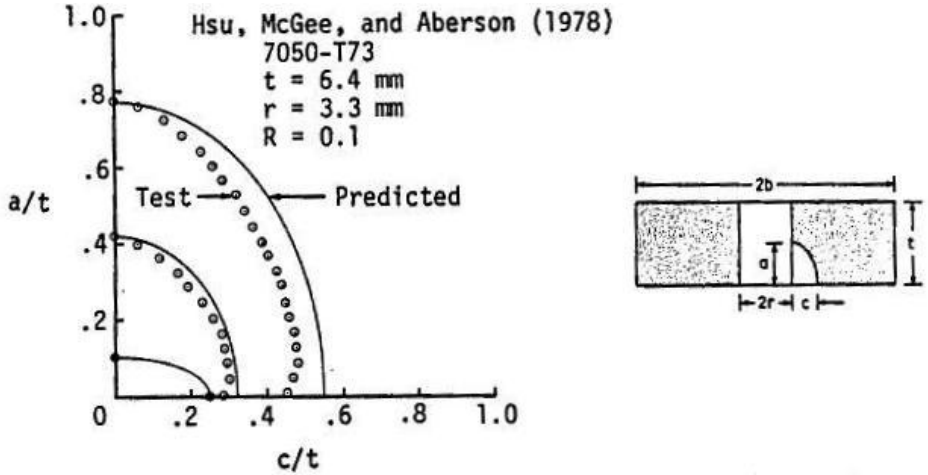

Fig. 11. Experimental and predicted fatigue crack-growth patterns for a corner crack at a hole under tension.

Ref.: J.C. Newman, Jr., I.S. Raju, **Prediction of Fatigue Crack-Growth Patterns and Lives in Three-Dimensional Cracked Bodies**, NASA-TM-85787, April 1984, pg 12.

Fatigue Crack Closure

In the vicinity of the crack tip there is appreciable localized plastic deformation. During the unloading phase of the loading cycle the surrounding elastic volume induces a reverse yielding response that results in a wake of deformed material that acts to close the crack flanks at loads greater that zero.

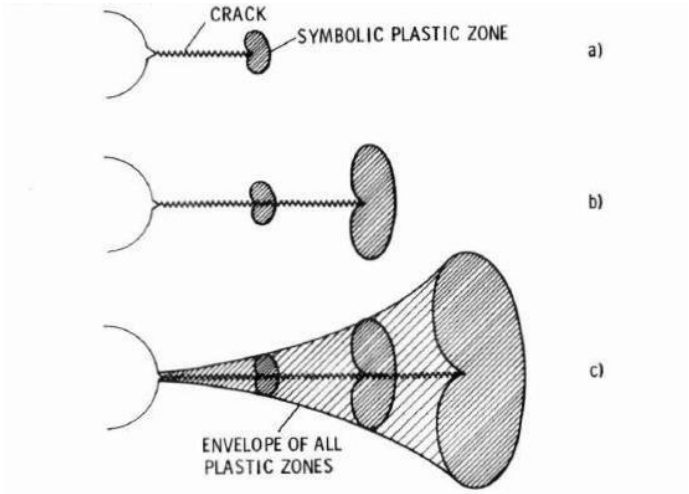

FIG. 1—*Development of a plastic zone envelope around a fatigue crack.*

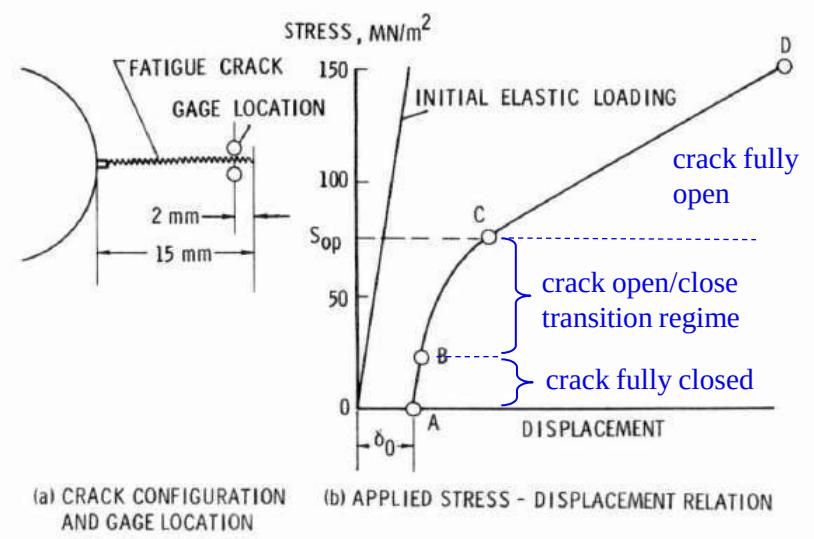

FIG. 5—*Crack configuration and applied stress-displacement relationship.*

Ref.: Elber, Wolf, "**The Significance of Fatigue Crack Closure**", *Damage Tolerance in Aircraft Structures*, *ASTM STP 486*, American Society for Testing and Materials, 1971, pp. 232, 235.

Fatigue Crack Closure ; (cont.)

Within variable amplitude loading fatigue crack closure (mode I) plasticity induced fatigue crack closure accounts for load interaction effects (acceleration/deceleration) on the resulting fatigue crack growth rates. The resulting cyclic capability is very sensitive to the spectrum composition and sequencing.

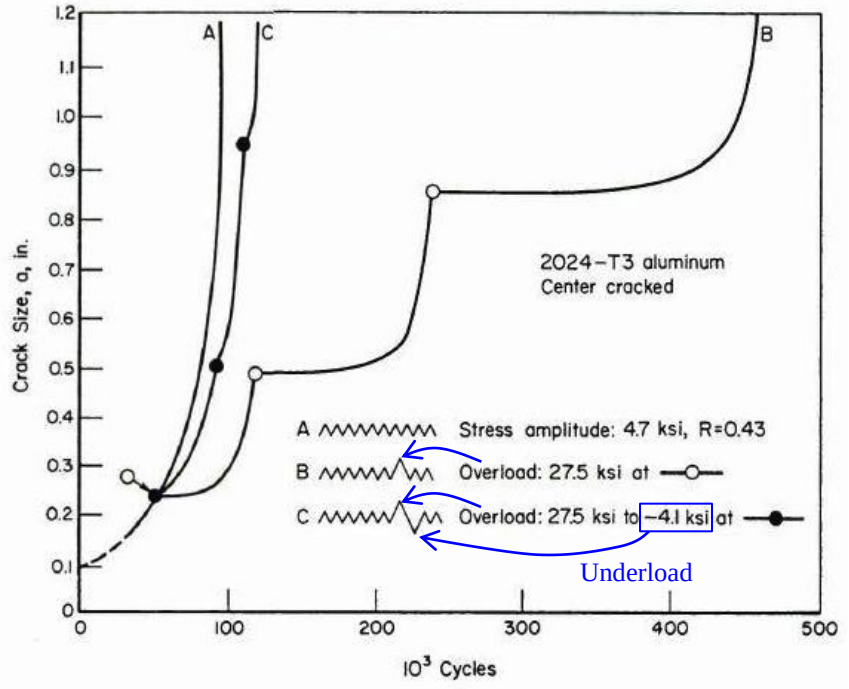

Figure 5.2.1. Retardation Due to Positive Overloads, and Due to Positive-Negative Overload Cycles (Ref. 40).

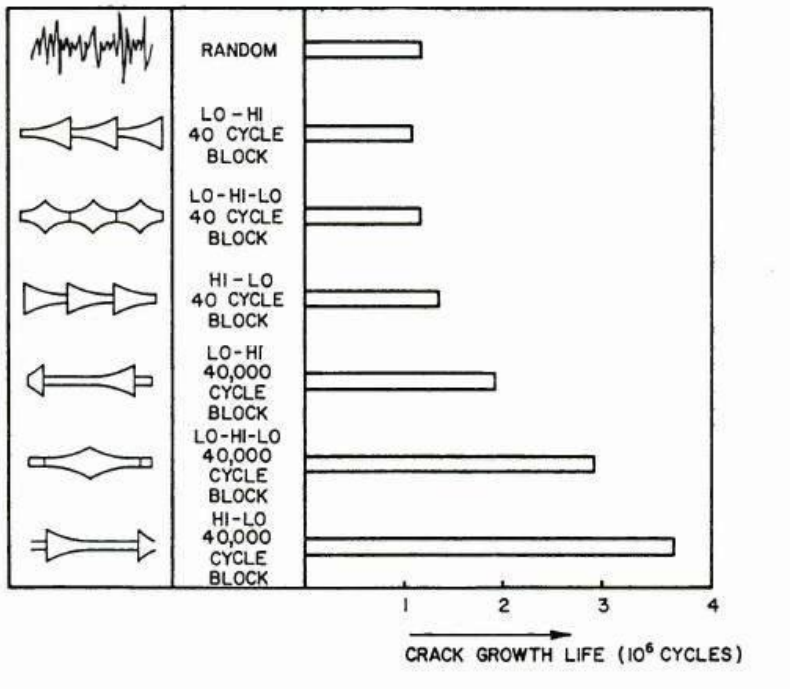

Figure 5.2.5. Effect of Block Programming and Block Size On Crack Growth Life (All Histories Have Same Cycle Content) Alloy: 2024-T3 Aluminum (Ref. 27).

Ref.: Gallagher, Giessler, Berens, Engle, **USAF Damage Tolerant Design Handbook**, AFWAL-TR-82-3073, 1984, pp. 5.2.20, 5.2.24.

Fatigue Crack Closure – Overload/Underload Influences ; (cont.)

The influence of periodic overload fatigue testing and periodic underload testing on the resulting cyclic capability is provided below. It is noted that the results are dependent upon the overload frequency and specimen/notch geometry.

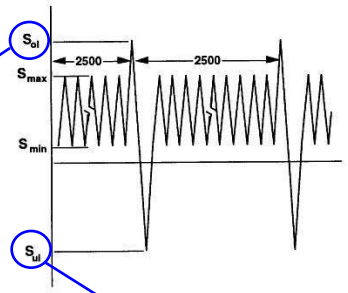

Figure 2 Schematic of overload/underload spectra.

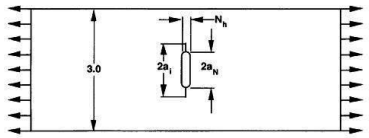

Figure 1 Middle-crack tension specimen with crack starting from notch.

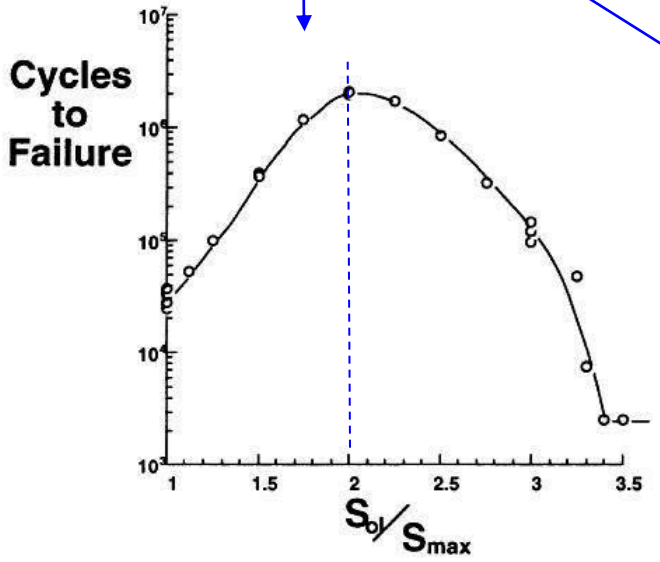

Figure 3 Fatigue test results for the tests conducted with repeated spike overloads (S_{ul} = 0.2 ksi).

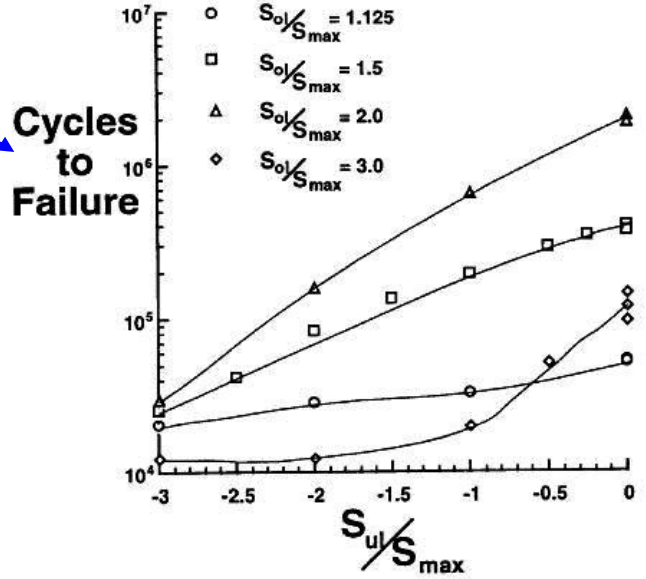

Figure 4 Fatigue test results for the tests conducted with repeated spike overloads followed by spike underloads.

Ref.: David S. Dawicke, **Overload and Underload Effects on the Fatigue Crack Growth Behavior of the 2024-T3 Aluminum Alloy**, NASA-CR-201668, 1997, pp. 4-7.

Fatigue Crack Closure – Overload/Underload Influences ; (cont.)

NASGRO linear damage accumulation (no-interaction) is typically conservative for tensile overload dominated spectra, but can become non-conservative for spectra with appreciable underload events.

TABLE 3. SPECTRUM CYCLES, STRESSES AND INITIAL CRACK SIZES FOR ALL TEST SPECIMENS.

Test ID	Spectrum Cycles	σ_{max} (ksi)	σ_{min} (ksi)	$a_{initial}$ (inch)
TTC-1A	42,290	34.6	-39.7	0.239
TTC-2	42,290	26.2	-26.2	0.166

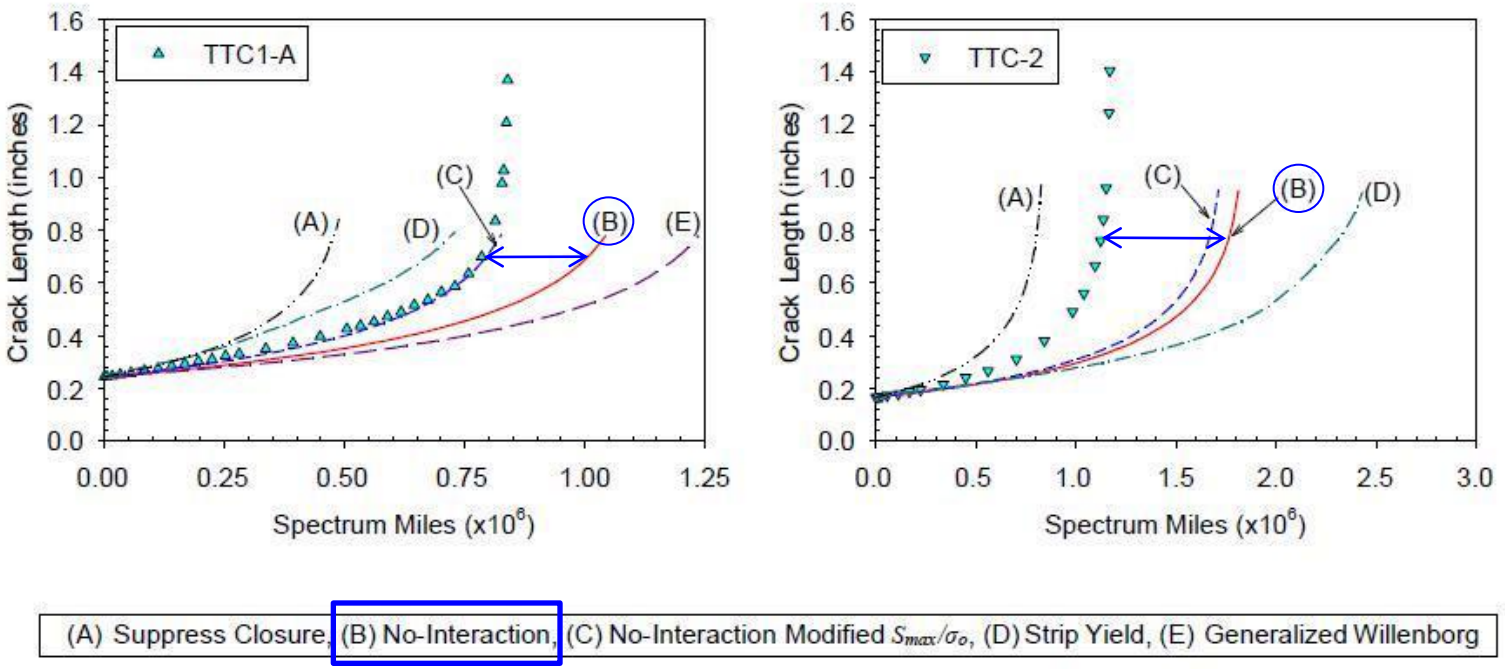

Ref.: Garcia, Feiger, McKeighan, Cardinal, Jeong, **Fatigue Crack Growth Behavior of TC-128-B Steel Under Variable Amplitude Loading**, RTD2001-46007, 2007 ASME Rail Transportation Conference, pp. 8-9.

Fatigue Crack Closure – Block Loading Induced Fatigue Crack Striations; (cont.)

Striations in 2024-T3 aluminum for low-hi-low block loading are presented below.

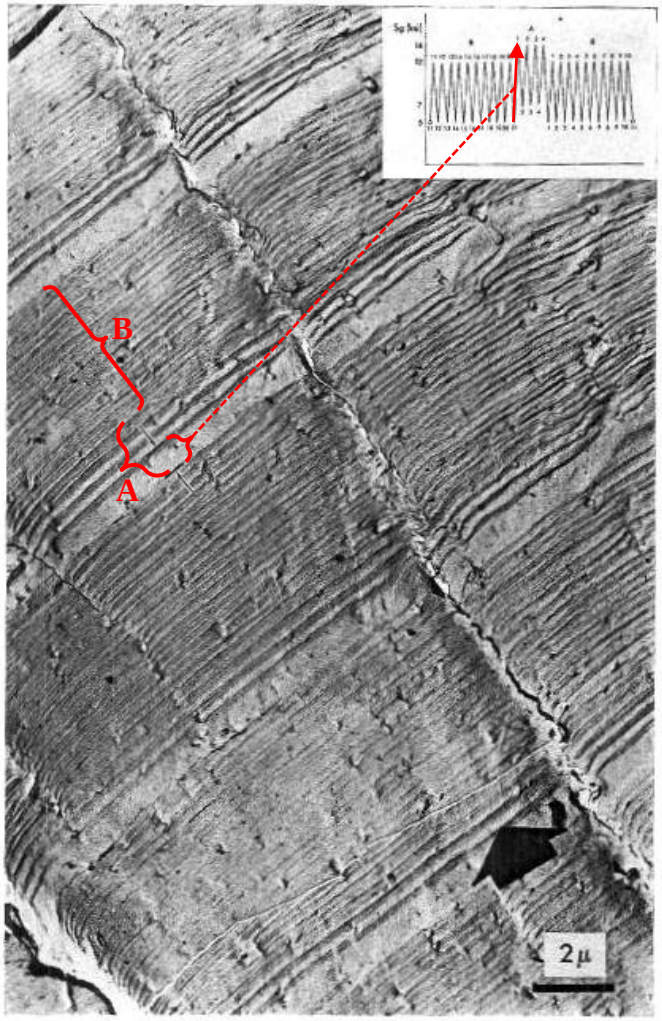

FIG. 6—*Typical fracture surface resulting from Program P11. Note the large striation spacing (marked with small arrows) due to the load amplitude B21-A1 (9000 psi), followed by three large striations corresponding to the load cycles of Spectrum A (2a = 1.7 in.).*

Ref.: J.C. McMillan and R.M.N. Pelloux,, "**Fatigue Crack Propagation Under Program and Random Loads**", *Fatigue Crack Propagation ASTM STP 4815* American Society for Testing and Materials, 1967, pp. 516.

LEFM Limitations

NASGRO incorporates the net section yield failure criterion as a reasonable measure to prevent the LEFM based fracture toughness predictions from being grossly nonconservative in certain applications.

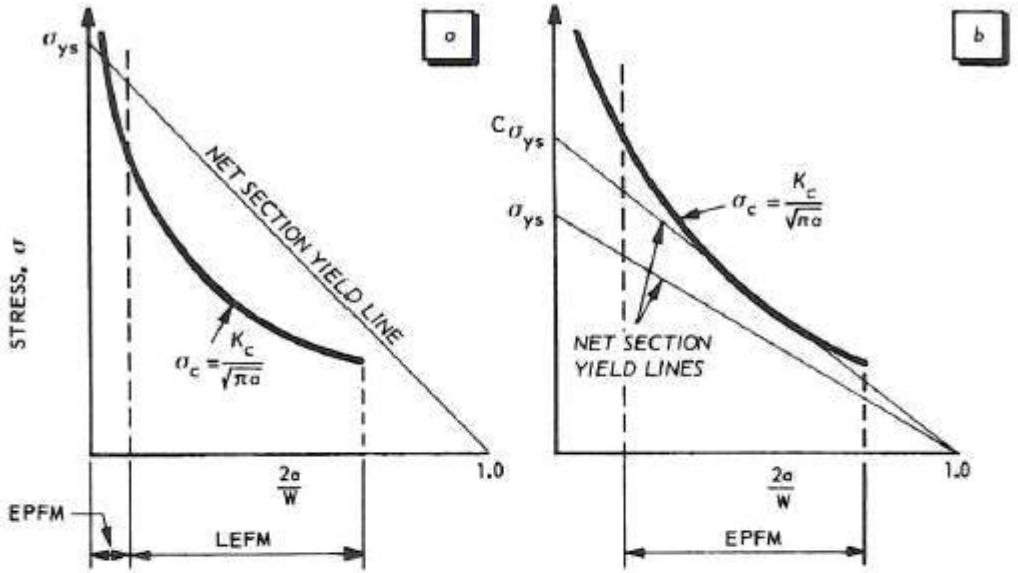

Figure 6.2. Schematic residual strength diagrams for (a) relatively brittle and (b) relatively ductile materials.

Figure 6.2.a gives a schematic residual strength diagram for a relatively brittle material in terms of the dimensionless crack length, 2a/W (W = panel width), of a centre cracked panel. Except for very short cracks the residual strength is determined by the stress intensity factor, since the K_c curve lies well below the line representing net section yield (and hence plasticity induced failure) of the uncracked ligaments. Thus LEFM is applicable for most cases. However, for very short cracks the plastic zone size is no longer relatively small, and EPFM concepts will have to be used.

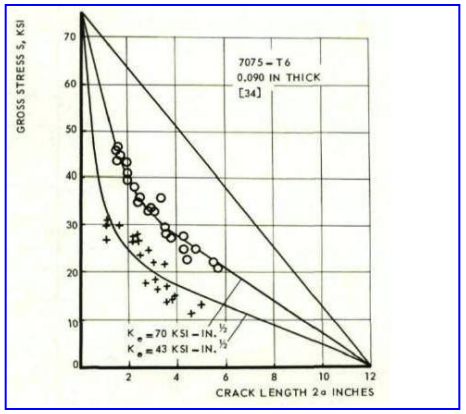

LEFM applicable test data

Ref.: H.L. Ewalds, R.J.H. Wanhill,, **Fracture Mechanics**, Edward Arnold, 1984, pg. 119.

From Safe-Life (S-N fatigue) to Damage Tolerance (Fracture Mechanics) :
The F-111 Wing Pivot Failure

The F-111 was qualified for 4,000 flight hours via full-scale static and fatigue test articles. The sensitivity of the high strength steel to initial defects was known and numerous inspections were performed on critical primary structure. On December 22, 1969 an F-111 with ~100 flight hours crashed due to a wing pivot failure resulting from an undetected forging defect resulting in loss of the crew.

Ref.: **The Surface Crack: Physical Problems and Computational Solutions**, ASME, 1972, pp. 22.

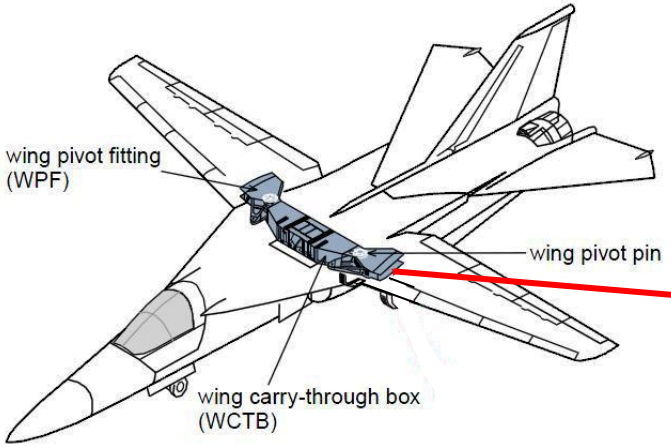

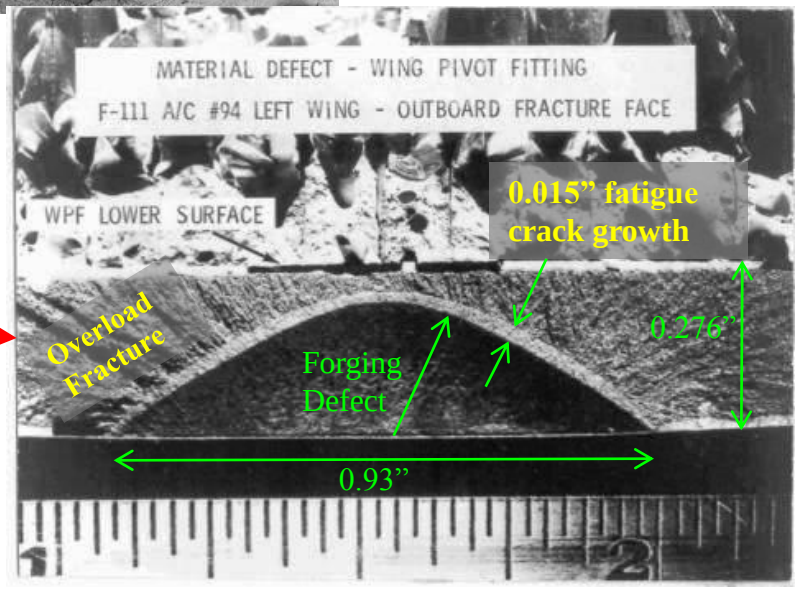

Fatigue Example Problem

iLIDS Latch Hook Service Life Assessment

The international Low Impact Docking System (iLIDS) provides a structural arrangement that allows for visiting vehicles to dock with the International Space Station (ISS).

The docking units are mechanically joined together by a series of 12 sets of active and passive latch hooks.

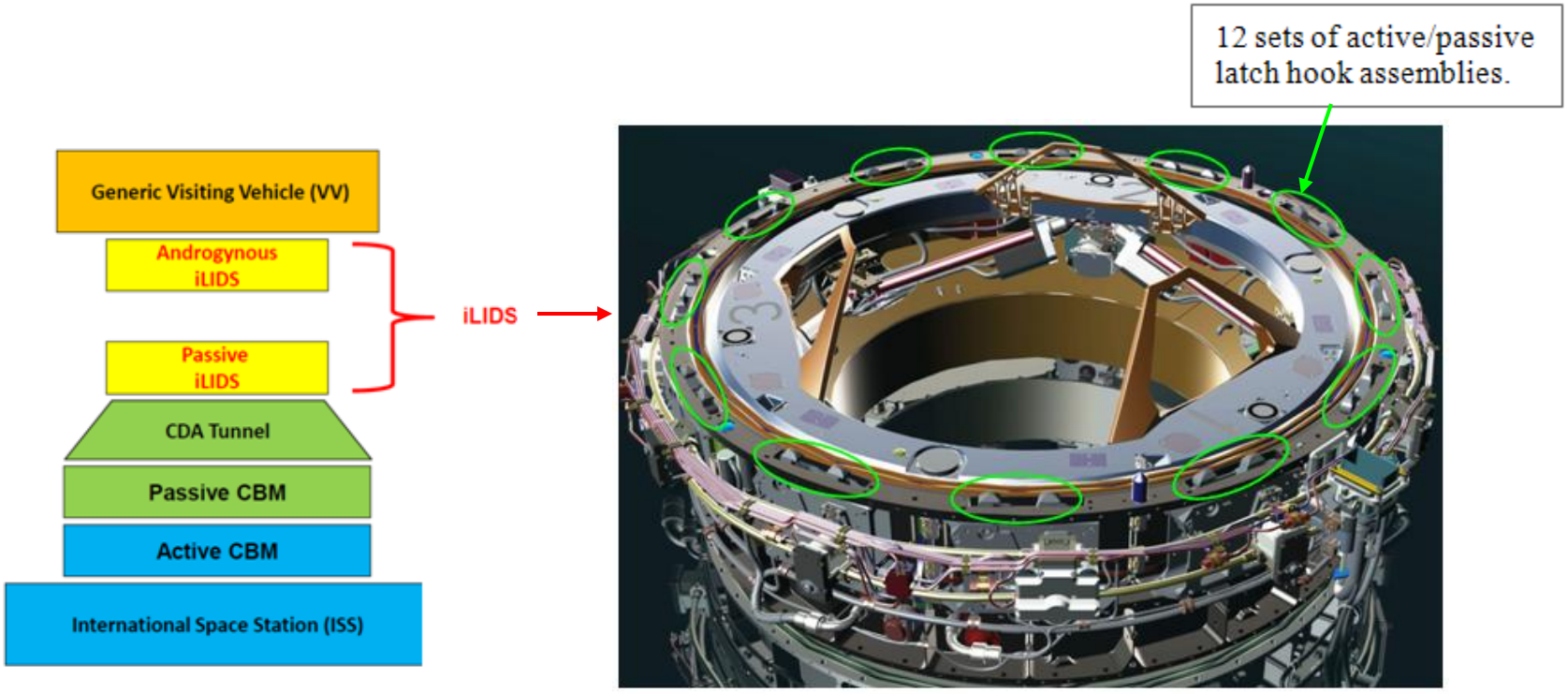

Introduction

In order to preserve docking capability at the existing Russian docking interfaces the iLIDS latch hooks are required to conform to the existing Russian design.

The passive hook is stationary with a series of Bellville springs located on the mounting stem. The Bellville spring compliance allows for the resulting hook loads to be more uniformly distributed throughout the 12 sets of latch hook assemblies. The active hook is driven by a motor that rotates the hook through a small angular displacement followed by an inward translation which allows for engagement and preloading with the passive hook.

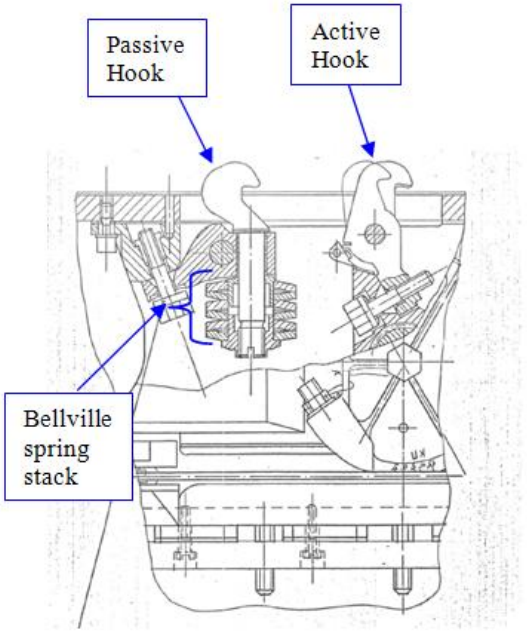

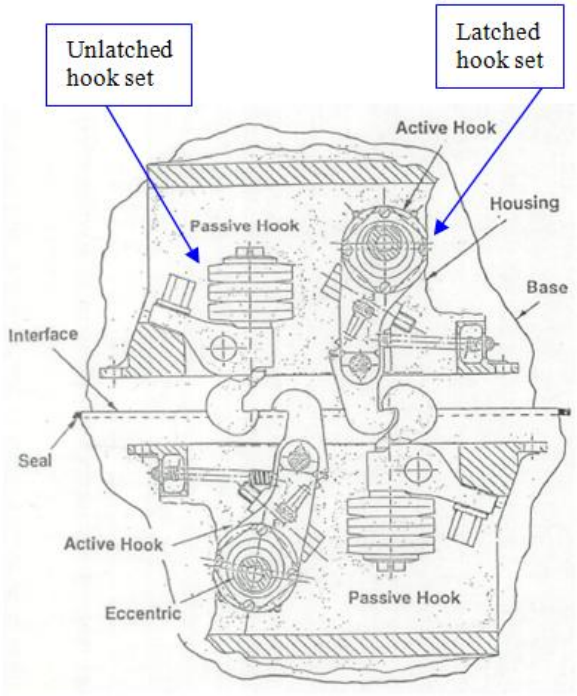

Introduction (cont.)

The latch hooks are classified as ‘fail-safe’ due to the structural redundancy that exists. Since the hooks are not fracture critical (failure does not directly results in a catastrophic event) only a fatigue life demonstration is required via the structures requirements.

A demonstration of the fail-safe capability is provided via the Shuttle/Mir program certification testing wherein static and fatigue testing is performed for 24 engaged hooks and 12 engaged hooks.

CERTIFICATION REQUIREMENTS TEST / ANALYSIS DESCRIPTION

DATE ISSUED 4/29/98 DATE REVISED _____ CR NO. 28-621-0087-6001 CR SERIES NO. 1 PART NO. MC621-0087-6001

Table 10: Structural Integrity Test

	APDS	Hooks Active	Bending Moment	Torsion	Axial	Shear	Cycles
Limit Loading	-6001/-8001	12	6650	6650	500	500	2
	-7001	24	6650	6650	500	500	2
Fatigue Loading	-6001/-8001	12	6650	4000	n/a	n/a	10
			5985	3600			50
			5320	3200			100
			4655	2800			700
			3990	2400			1000
			3325	2000			7000
			2660	1600			40000
			1995	1200			80000
			1330	800			100000
	-6001/-8001	12	4000	6650	n/a	n/a	10
			3600	5985			50
			3200	5320			100
			2800	4655			700
	-6001/-8001	12	1000	1000	n/a	n/a	800000
	-7001	24	7930	4330	n/a	n/a	10
			7137	3897			50
			6344	3464			100
	-7001	24	5090	7630	n/a	n/a	10
			4581	6867			50
			4072	6104			100
Ultimate Loading	-6001/-8001	12	9975	9975	750	750	1
	-7001	24	11900	11450	890	900	1

iLIDS Latch Hook Static Strength Testing

Representative component level static strength testing was performed on the active and passive latch hooks. The design features of the active and passive hooks are consistent with the Russian drawings. The passive hook Bellville spring stack is omitted without any loss in similitude with respect to static strength definition.

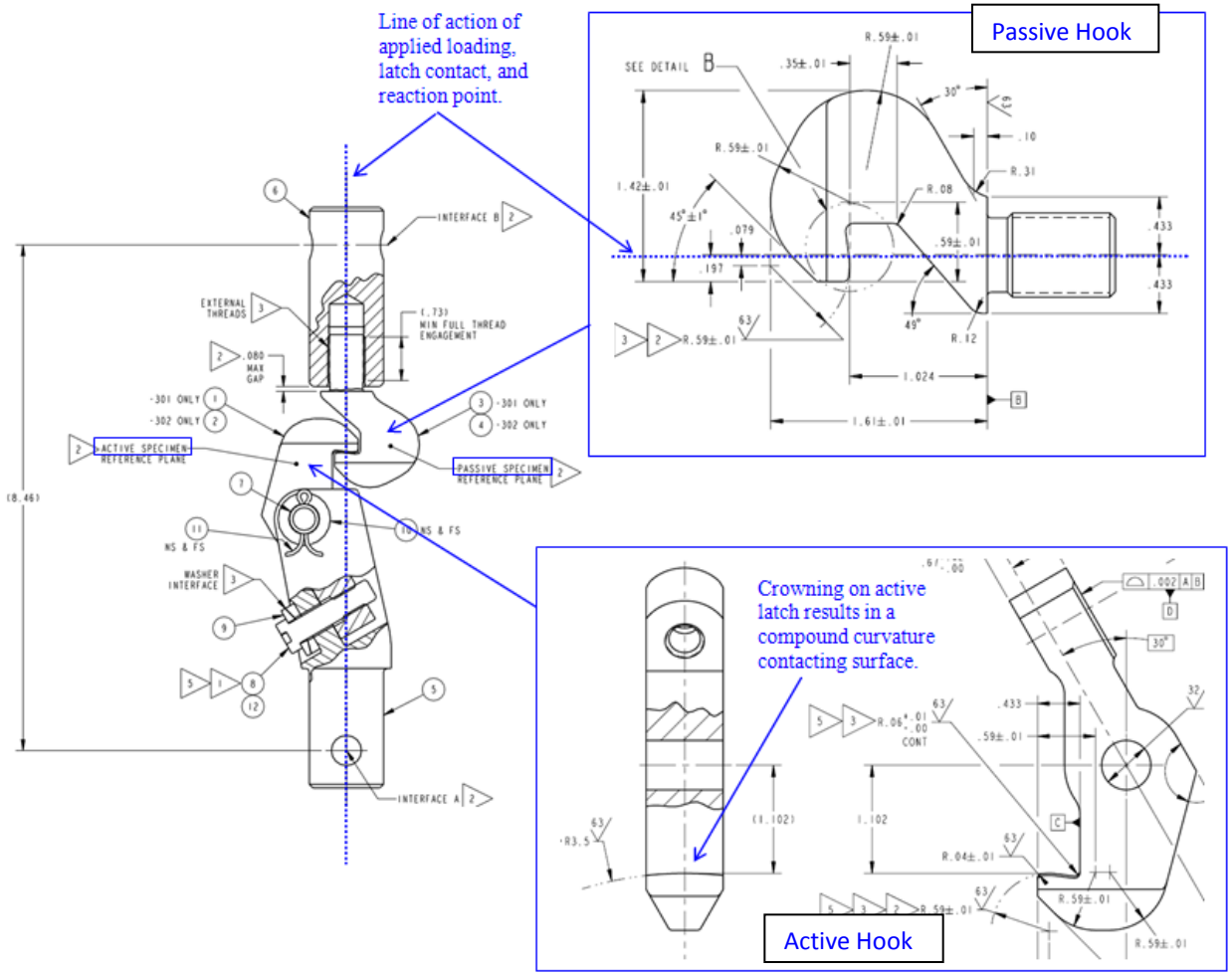

iLIDS Latch Hook Static Strength Testing (cont)

The tensile coupon test data from the two candidate titanium alloys incorporated in the component level static strength testing.

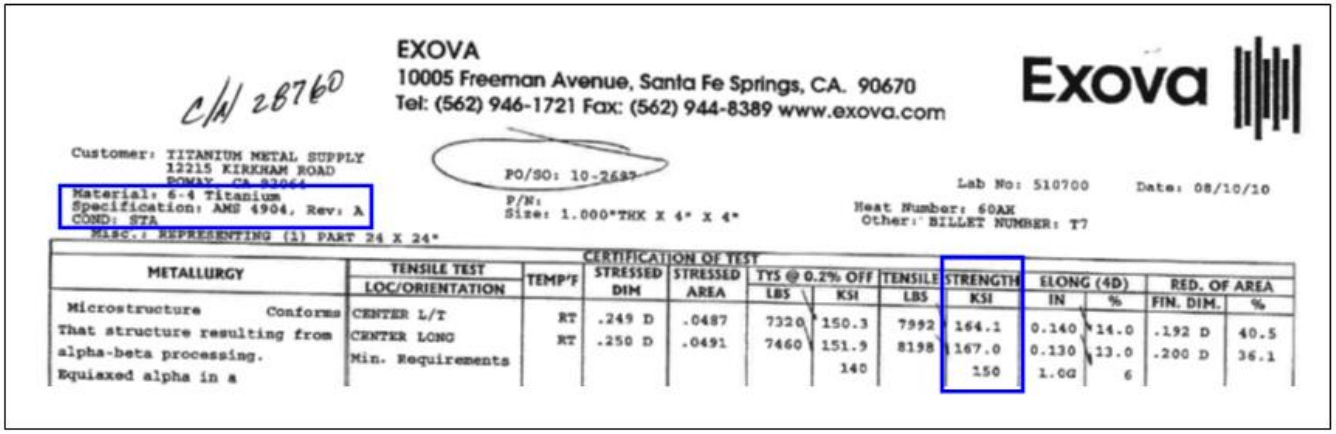

EXOVA
10005 Freeman Avenue, Santa Fe Springs, CA. 90670
Tel: (562) 946-1721 Fax: (562) 944-8389 www.exova.com

C/N 28760

Customer: TITANIUM METAL SUPPLY
12215 KIRKHAM ROAD
POWAY, CA 92064

Material: 6-4 Titanium
Specification: AMS 4904, Rev: A
COND: STA
MISC.: REPRESENTING (1) PART 24 X 24"

PO/SO: 10-2683
P/N:
Size: 1.000"THK X 4" X 4"

Lab No: 510700 Date: 08/10/10
Heat Number: 60AK
Other: BILLET NUMBER: T7

CERTIFICATION OF TEST

METALLURGY	TENSILE TEST LOC/ORIENTATION	TEMP'F	STRESSED DIM	STRESSED AREA	TYS @ 0.2% OFF LBS	TYS @ 0.2% OFF KSI	TENSILE LBS	STRENGTH KSI	ELONG (4D) IN	ELONG (4D) %	RED. OF AREA FIN. DIM.	RED. OF AREA %
Microstructure Conforms	CENTER L/T	RT	.249 D	.0487	7320	150.3	7992	164.1	0.140	14.0	.192 D	40.5
That structure resulting from alpha-beta processing.	CENTER LONG	RT	.250 D	.0491	7460	151.9	8198	167.0	0.130	13.0	.200 D	36.1
Equiaxed alpha in a	Min. Requirements					140		150	1.0G	6		

(a) Ti-6Al-4V STA tensile test coupon data.

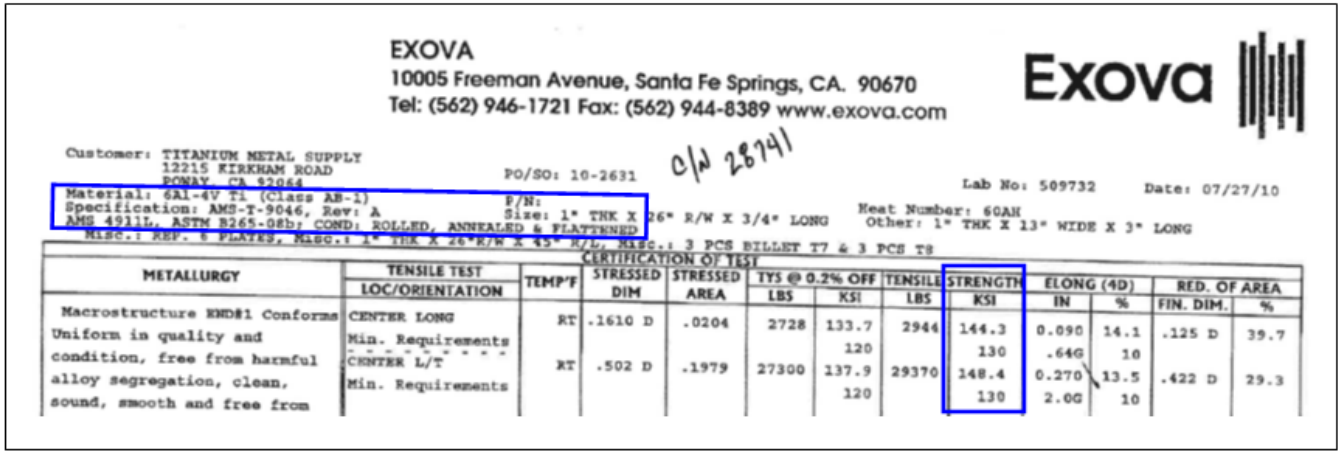

EXOVA
10005 Freeman Avenue, Santa Fe Springs, CA. 90670
Tel: (562) 946-1721 Fax: (562) 944-8389 www.exova.com

C/N 28741

Customer: TITANIUM METAL SUPPLY
12215 KIRKHAM ROAD
POWAY, CA 92064

Material: 6Al-4V Ti (Class AB-1)
Specification: AMS-T-9046, Rev: A
AMS 4911L, ASTM B265-08b; COND: ROLLED, ANNEALED & FLATTENED
MISC.: REF. 6 PLATES, MISC.: 1" THK X 26"R/W X 45" R/L, MISC.: 3 PCS BILLET T7 & 3 PCS T8

PO/SO: 10-2631
P/N:
Size: 1" THK X 26" R/W X 3/4" LONG

Lab No: 509732 Date: 07/27/10
Heat Number: 60AH
Other: 1" THK X 13" WIDE X 3" LONG

CERTIFICATION OF TEST

METALLURGY	TENSILE TEST LOC/ORIENTATION	TEMP'F	STRESSED DIM	STRESSED AREA	TYS @ 0.2% OFF LBS	TYS @ 0.2% OFF KSI	TENSILE LBS	STRENGTH KSI	ELONG (4D) IN	ELONG (4D) %	RED. OF AREA FIN. DIM.	RED. OF AREA %
Macrostructure RND#1 Conforms	CENTER LONG	RT	.1610 D	.0204	2728	133.7	2944	144.3	0.090	14.1	.125 D	39.7
Uniform in quality and	Min. Requirements					120		130	.64G	10		
condition, free from harmful	CENTER L/T	RT	.502 D	.1979	27300	137.9	29370	148.4	0.270	13.5	.422 D	29.3
alloy segregation, clean,	Min. Requirements					120		130	2.0G	10		
sound, smooth and free from												

(b) Ti-6Al-4V annealed tensile test coupon data.

iLIDS Latch Hook Static Strength Testing (cont)

The static strength testing was performed at 3 different temperatures in each of the 2 material candidates.

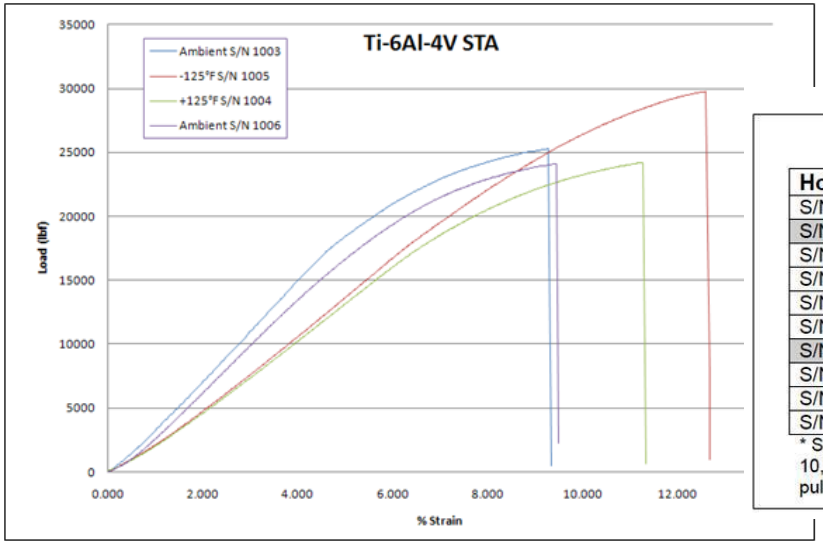

Table 1 – Test Data Summary

Hook Set	Material	Environment	~ Yield load	Failure load	Failed Hook Unit
S/N 1001	Ti- 6Al-4V Annealed	Ambient	12,000 lbs *	23201.123 lbs	Passive
S/N 1002	Ti- 6Al-4V Annealed	Not tested			
S/N 1003	Ti- 6Al-4V STA	Ambient	17,000 lbs	25283.569 lbs	Active
S/N 1004	Ti- 6Al-4V STA	+125°F	18,000 lbs	24177.721 lbs	Active
S/N 1005	Ti- 6Al-4V STA	-125°F	23,000 lbs	29786.550 lbs	Active
S/N 1006	Ti- 6Al-4V STA	Ambient	17,500 lbs	24091.402 lbs	Passive
S/N 1007	Ti- 6Al-4V STA	Not tested			
S/N 1008	Ti- 6Al-4V Annealed	-125°F	21,000 lbs	27445.407 lbs	Active
S/N 1009	Ti- 6Al-4V Annealed	+125°F	17,000 lbs	22756.365 lbs	Active
S/N 1010	Ti- 6Al-4V Annealed	Ambient	14,000 lbs	23229.771 lbs	Active

* Specimen was pulled 10 times with increasing loads with yielding being evident as low as perhaps 10,000 lbs. The resulting strain hardening of the specimen provides an artificially high yield point in the pull to failure curve, and finding a distinct yield point from the lower load curves is quite challenging.

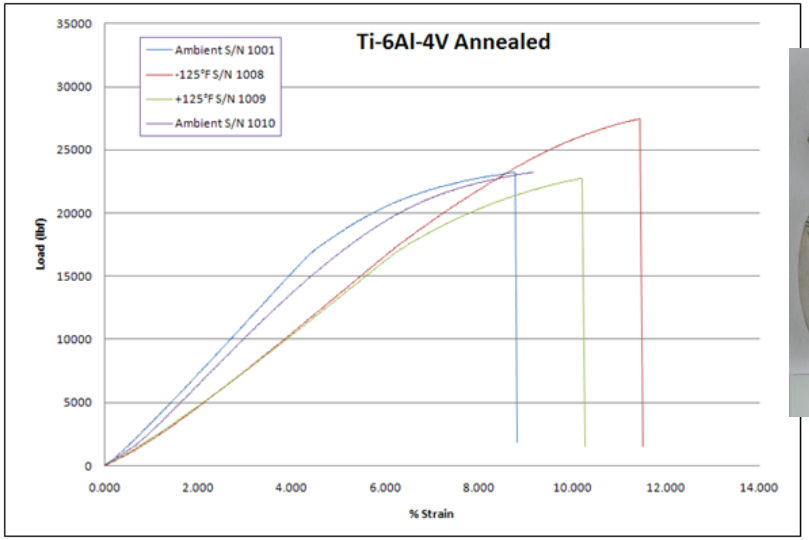

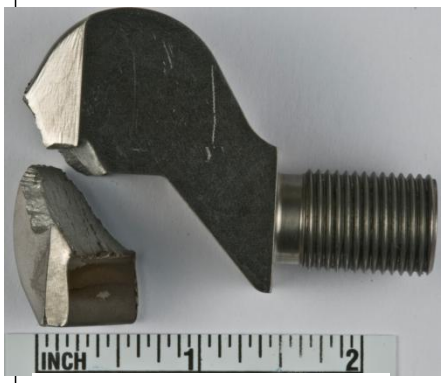

Passive latch hook static load failure location at the hook ledge transition radius.

Active latch hook static load failure location at the hook ledge transition radius.

2D Active/Passive Hook Linear Elastic Stress Result

The stress gradient in the passive and active hooks are defined with 2D models and a unit point load along the test fixture defined line of action.

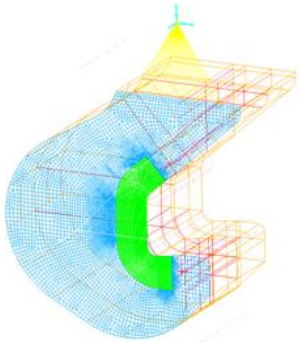

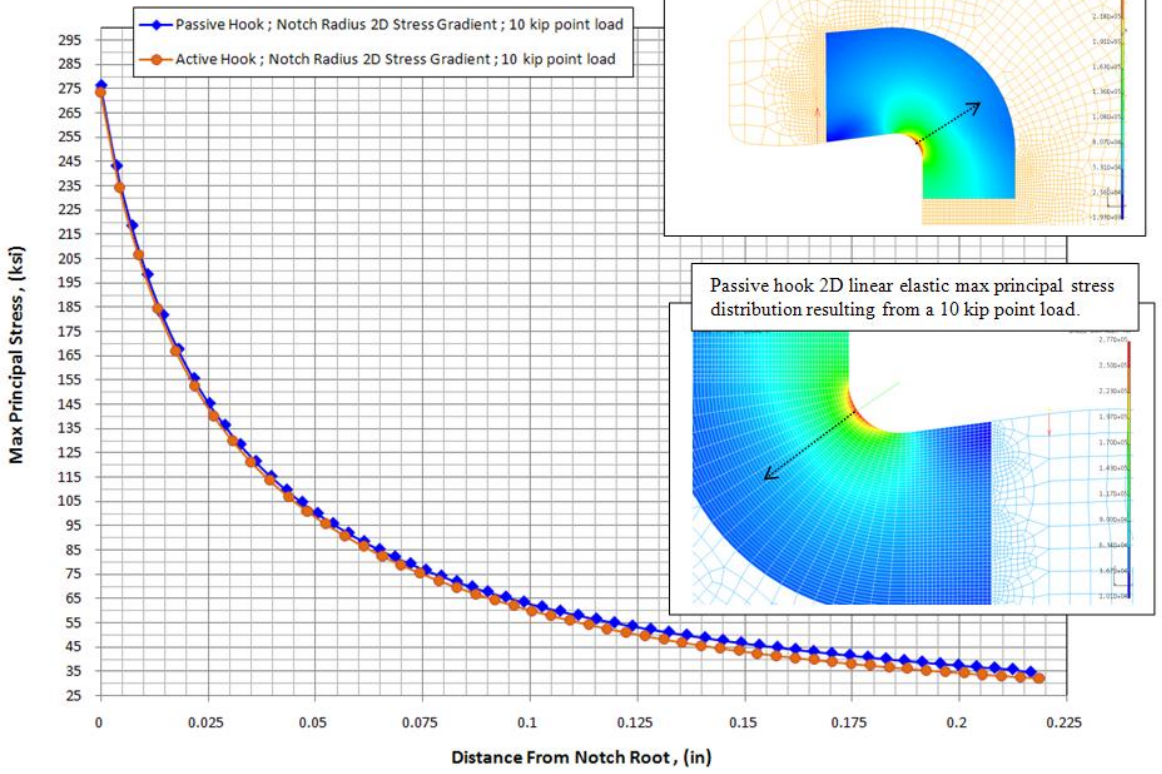

2D FEM Failure Load Prediction (Passive Hook)

The annealed titanium data is utilized since a representative lower bound correlation is desired for some measure of added conservatism in the resulting service life projections. An elastic-perfectly plastic material response is assumed (tensile test σ-ε curve not provided). A flow stress of 140 ksi (average of yield and ultimate stress) defines the material nonlinear response.

PO/SO: 10-2631 Lab No: 509732 Date: 07/27/10

P/N:
Size: 1" THK X 26" R/W X 3/4" LONG
Heat Number: 60AH
Other: 1" THK X 13" WIDE X 3" LONG

ND: ROLLED, ANNEALED & FLATTENED
.: 1" THK X 26"R/W X 45" R/L, Misc.: 3 PCS BILLET T7 & 3 PCS T8

CERTIFICATION OF TEST

TENSILE TEST LOC/ORIENTATION	TEMP'F	STRESSED DIM	STRESSED AREA	TYS @ 0.2% OFF LBS	TYS @ 0.2% OFF KSI	TENSILE STRENGTH LBS	TENSILE STRENGTH KSI	ELONG (4D) IN	ELONG (4D) %	RED. OF AREA FIN. DIM.	RED. OF AREA %
CENTER LONG	RT	.1610 D	.0204	2728	133.7	2944	144.3	0.090	14.1	.125 D	39.7
Min. Requirements					120		130	.64G	10		
CENTER L/T	RT	.502 D	.1979	27300	137.9	29370	148.4	0.270	13.5	.422 D	29.3
Min. Requirements					120		130	2.0G	10		

$\sigma_{flow} = (133.7+144.3) / 2 = 139.0$ ksi

$\sigma_{flow} = (137.9+148.4) / 2 = 143.2$ ksi

$\sigma_{flow} \approx 140$ ksi

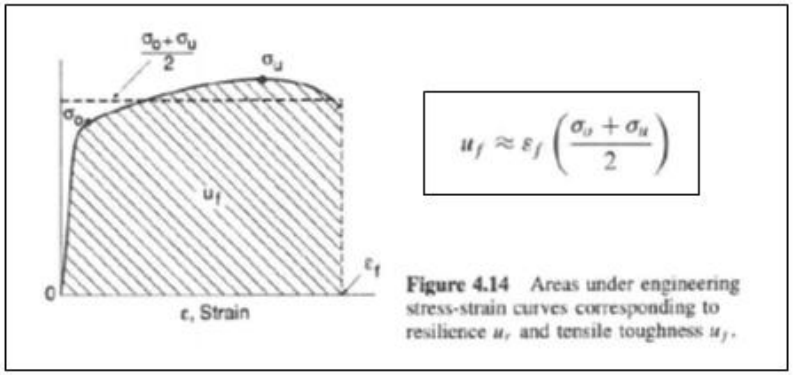

$$u_f \approx \varepsilon_f \left(\frac{\sigma_o + \sigma_u}{2} \right)$$

Figure 4.14 Areas under engineering stress-strain curves corresponding to resilience u_r and tensile toughness u_f.

2D FEM Failure Load Prediction (Passive Hook) – (cont)

The latch hook structural response results in localized yielding encapsulated by a large elastic volume. The localized nonlinear response results in the strain concentration increasing with increasing loading beyond yield. Based upon this response (as opposed to a net-section collapse) the failure criterion utilized in this assessment is a strain to failure exceedance. The longitudinal direction elongation for annealed titanium in the MIL-Handbook is on the order of 10%, and the while the tensile coupons demonstrate elongation values on the order of 14%. A failure load range will be established by quantifying the load levels required to exceed strain levels of 0.1 and 0.14.

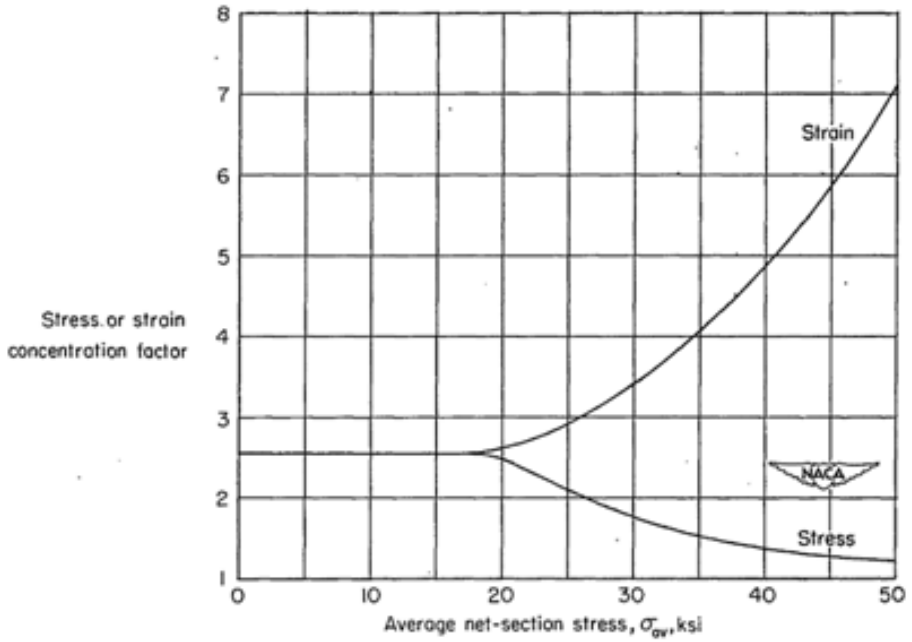

Figure 5.– Stress and strain concentration factors for first load cycle.

2D FEM Failure Load Prediction (Passive Hook) – (cont)

The passive hook material nonlinear stress and strain responses for various hook load magnitudes defines a failure load range of 19 kip to 21 kip.

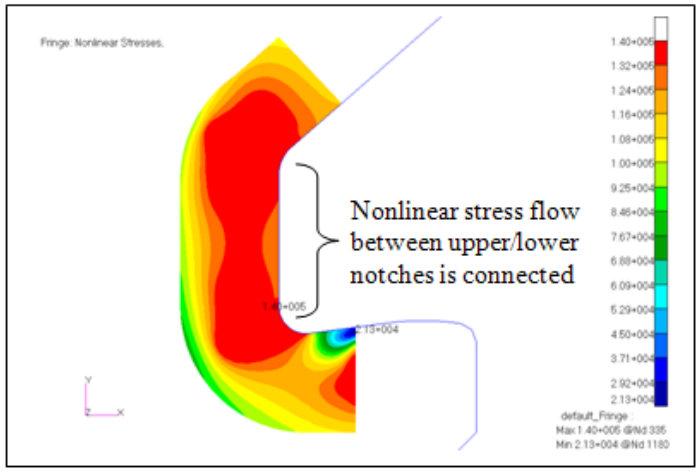

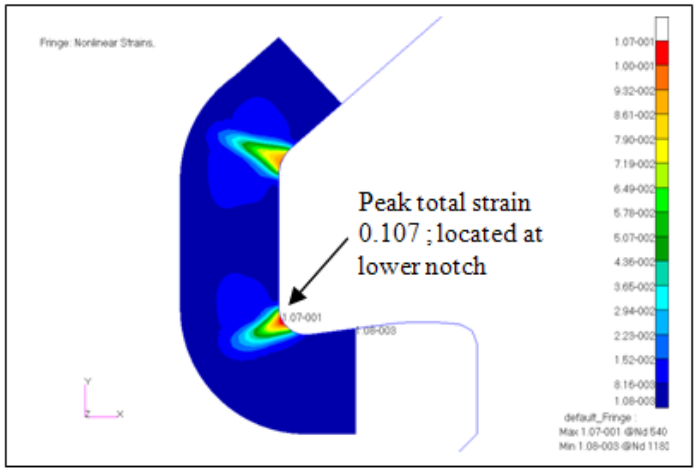

19 kip hook load induces a strain response of 0.107 constitutes failure as per the MIL-HNDBK strain to failure result of 0.1

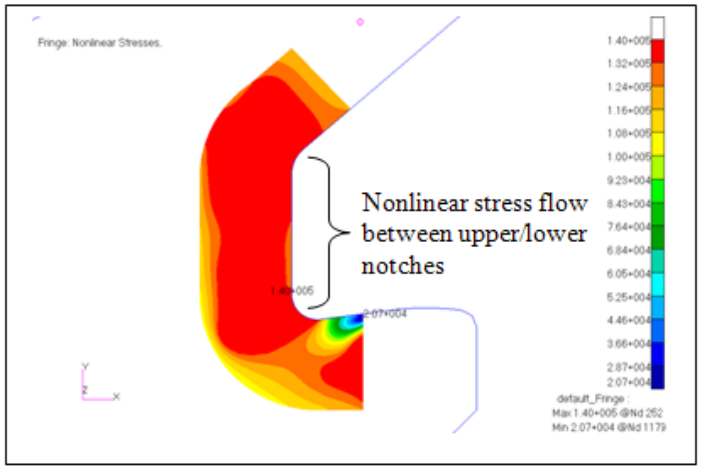

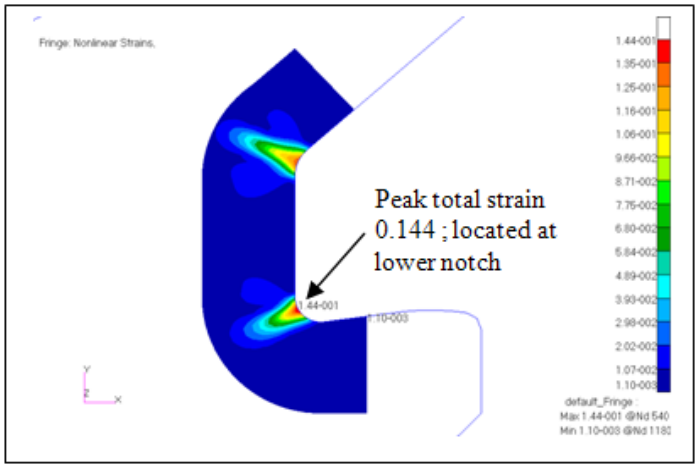

21 kip hook load induces a strain response of 0.144 constitutes failure as per the tensile coupon test data result of 0.14

2D Failure Load Prediction (Active Hook)

The active hook analytical failure load projection methodology will duplicate what was incorporated for the passive hook. The analytical failure criterion will be a strain to failure exceedance at strain levels of 0.1 and 0.14 ; the 19 and 21 kip total strain responses of 0.105 and 0.141 define the analytical failure load range as per the established failure criterion – identical to the passive hook analytical result.

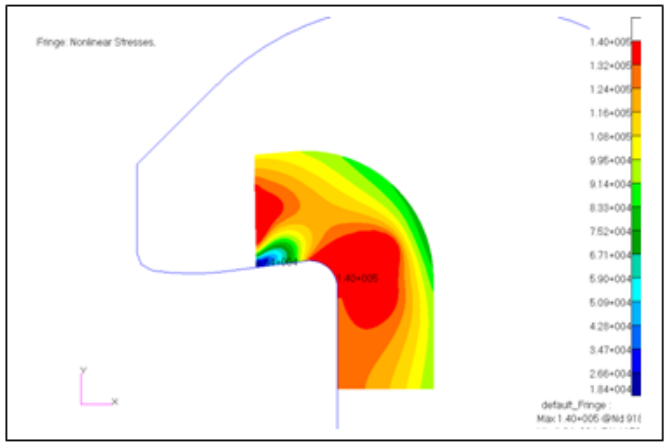

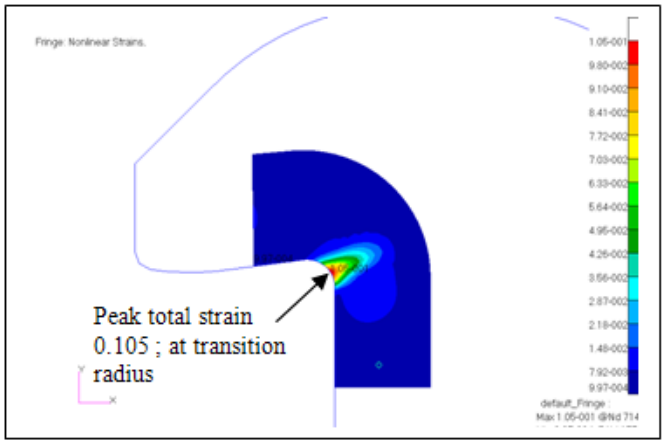

19 kip hook load induces a strain response of 0.105 constitutes failure as per the MIL-HNDBK strain to failure result of 0.1

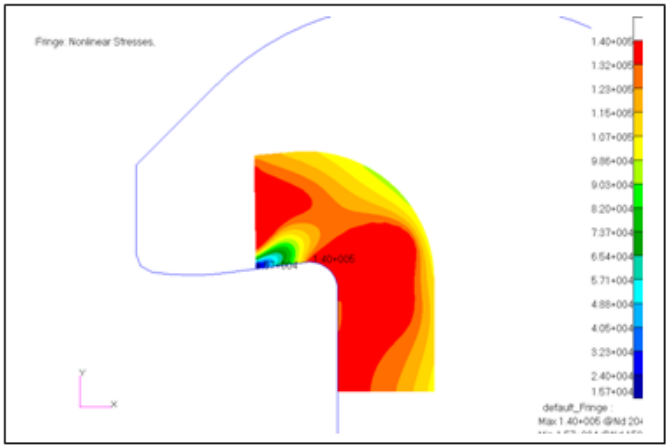

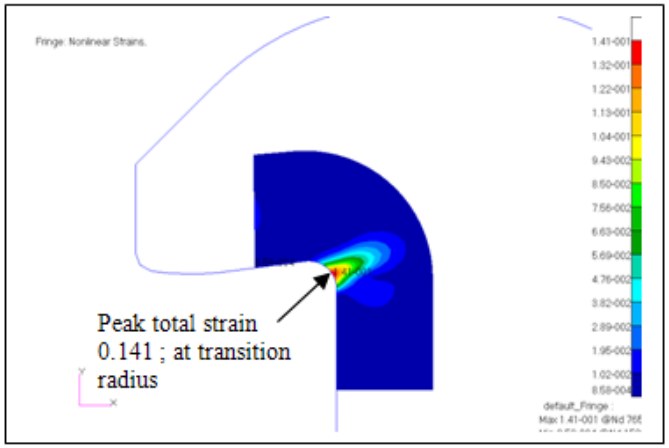

21 kip hook load induces a strain response of 0.141 constitutes failure as per the tensile coupon test data.

2D FEM Active/Passive Hook Stiffness Results

The active hook 2D FEM analytical stiffness response for the linear and nonlinear material responses is computed and compared with passive hook 2D stiffness result. The analysis results demonstrate that the active hook is less stiff than the passive hook and that the active hook demonstrates less nonlinear deviation from the linear elastic projection than the passive hook.

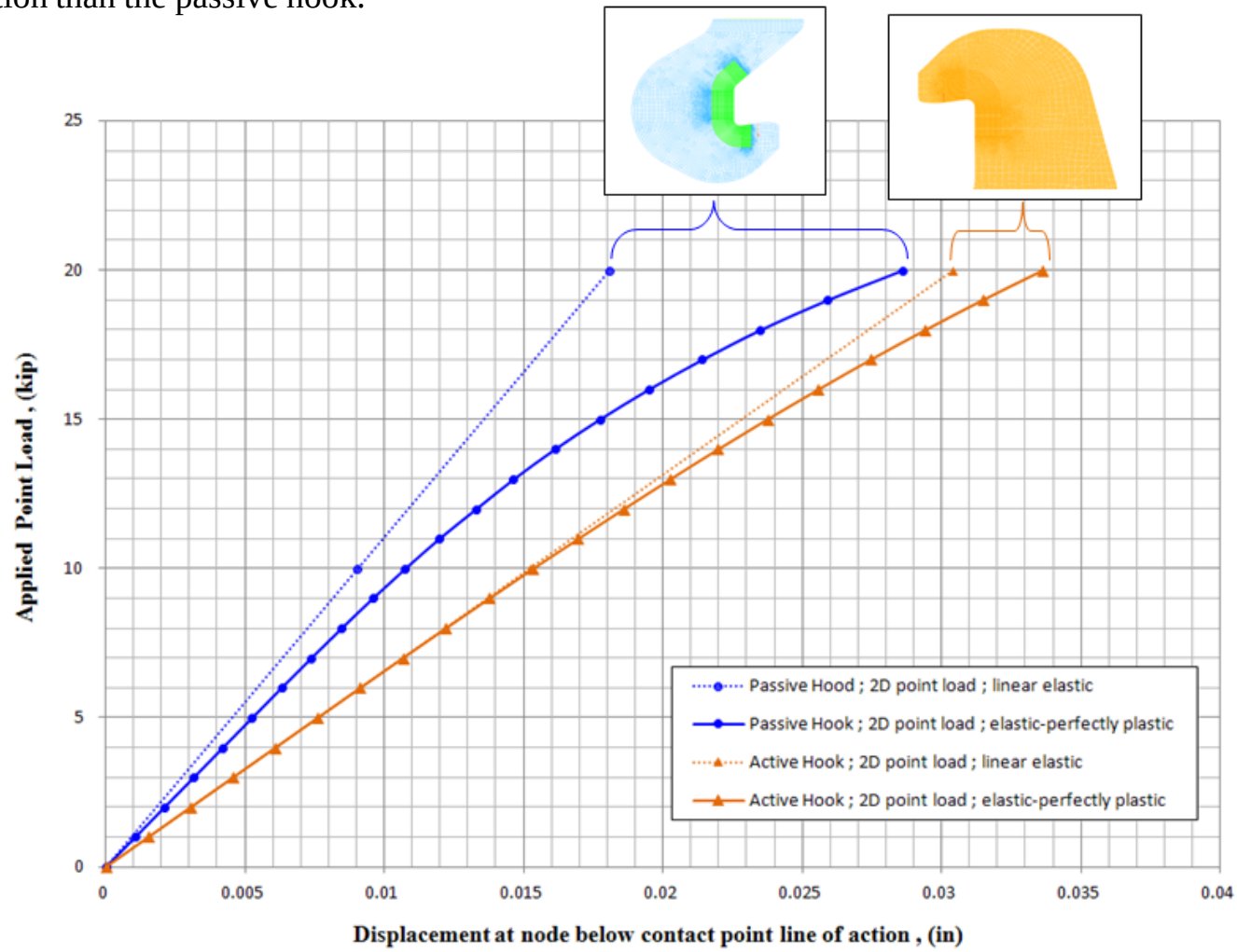

3D Linear Elastic FEM (Active/Passive Hooks Engaged)

The active/passive hook geometry 3D finite element model incorporates a vertical plane of symmetry to reduce the overall model size and computational effort. Only the upper portion of the active hook is modeled and the required reaction constraints are applied to the model defined sectioning plane. A 10,000 pound unit load (5,000 within the model due to symmetry) is applied to the passive hook along the test defined line of action. Contact definition between the active and passive hooks is also incorporated.

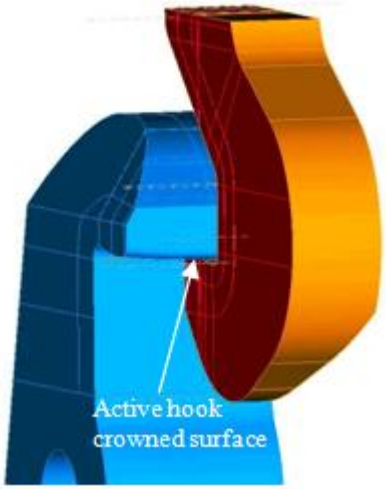

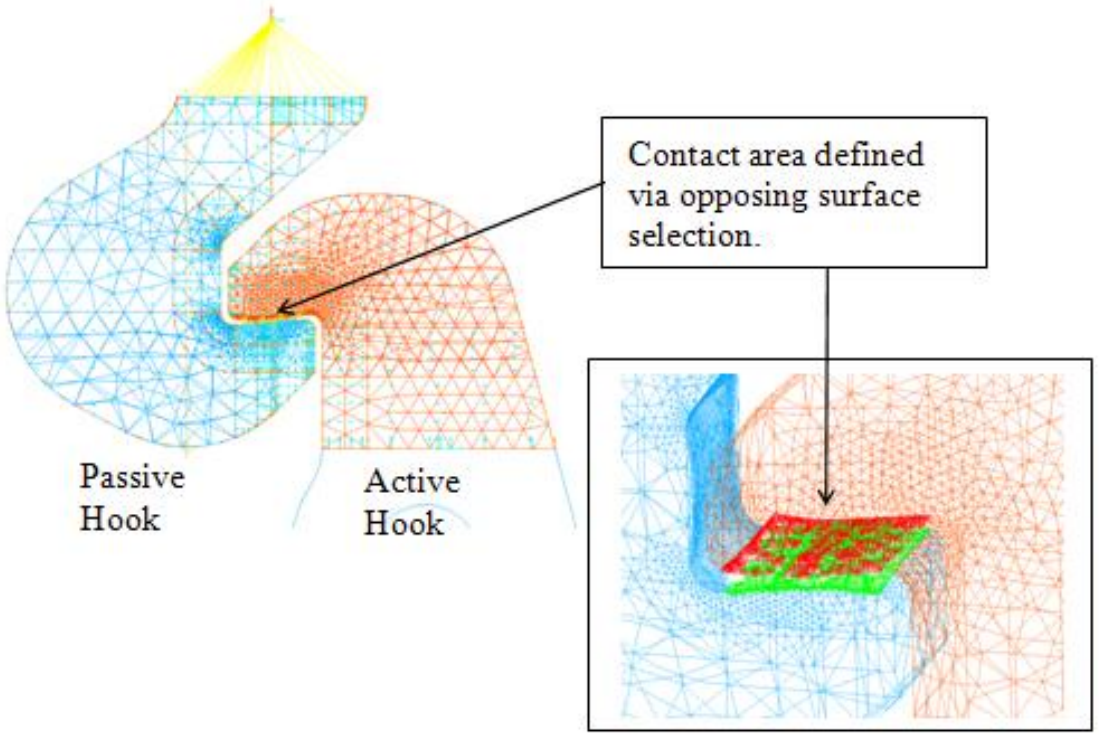

3D Linear Elastic FEM (Active/Passive Hooks Engaged) – (cont)

Passive hook maximum principal stress contour plots (outside surface and mid-plane views) for a 10 kip applied load are provided below (IDEAS solver & linear elastic material response). The peak linear elastic stress of 395 ksi occurs at the mid-plane of the section in the transition radius adjacent to the hook shelf. The peak linear elastic stress at the upper transition radius is on the order of 225 ksi, and the peak stress on the outer surface is on the order of 197 ksi (approximately half of the mid-plane value).

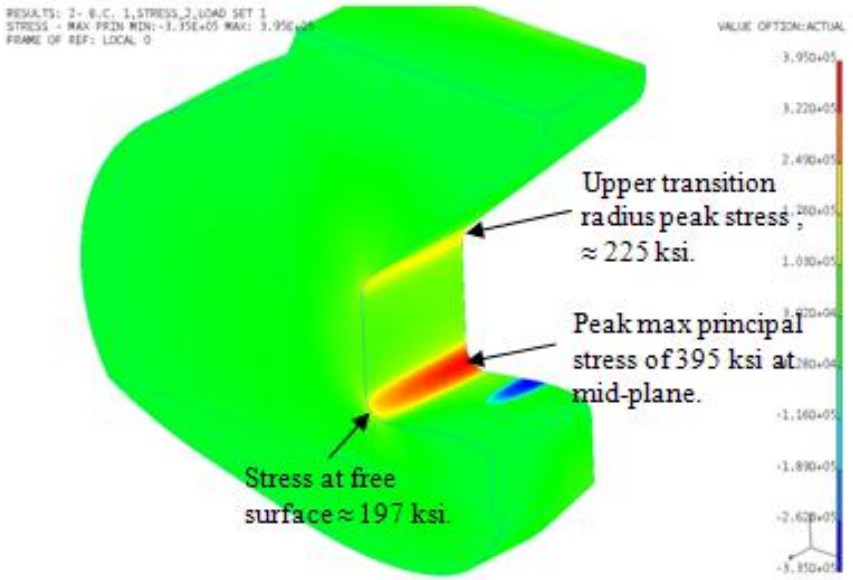

Passive Hook - Outside surface view.

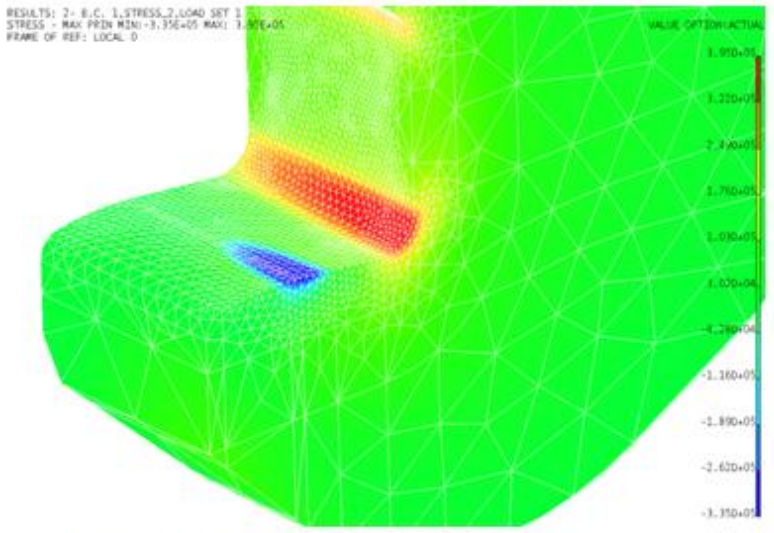

Passive Hook - Mid-plane surface view.

3D Linear Elastic FEM (Active/Passive Hooks Engaged) – (cont)

Active hook maximum principal stress contour plots (outside surface and mid-plane views) for a 10 kip applied load are provided below (IDEAS solver & linear elastic material). The peak linear elastic stress of 414 ksi occurs at the mid-plane of the section in the transition radius adjacent to the hook shelf. The peak stress on the outer surface is on the order of 178 ksi.

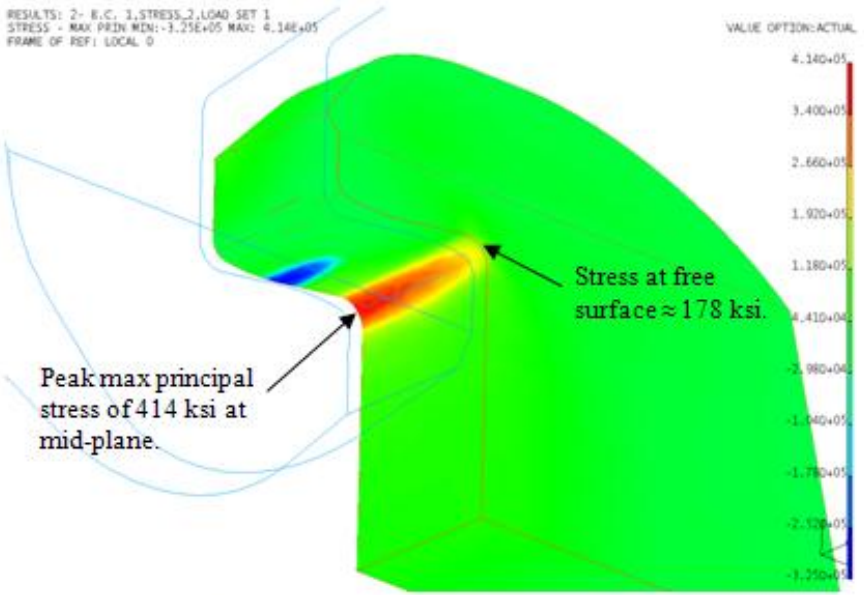

Active Hook - Outside surface view.

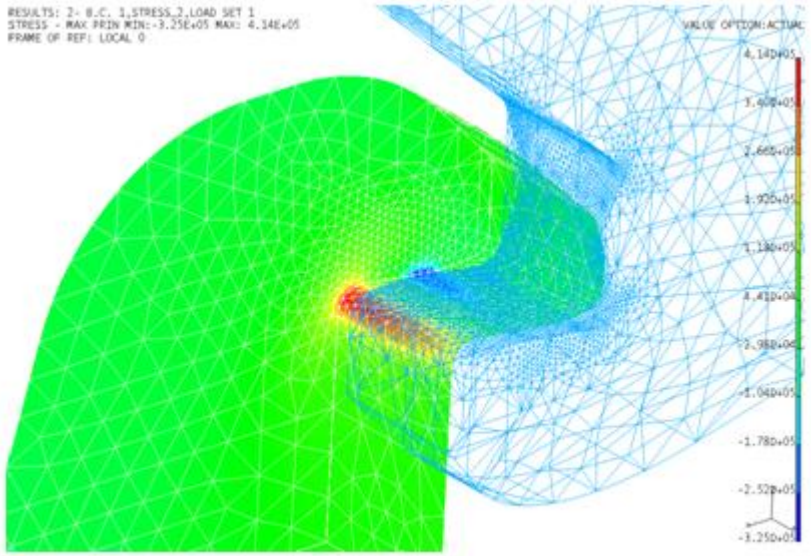

Active Hook - Mid-plane surface view.

3D Linear Elastic FEM (Active/Passive Hooks Engaged) – (cont)

A contour plot of the passive and active hook analytical contact pressure distribution (IDEAS solver, 10 kip loading, and linear elastic material response) is provided below along with the contact witness marks on failed passive hooks from static testing. The analysis demonstrates a similar contact location and distribution pattern.

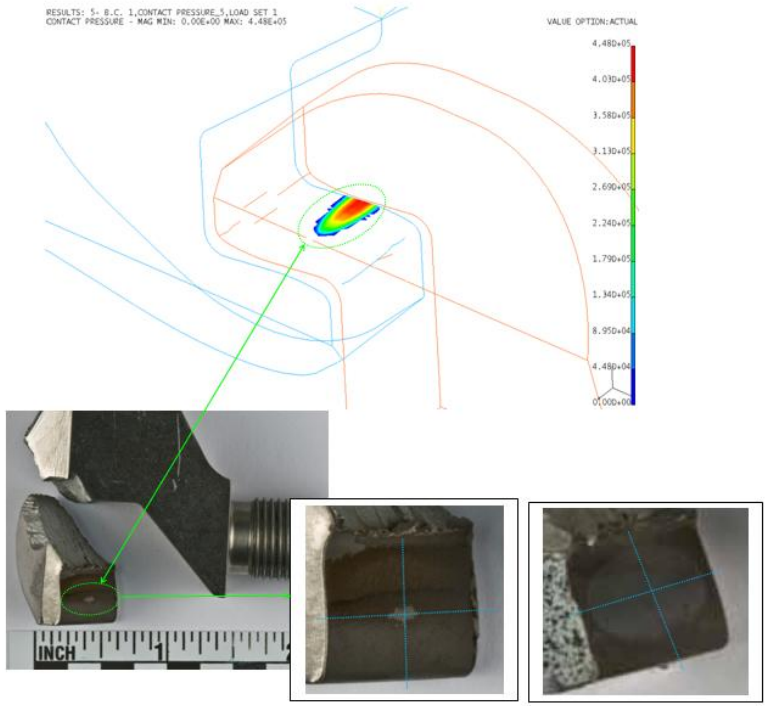

passive hook

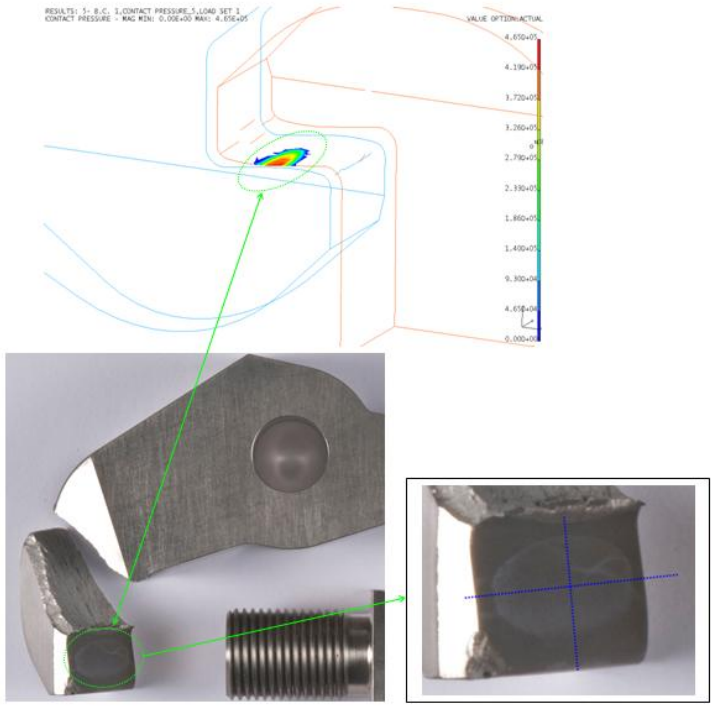

active hook

2D/3D FEM Analytical Failure Load Prediction

Based upon a strain-to-failure exceedance for 10 and 14% elongation values the analytical failure load prediction via the 2D and 3D models failure loads ranged from 19 to 21 kips (23 to 25 kips is the ambient temp static strength test result).

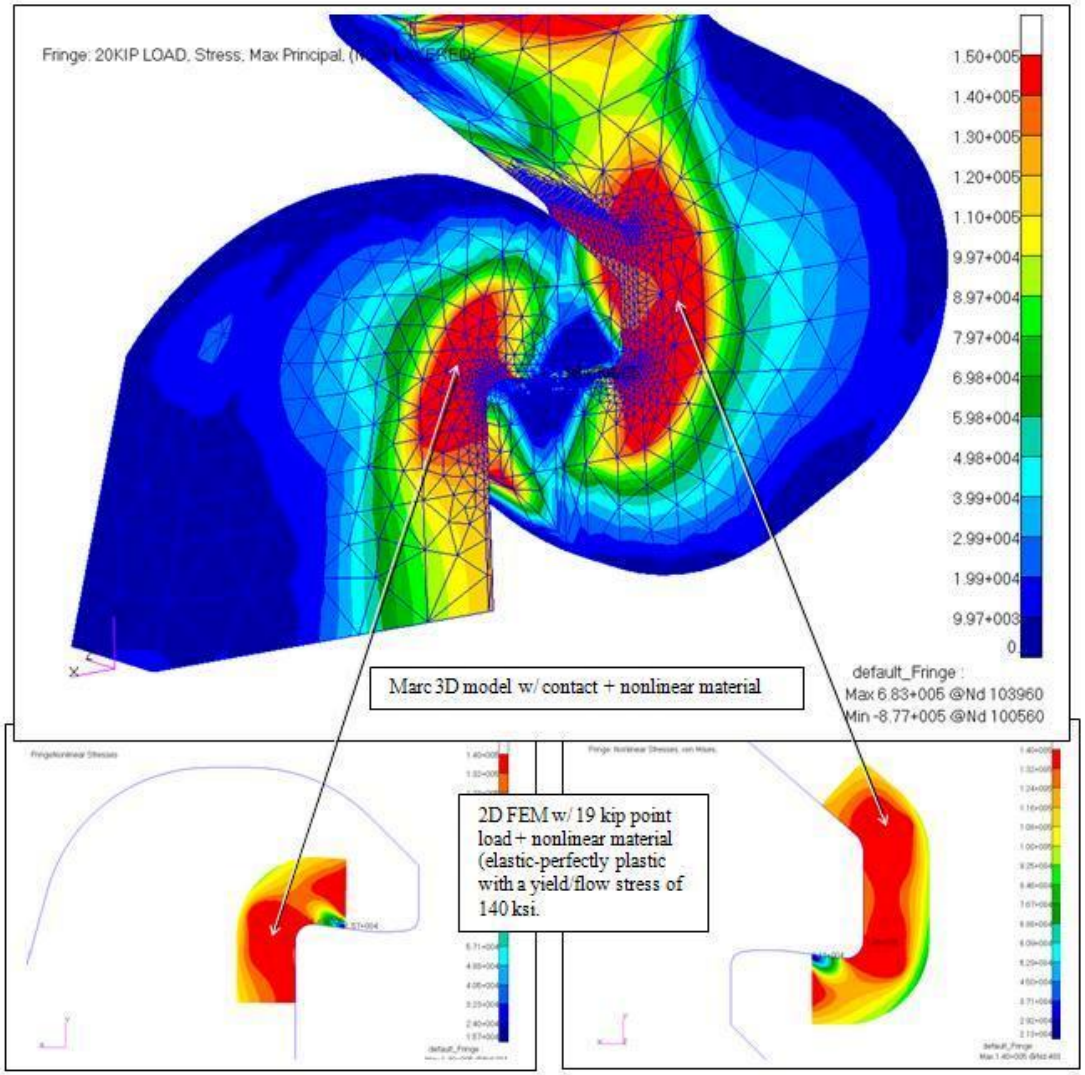

3D FEM Failure Load Prediction (Active/Passive Hook Contact Pressure)

A plot of the active and passive hook contact normal force distribution for a 20 kip loading with nonlinear material response is provided below. The contact footprint on both hook surfaces is characteristically similar to the witness mark observed on an active hook failed during static strength testing.

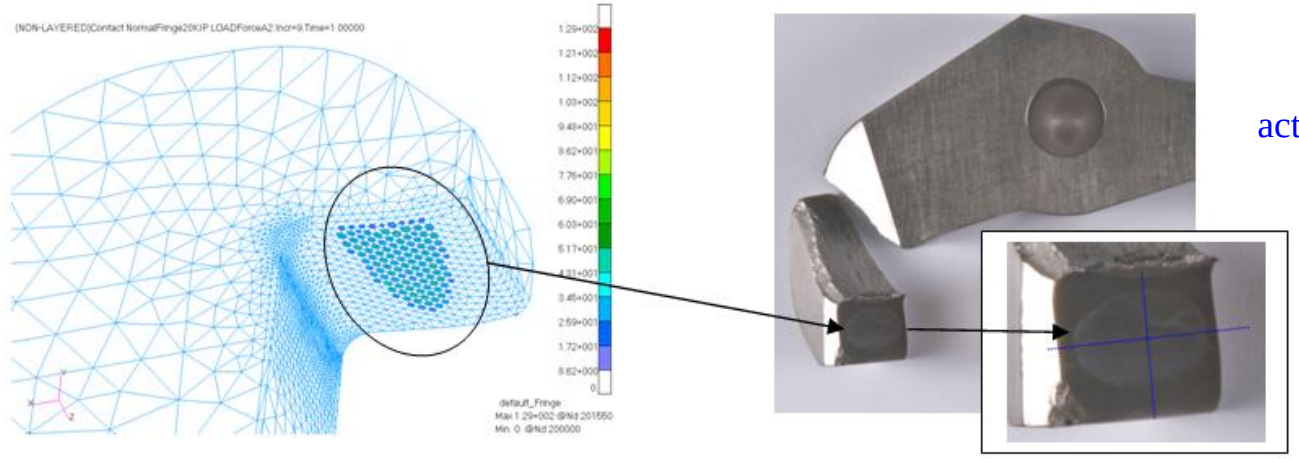

active hook

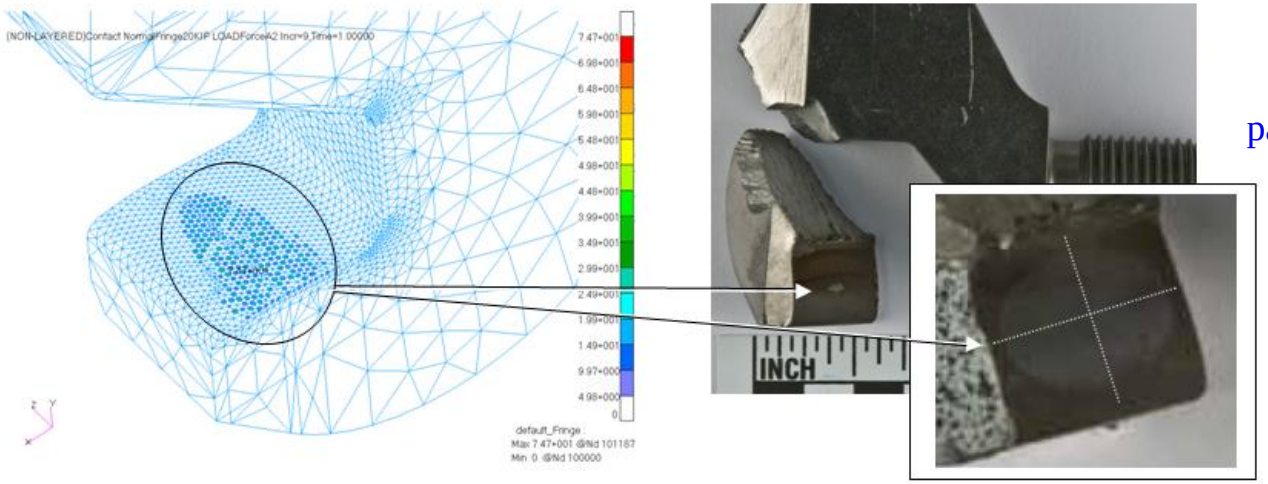

passive hook

2D/3D Analytical Stiffness

The 2D engaged hook analytical stiffness is achieved by a summation of the active/passive hook results and it demonstrates a good correlation with the 3D analytical result up to 15 kips.

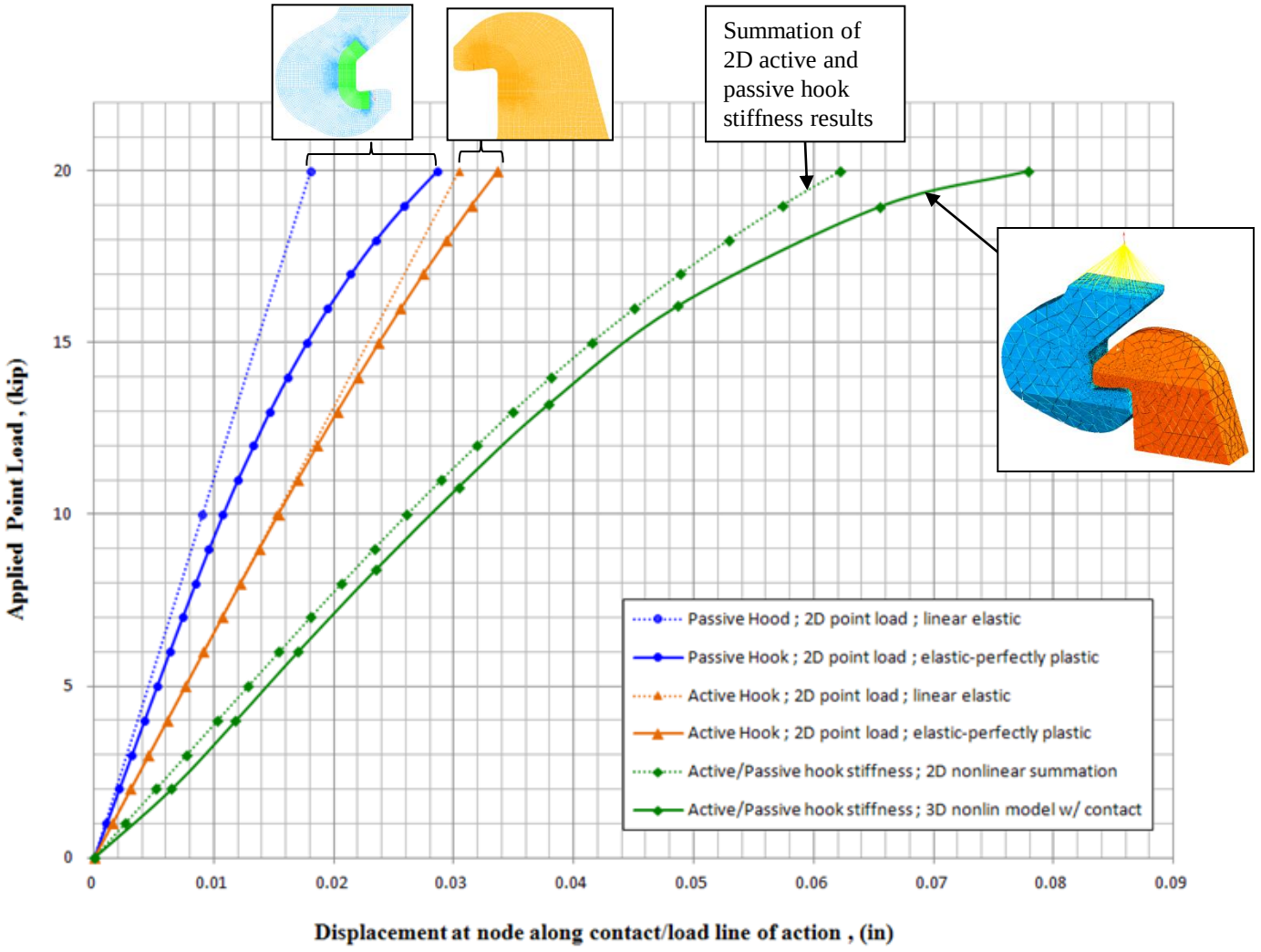

2D/3D FEM Correlation to Static Test Results

The finite element models are correlated to the static strength test results – failure load (end point) and stiffness (load-displacement).

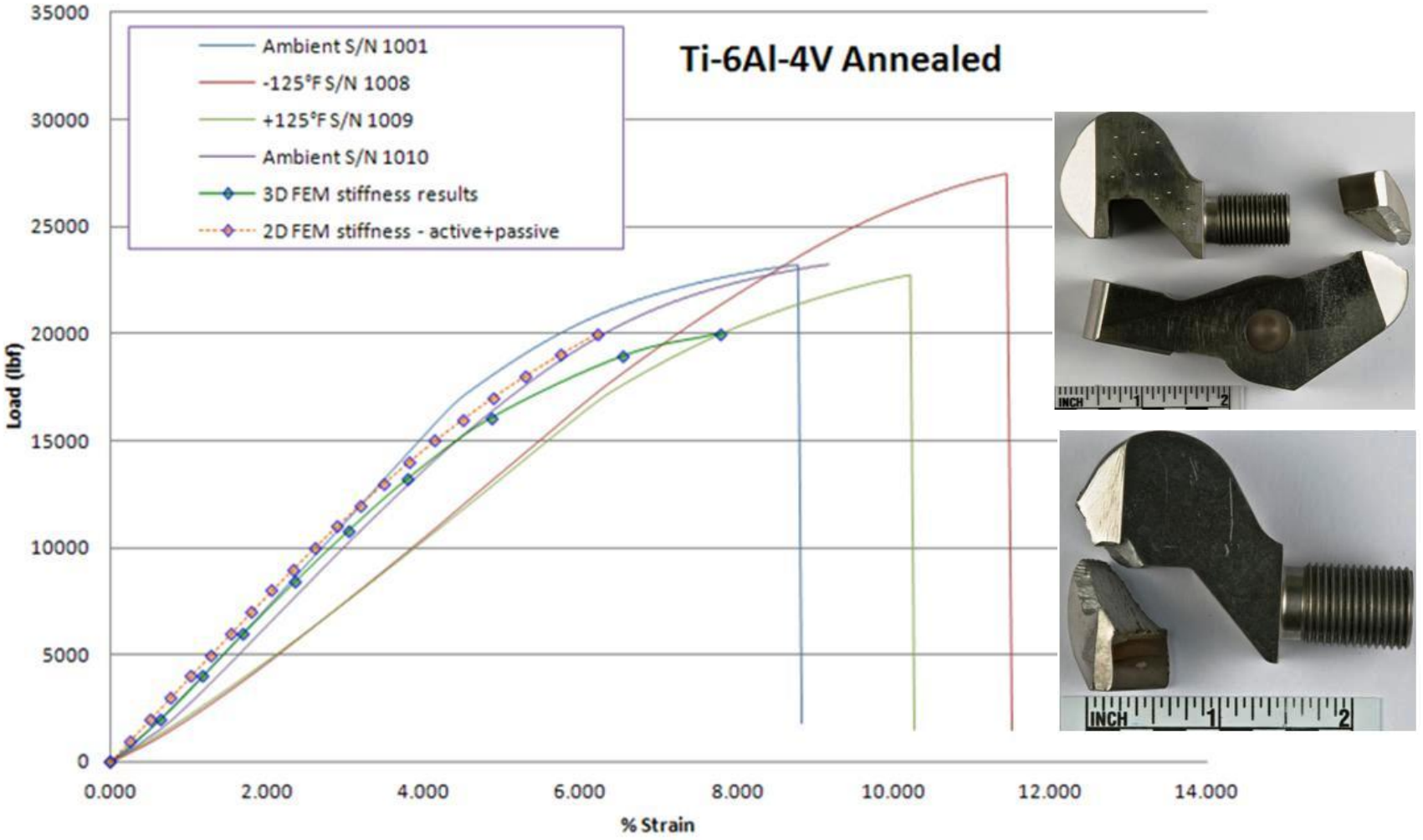

Fracture Based Service Life Assessment – Equivalent Initial Flaw Size

The analytical initial flaw size that realistically captures the influence of microstructural imperfections and processing defects with respect to the overall fatigue life is known as the equivalent initial flaw size.

Test coupons representative of standard manufacturing processing are cycled to failure and the resulting test data is correlated analytically via the initial crack size. USAF durability EIFS (0.005”) is characteristic of manufacturing related surface finish features.

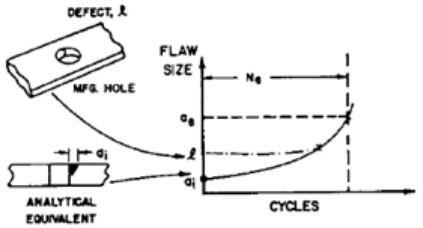

Figure 3.4.2. Definition of Equivalent Initial Quality (Reference 27).

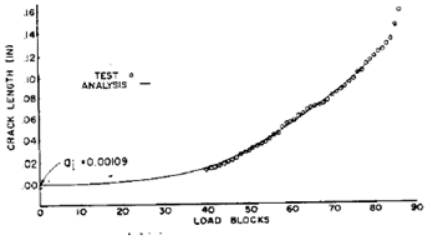

Figure 3.4.4. Equivalent Initial Quality Results for A-7A Wing Fatigue Test (Reference 27).

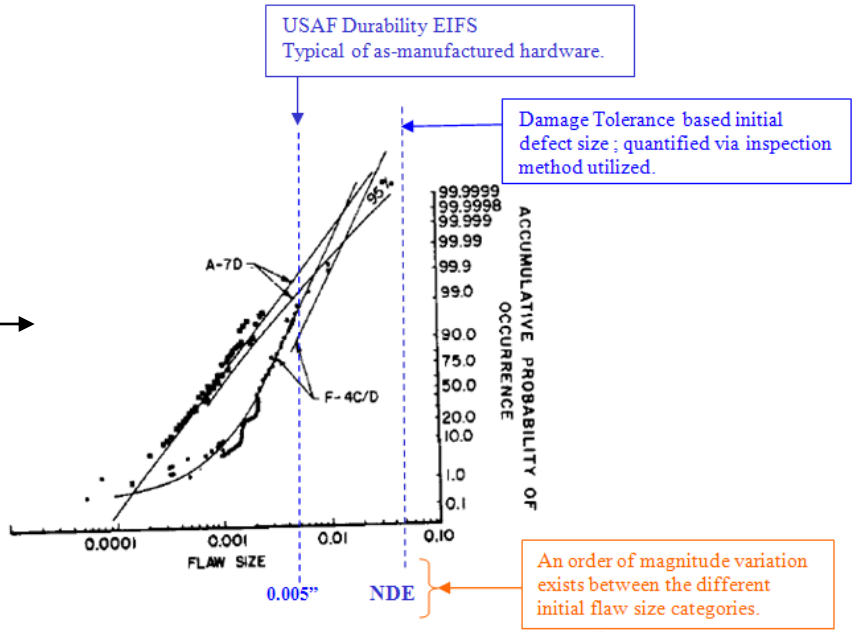

Figure 3.4.9. Cumulative Probability of Occurrence of A-7D Equivalent Initial Quality (Reference 27).

Fracture Based Service Life Assessment – Equivalent Initial Flaw Size (cont)

Stress-Life (S-N) test coupons typically employ a very high quality surface finish in order to reduce the overall scatter in results. Newman et al. (ASTM STP 1122) demonstrate EIFS an order of magnitude less than USAF durability for S-N correlation. Thus an EIFS of 0.0005" is used herein to define the analytical upper bound of the service life capability.

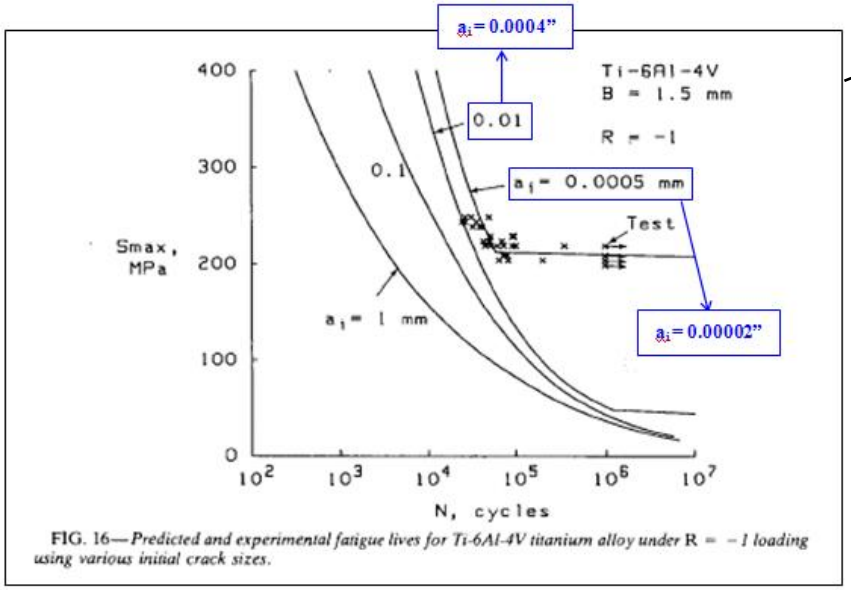

FIG. 16—*Predicted and experimental fatigue lives for Ti-6Al-4V titanium alloy under R = −1 loading using various initial crack sizes.*

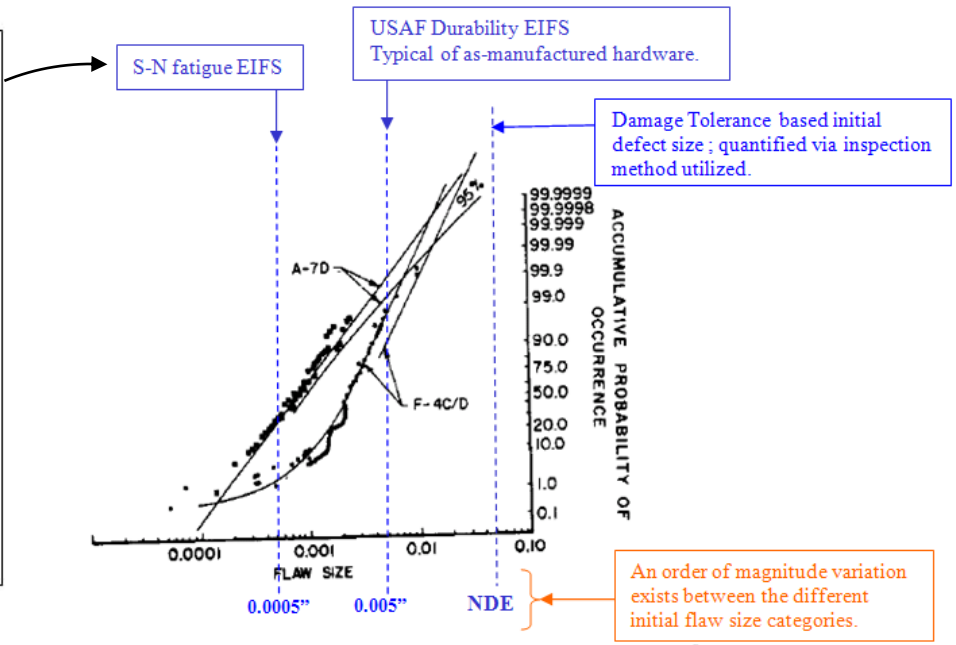

Figure 3.4.9. Cumulative Probability of Occurrence of A-7D Equivalent Initial Quality (Reference 27).

2D Fracture Based Service Life Assessment (Passive Hook)

The crack driving force in the passive latch transition radius is determined via a crack-tip element in the finite element model. A comparison of the stress intensity factor result with NASGRO defined plane-strain fracture toughness values indicates the potential for LEFM in an application with large magnitude linear elastic stresses (>>σult).

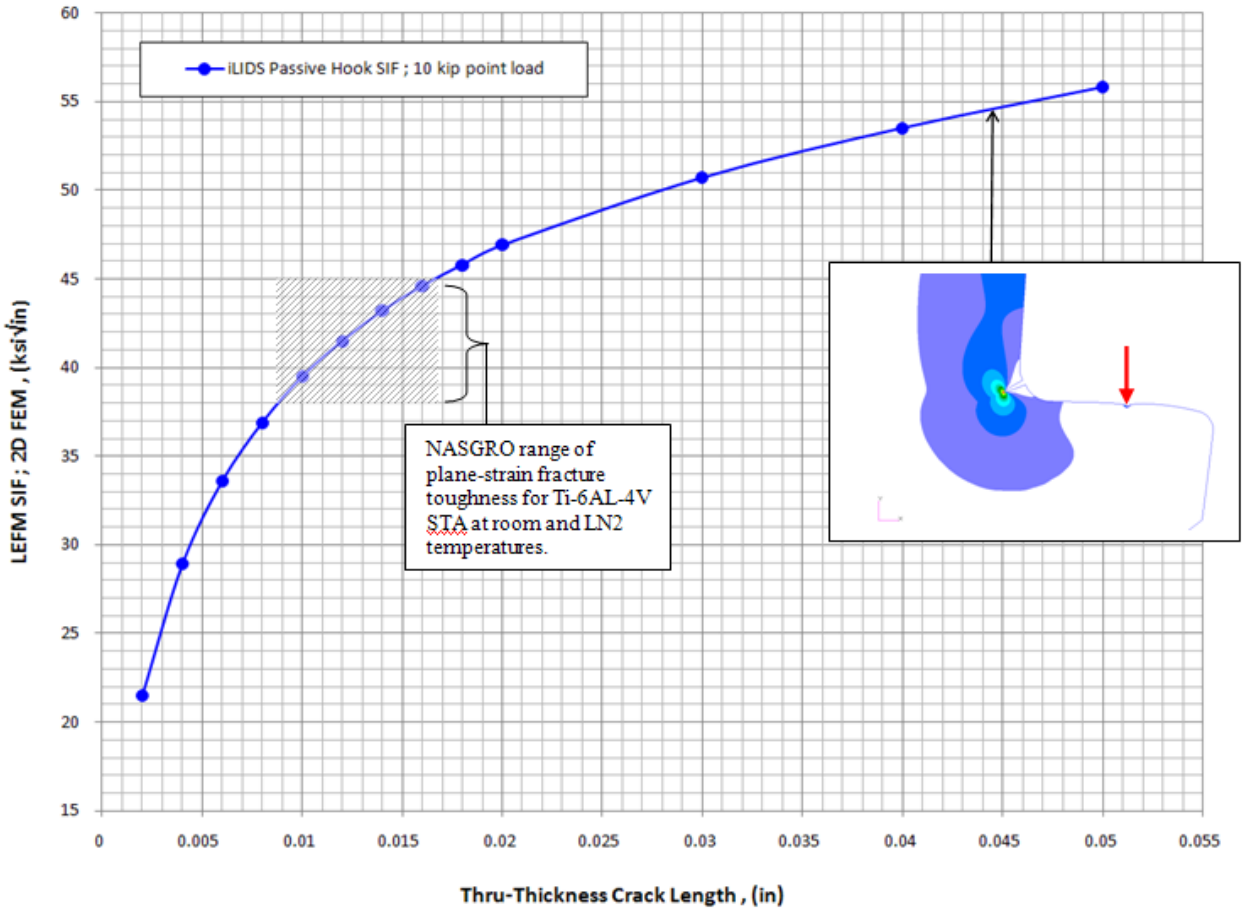

2D Fracture Based Service Life Assessment (Passive Hook) – (cont)

Fracture mechanics material data for the specific titanium alloys selected for this effort is not available. A representative alloy from NASGRO database is selected based upon product form similarity and the abundance of test data. An STA titanium is chosen in a somewhat conservative crack growth orientation.

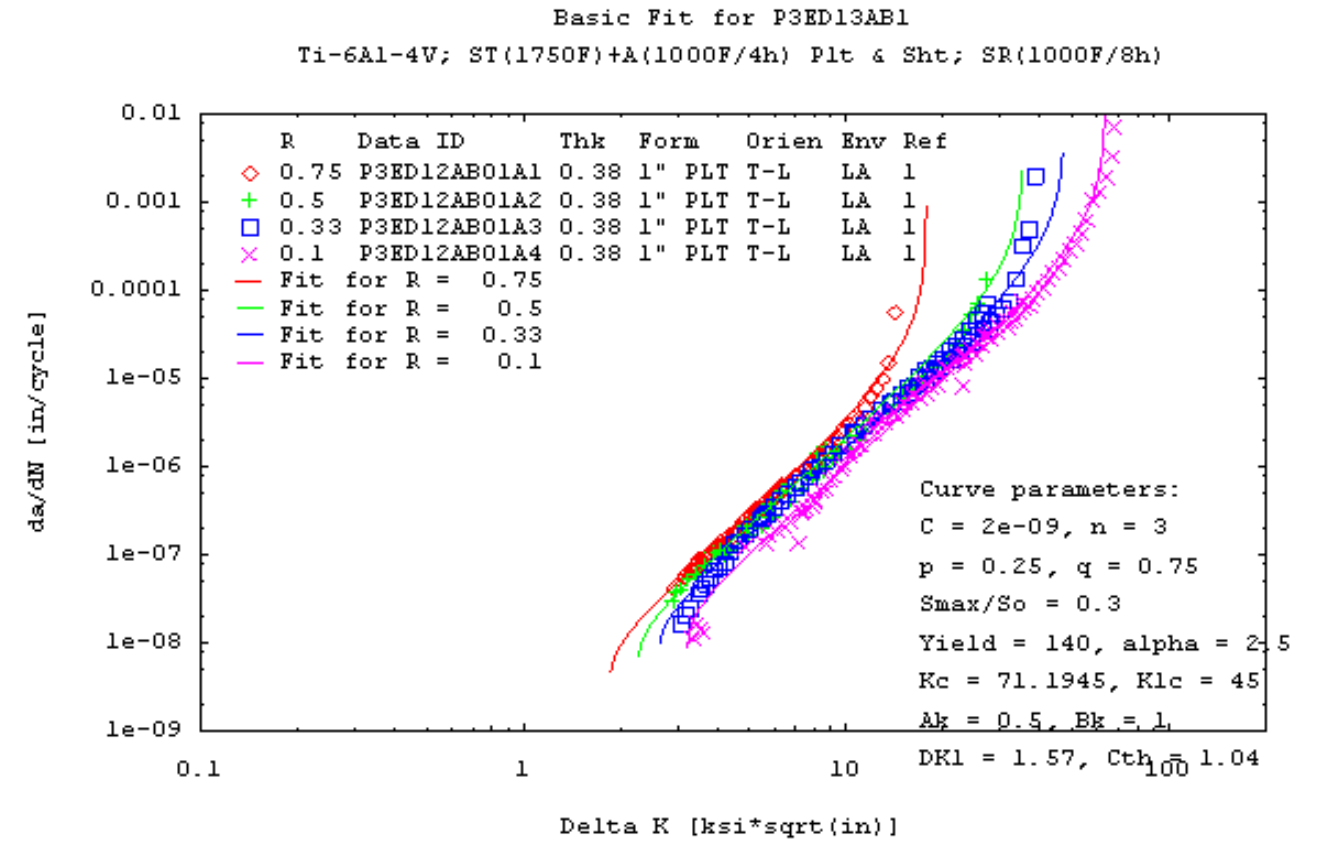

2D Fracture Based Service Life Assessment (Passive Hook) – (cont)

Crack case solution determination.

NASGRO provides a library of crack case solutions in the form of simplified geometric representations. Several are evaluated for use in the latch hook service life analysis.

Stress gradients associated with the geometry are embedded within these solution.

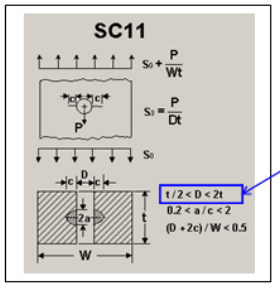

The SC11 crack case solution is for a surface crack in the bore of a hole.

This solution is valid for a specified range of hole diameters ($D > t/2 = 0.787"/2 = 0.394"$).

The hole diameter restriction will result in a local curvature (notch radius = 0.06") and the corresponding stress gradient may deviate from the actual structural response.

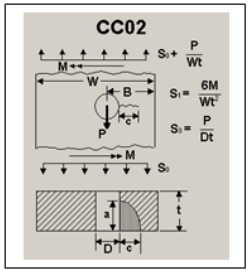

The CC02 crack case solution is for a corner crack in the bore of a hole.

Hole diameters of 0.4" (matches the SC11 solution) and 0.12" (matches the hook notch radius) are incorporated.

Stress gradients defined from the FEM in the uncracked configuration are input by the user.

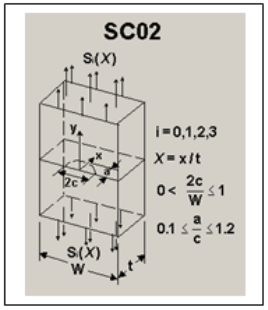

The SC02 crack case solution is for a surface crack in a flat plate (accounts for the free-surface and finite width geometrical features).

The stress gradient from the 2D FEM is incorporated ; (stress at the surface is constant over the width and varies in the depth direction as per the FEM definition).

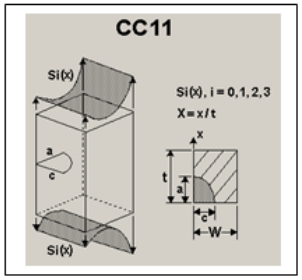

The CC11 crack case solution is for a corner crack in a flat plate (accounts for the free-surface and finite width geometrical features).

The stress gradient from the 2D FEM is incorporated ; (stress at the surface is constant over the width and varies in the depth direction as per the FEM definition).

2D Fracture Based Service Life Assessment (Passive Hook) – (cont)

Crack case solution determination.

The durability (0.005” initial crack) results for the various crack case solutions (constant amplitude loading 0-10 kips) are compared and the CC02 solution (dia=0.12”) demonstrates an appreciable deviation – due to the associated stress gradient and deformation constraint.

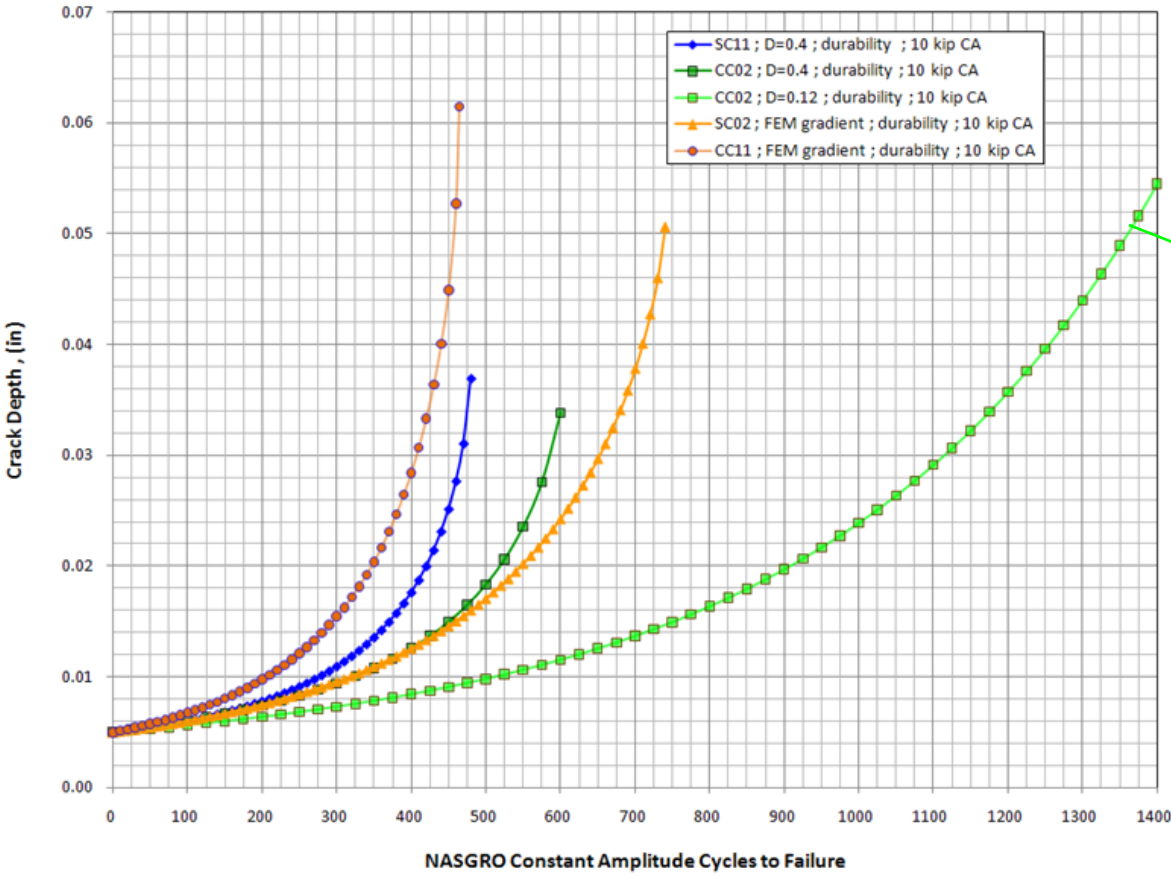

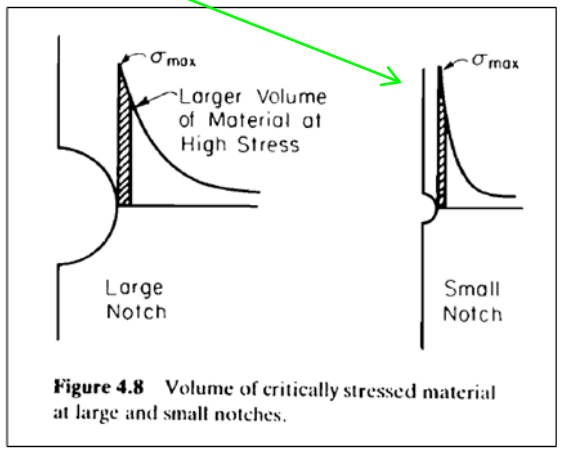

Figure 4.8 Volume of critically stressed material at large and small notches.

2D Fracture Based Service Life Assessment (Passive Hook) – (cont)

Crack case solution determination.

Correcting the SC02 crack case solution for the peak stress amplification at the mid-surface (inherent within the SC11 solution) results in good agreement between the SC11, CC11, and SC02 solutions. The SC11 solution is selected for use in the service life assessments since only knowledge of the peak local stress is required (not the entire gradient).

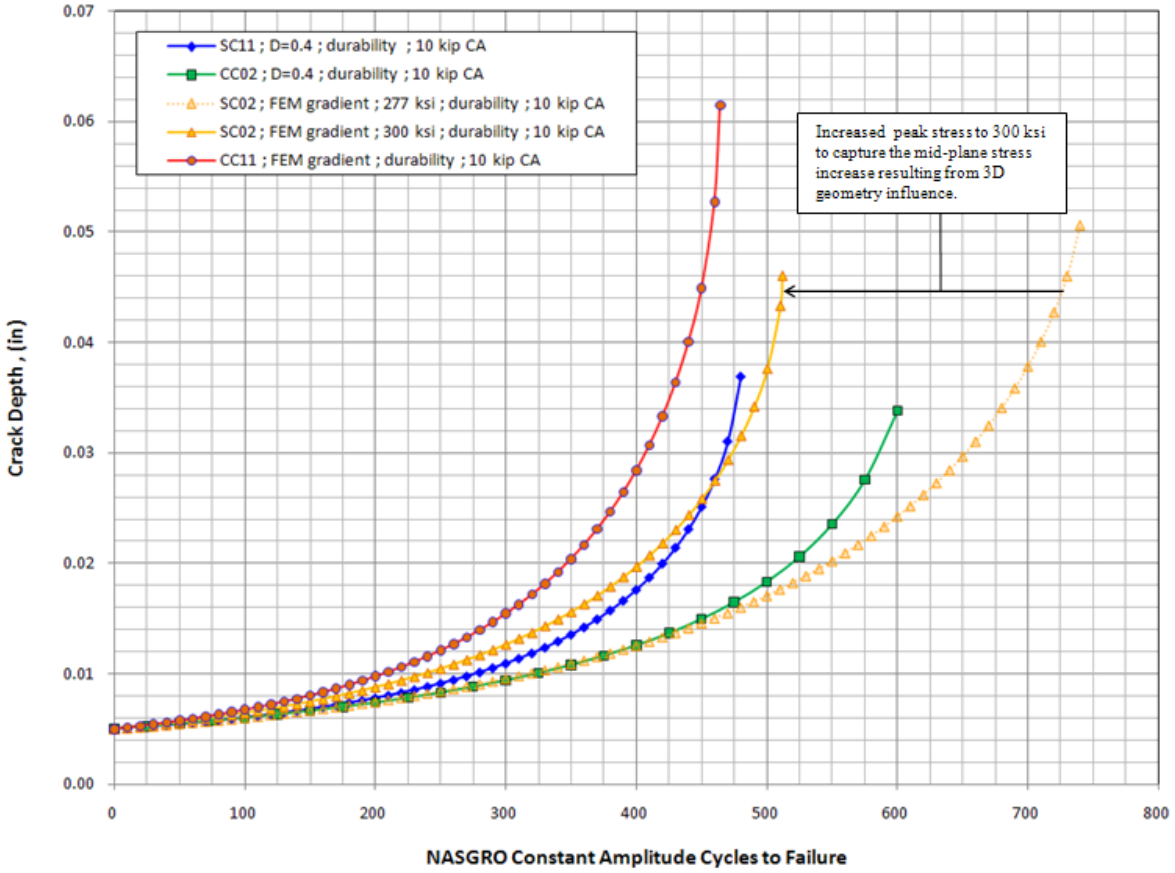

LEFM Constant Amplitude Projections

Peak linear elastic stresses from 2D and 3D models are combined with the SC11 crack case solution to define the constant amplitude cyclic capability for EIFS of 0.005” and 0.0005” for various hook load magnitudes.

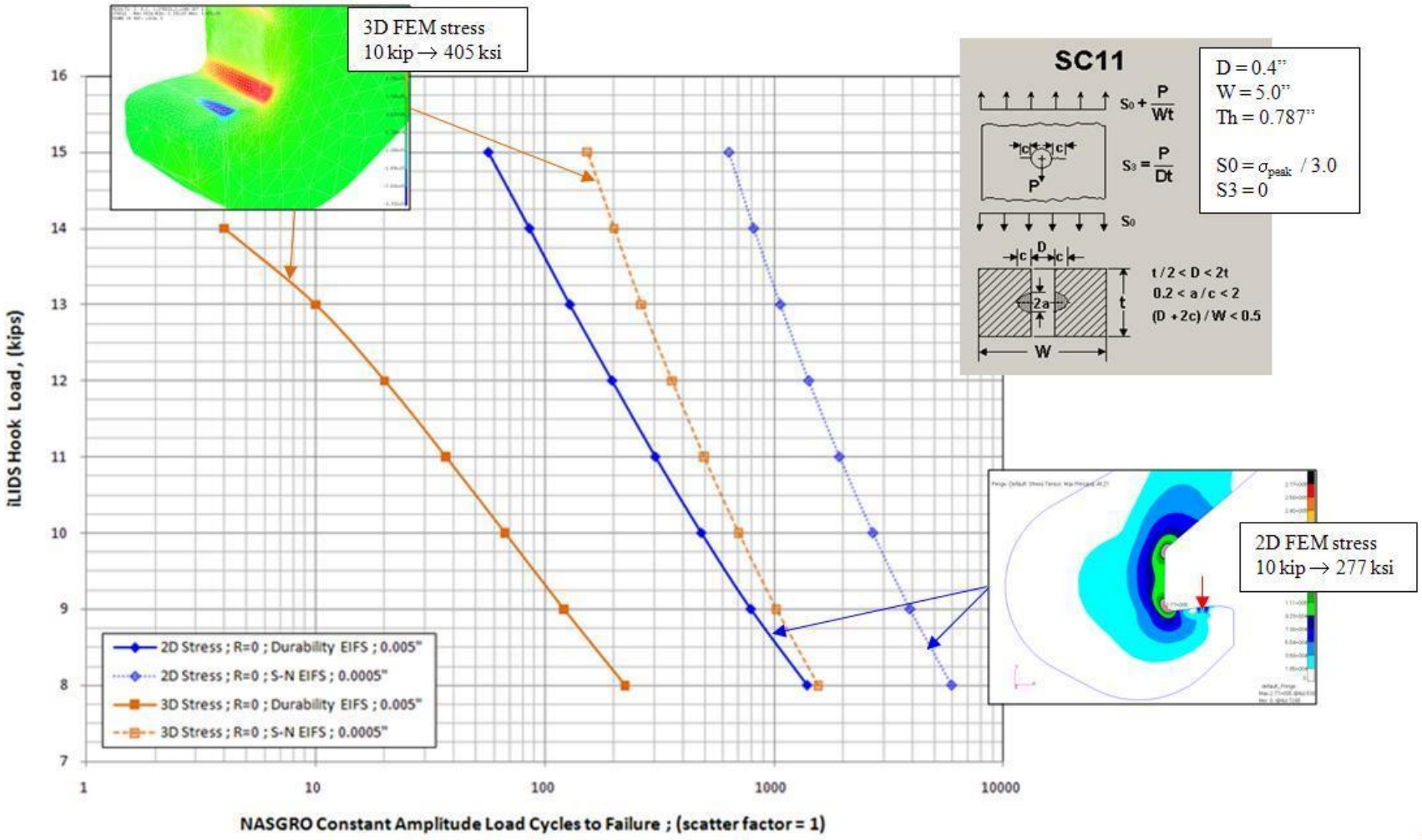

Strain-Life Methodology

The strain-life curve is the material characterization expression that quantifies the cyclic capability as a function of the applied strain range. In lieu of lot-specific strain-life material data the modified method of universal slopes (which utilizes monotonic tensile test data to define the resulting plastic and elastic life curve slopes ; Ref. Manson, S.S., Halford, G.R., **Fatigue and Durability of Structural Materials**, ASM International, 2006, pp 54-55, 81) is incorporated.

elastic modulus. For the plastic line, the intercept point at $N_f = 1.0$ was found to depend only on ductility D (= ln[100/(100 − %RA)]), where RA is the reduction of area in a tensile test). On the basis of these parameters, the Manson-Hirschberg Universal Slopes Equation becomes:

$$\Delta\varepsilon = (3.5S_u/E)(N_f)^{-0.12} + (D)^{0.6}(N_f)^{-0.60} \qquad \text{(Eq 3.3)}$$

Thus, only the tensile properties S_u, D, and E are required to determine the relations between cyclic life and strain range. We discuss the uses to

The Modified Method of the Universal Slopes Equation. By 1986, when the fatigue properties of many more materials had been characterized than the 29 materials used in 1964, a new study was undertaken to reexamine the relation with the intent of improving its accuracy. The study is reported in Ref 3.18. Least squares curve fitting using log-log coordinates of the strain-life data of the 50 materials listed in Table 3.1 resulted in the equation:

$$\Delta\varepsilon = 1.17\left(\frac{S_u}{E}\right)^{0.832}(N_f)^{-0.09} + 0.0266(D)^{0.155}\left(\frac{S_u}{E}\right)^{-0.53}(N_f)^{-0.56}$$

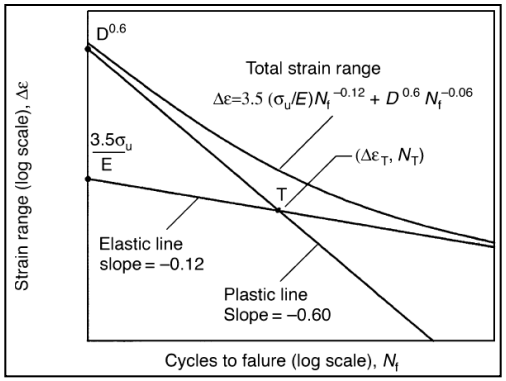

Strain-Life Methodology – (cont)

The two data sets of titanium material tensile test data were utilized to form 2 separate strain life formulations. A plot of the resulting strain-life curves via the modified method of universal slopes for the STA and annealed titanium alloys are provided below.

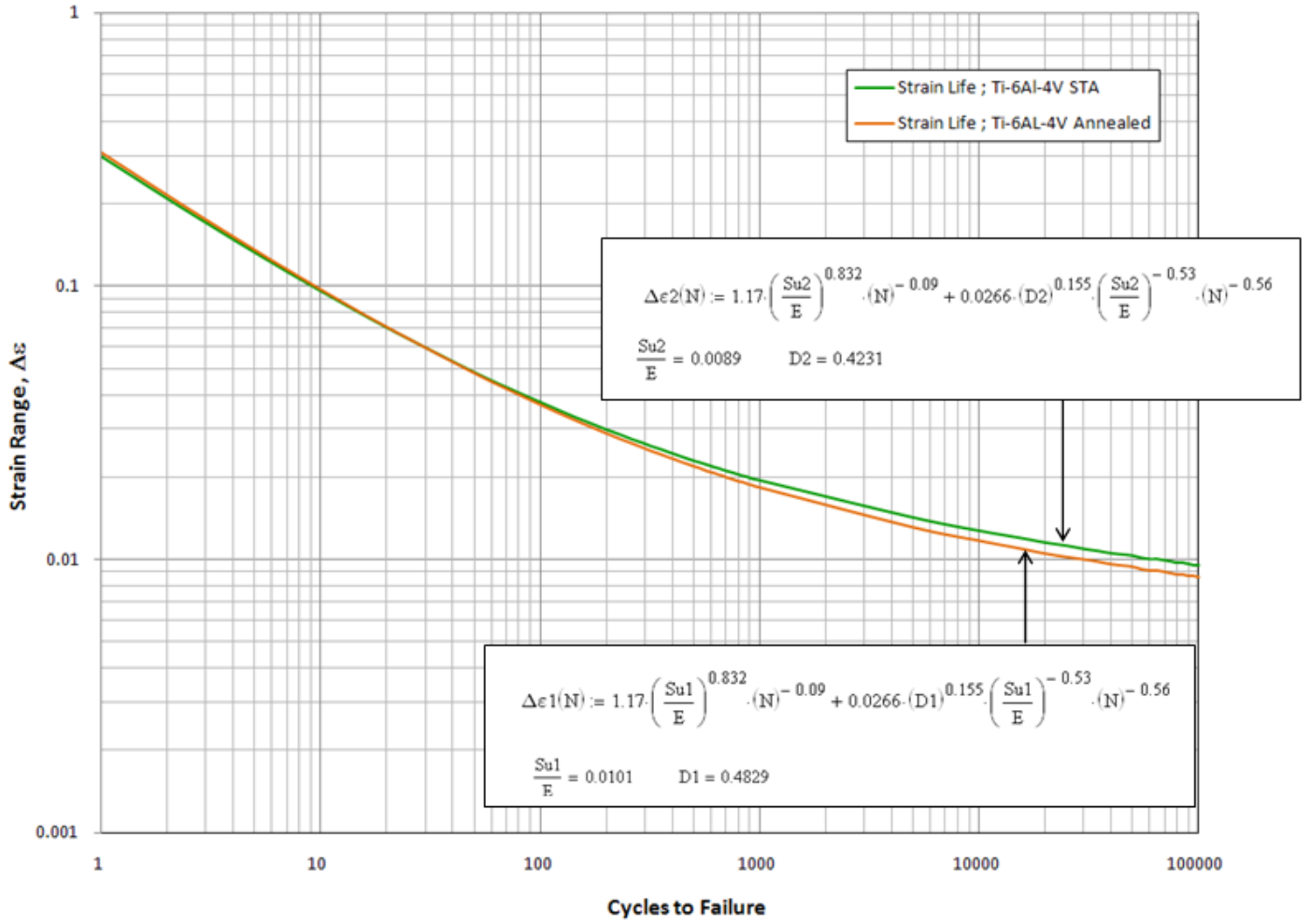

Latch Hook Nonlinear Strain Response

The 2D/3D latch hook nonlinear strain response for monotonic and cyclic loadings are generated. The monotonic strain response is doubled to compute a fully reversed (worst case ; R= -1) repsonse and the actual response (R=0) is generated analytically.

Monotonic nonlinear strain response

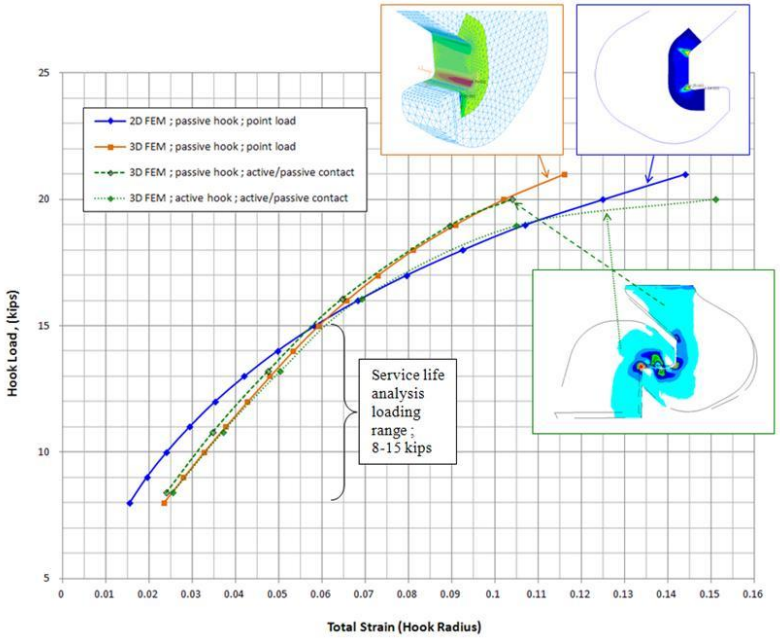

Cyclic nonlinear strain response

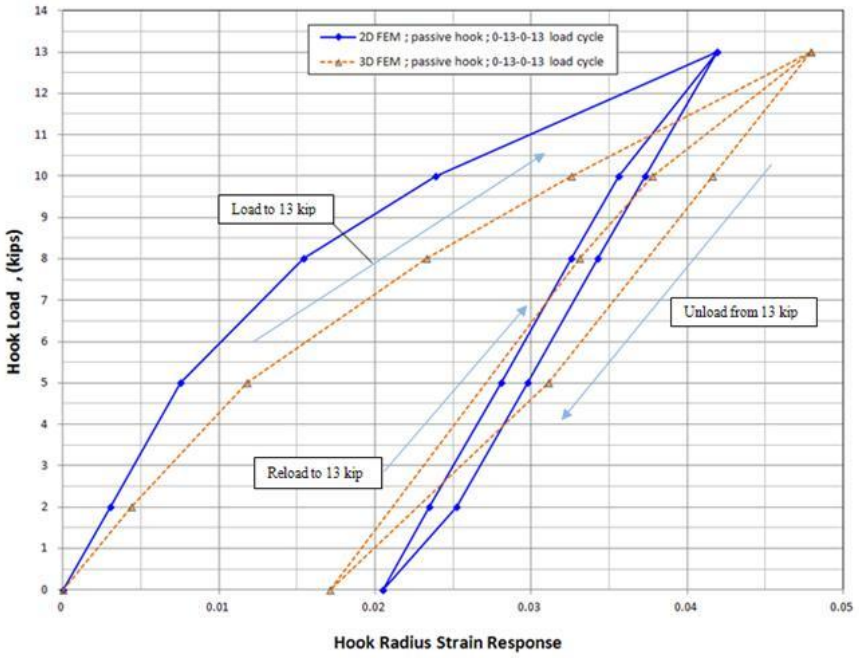

Strain-Life Analysis Comparison with LEFM Results

Strain-life analyses for fully R= -1 and R=0 are generated and compared with LEFM results.

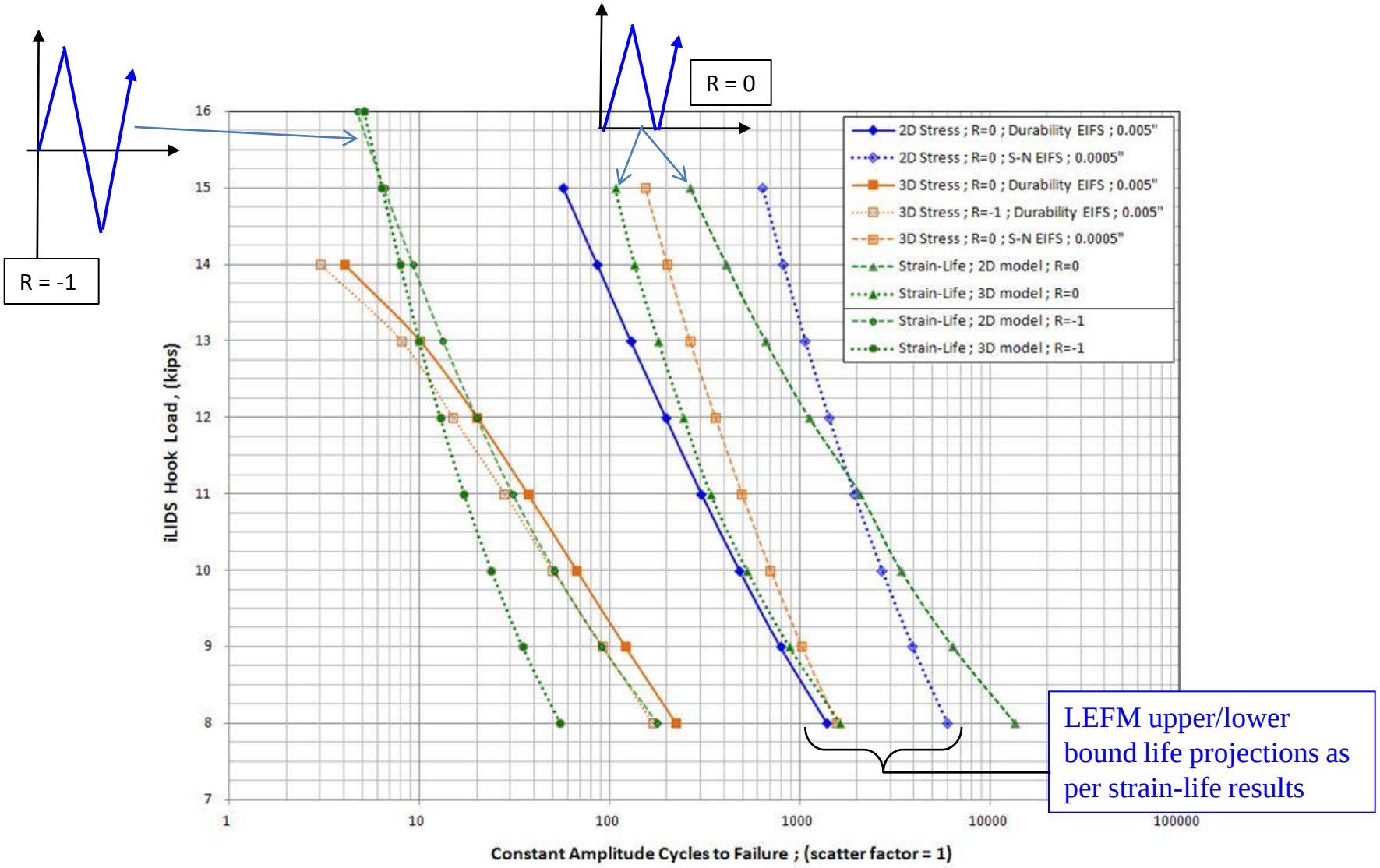

Latch Hook Service Life Projections – LEFM & Strain-Life

The fracture based upper & lower bound service life projections; verified via strain-life analysis.

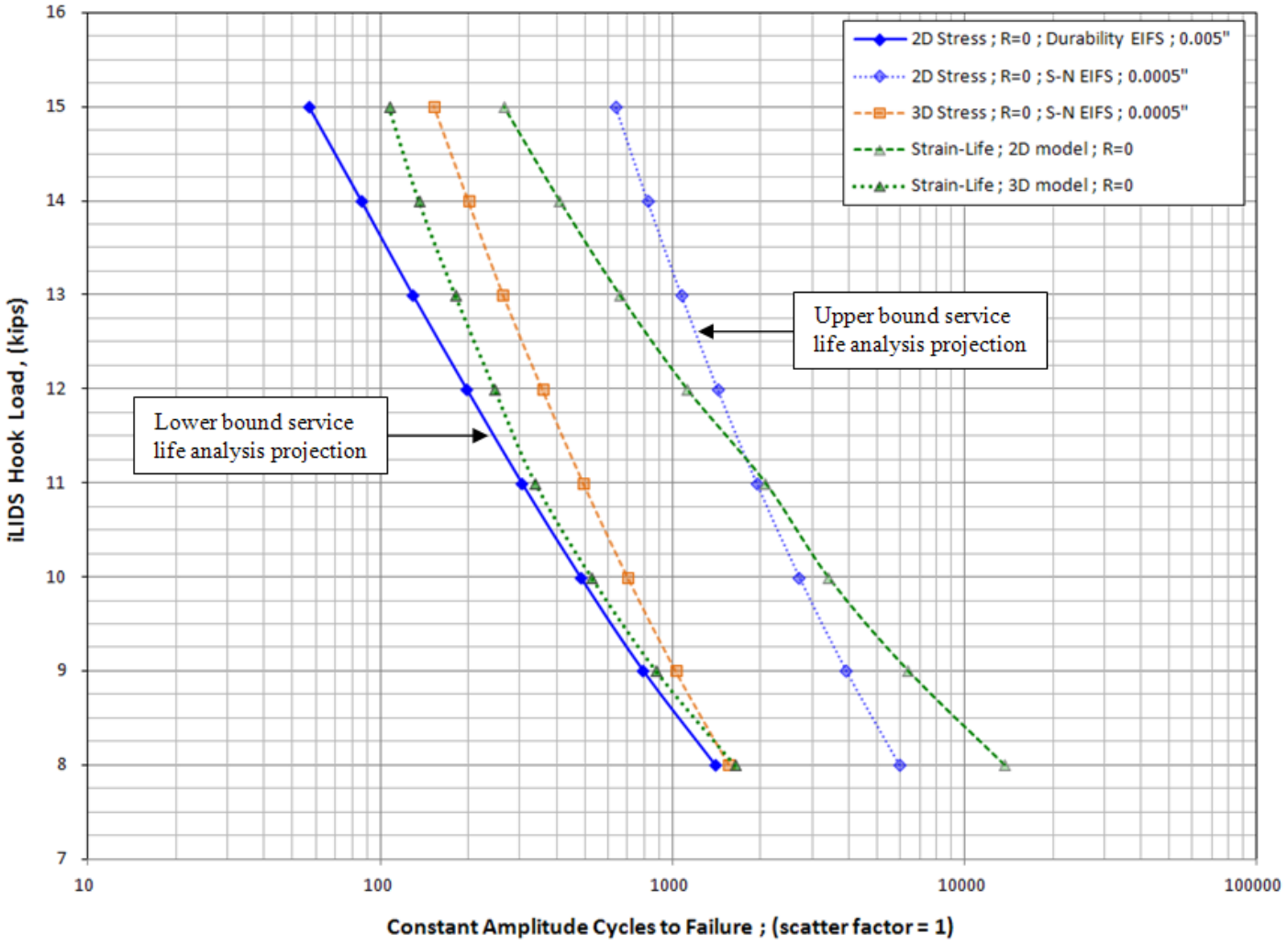

Latch Hook Fatigue Testing

The latch usage events consists of constant amplitude ground cycling to preload levels for integrated system checkouts. The operational usage of the latch hooks consists of the initial preload that joins the docking assemblies. Subsequent thermal, mechanical, and inertial induced loadings across the docking connection results in low-level loading oscillations about a high mean load.

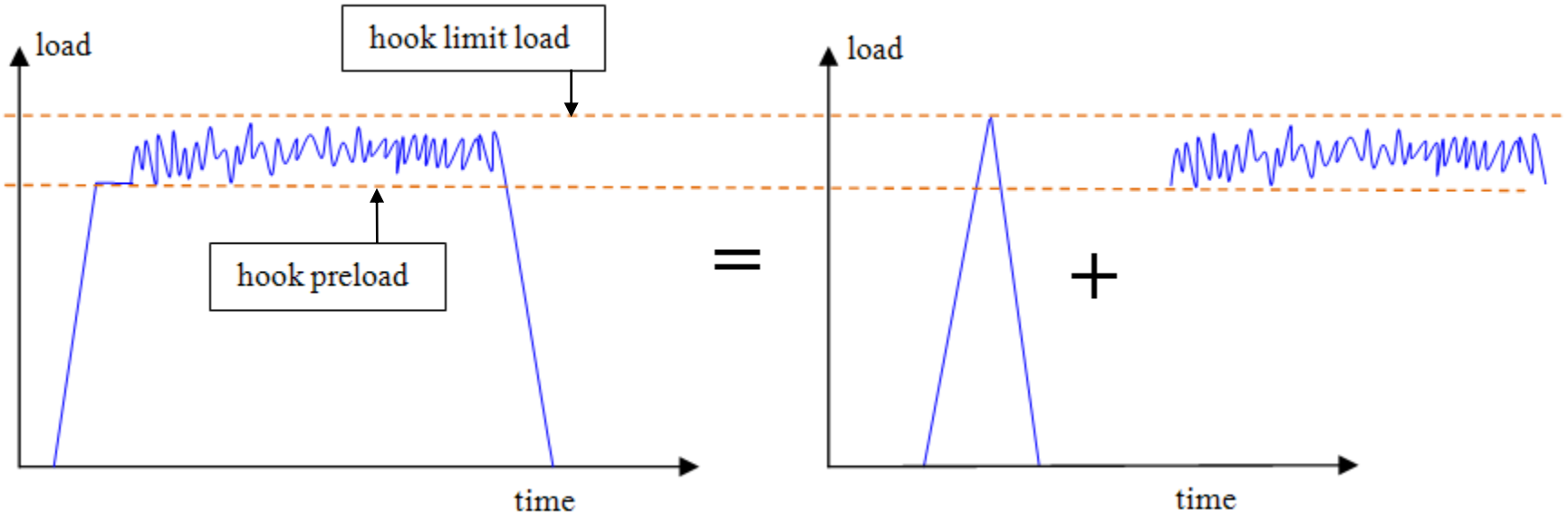

Latch Hook Fatigue Testing – (cont)

Constant amplitude fatigue testing of 4 sets of active and passive hooks to failure was conducted at hook loads of 10, 11, and 12 kips (2 hook sets were fatigue tested at 11 kips). Fatigue failure occurred in active hook at the contact shelf transition radius (consistent with the static strength failure location) for each test conducted.

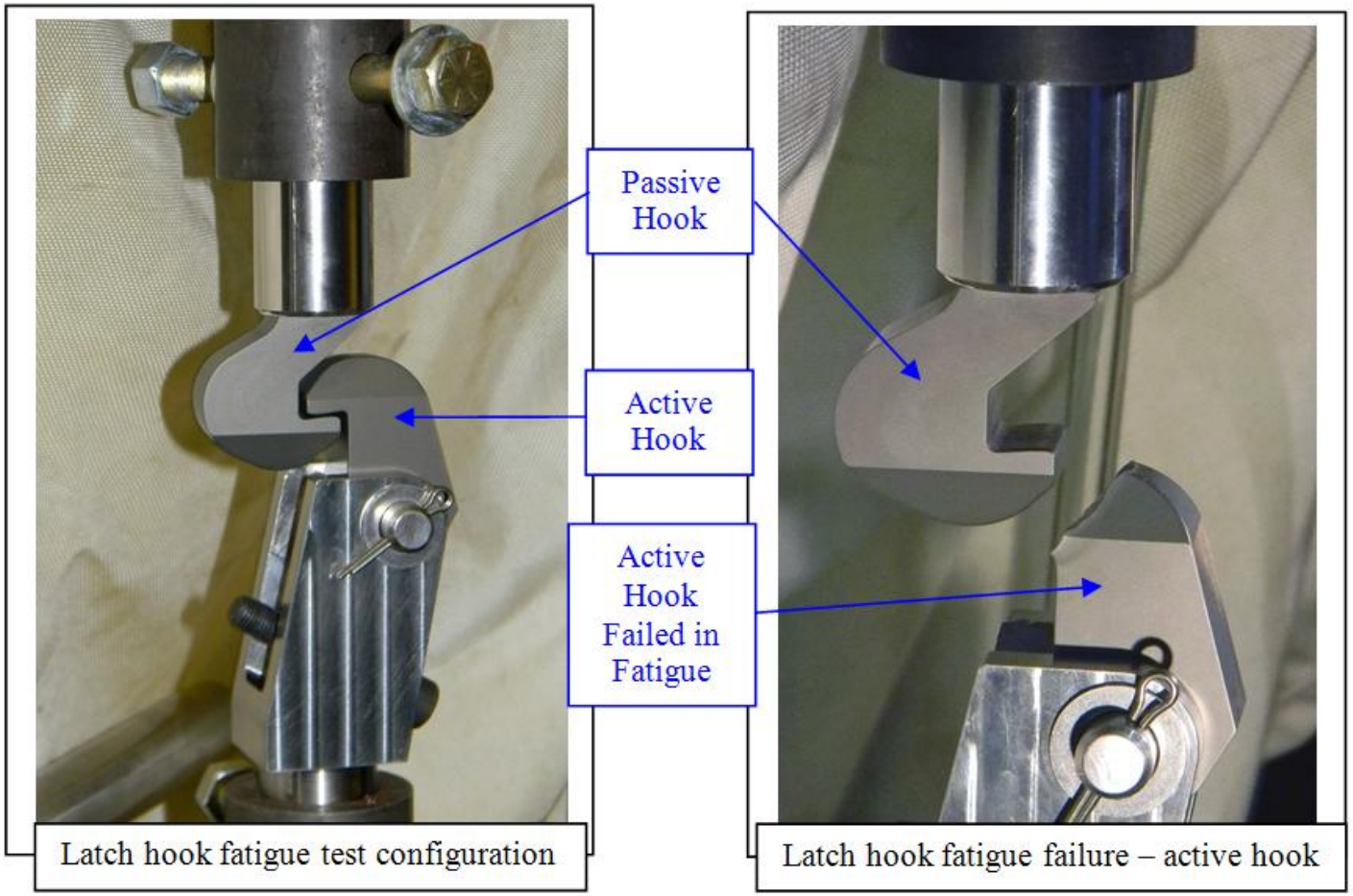

Latch Hook Fatigue Testing – (cont)

Frame by frame photographs of the 10 kip fatigue failure event are provided below.

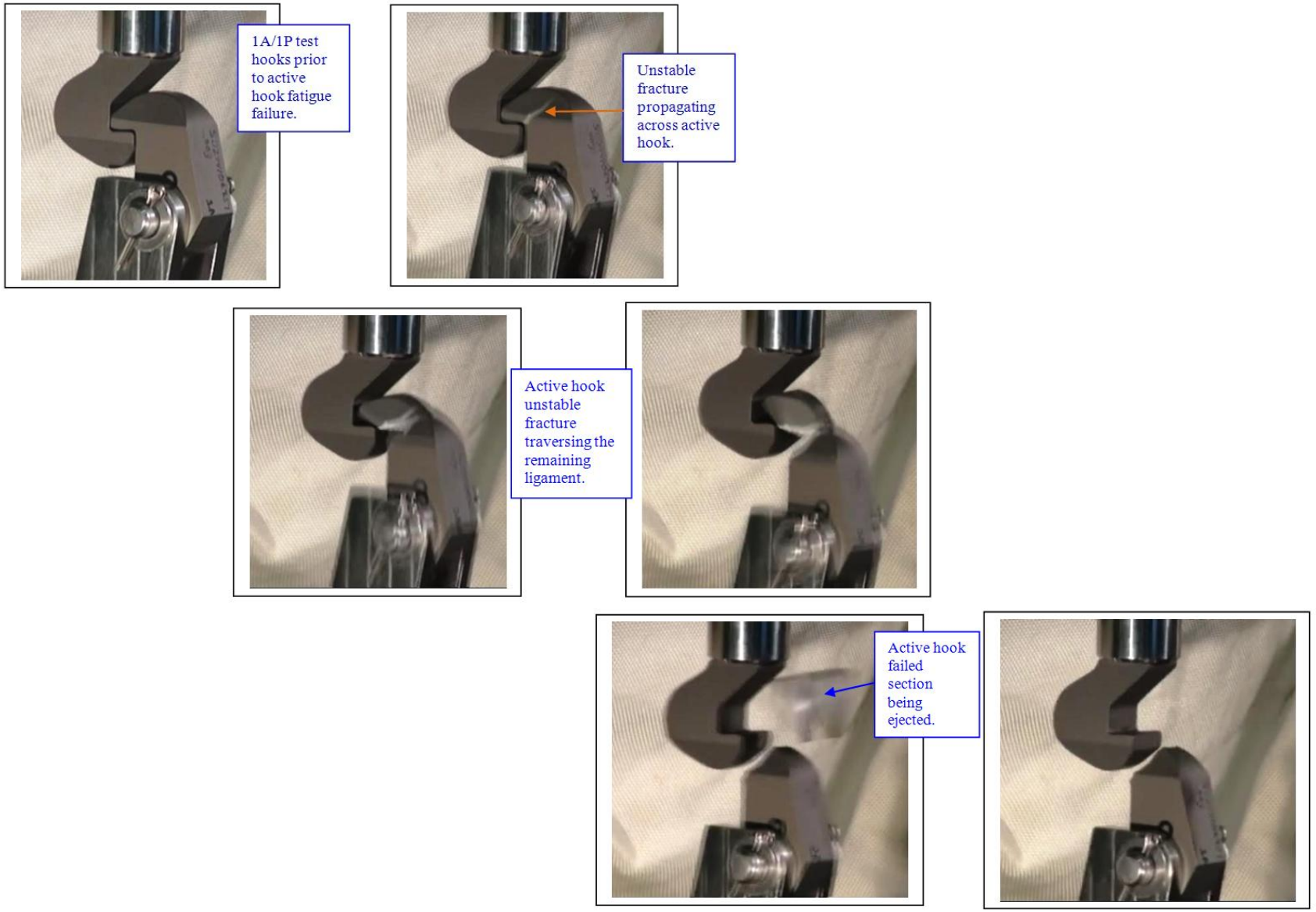

Latch Hook Fatigue Testing – (cont)

Post fatigue test photographs of the active and passive hook test article set are provided below.

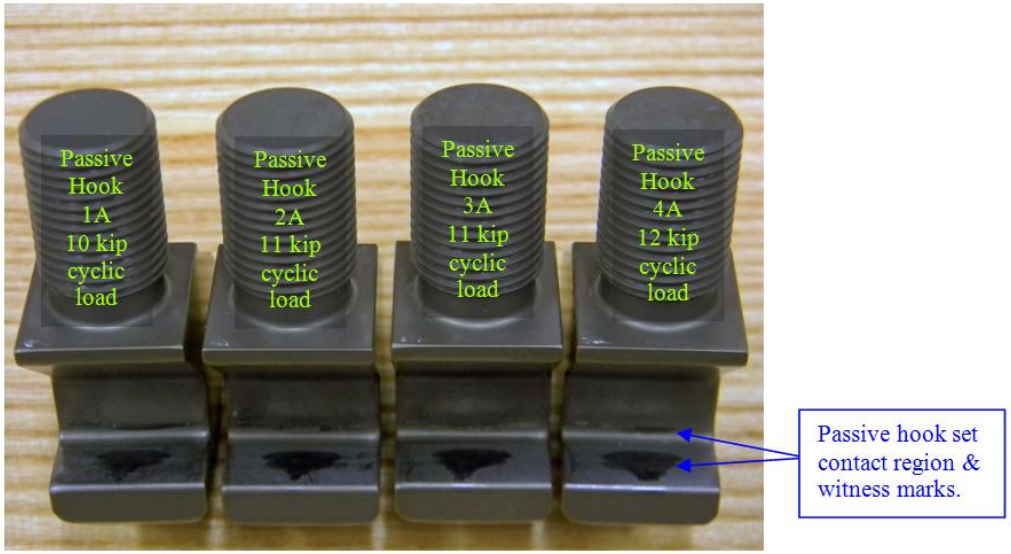

Latch Hook Fatigue Testing – (cont)

A tabular summary of the test results and a plot of the test data is provided below.

Test Number	Active/Passive Hook Set Test Id	Min / Max Cyclic Load (lb)	Constant Amplitude Cycles to Failure	Failed Hook & Failure Location
1	1A & 1P	150 / 10,000	**1,244**	Active / shelf transition radius
2	2A & 2P	158 / 11,050	**798**	Active / shelf transition radius
3	3A & 3P	184 / 11,000	**858**	Active / shelf transition radius
4	4A & 4P	134 / 11,996	**598**	Active / shelf transition radius

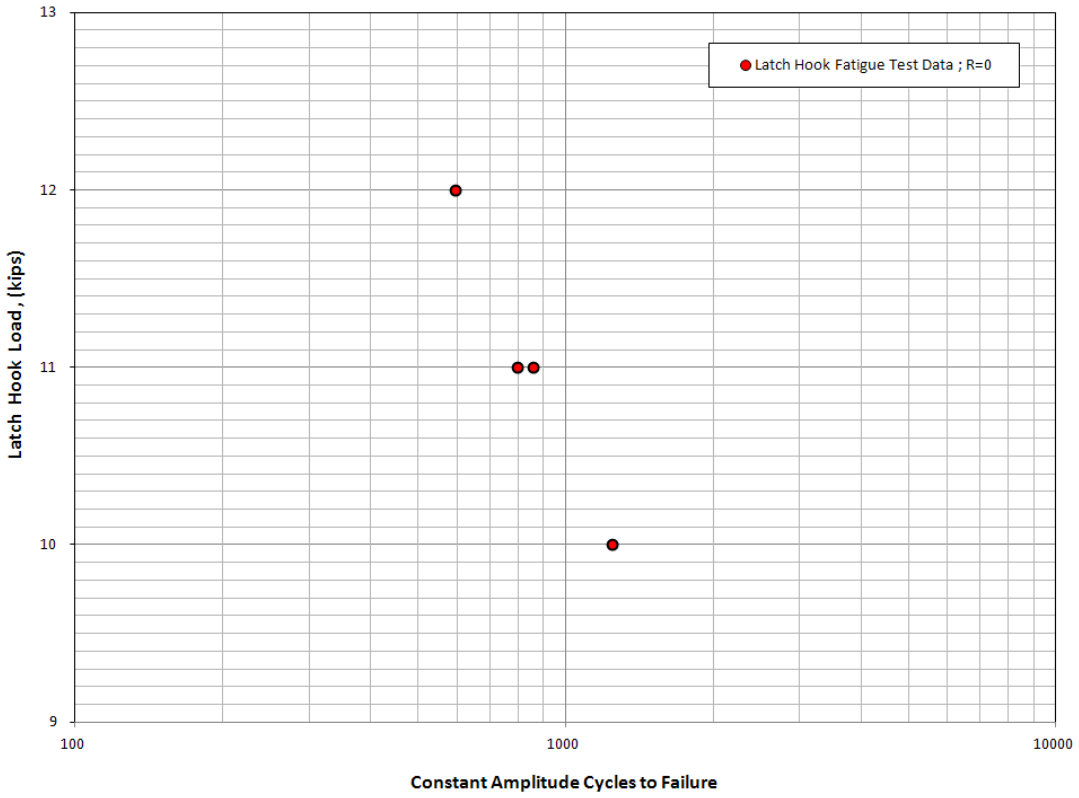

Comparison of Analytical Predictions With Fatigue Test Results

The test data was bounded by the analysis predictions and the overall trends are similar.

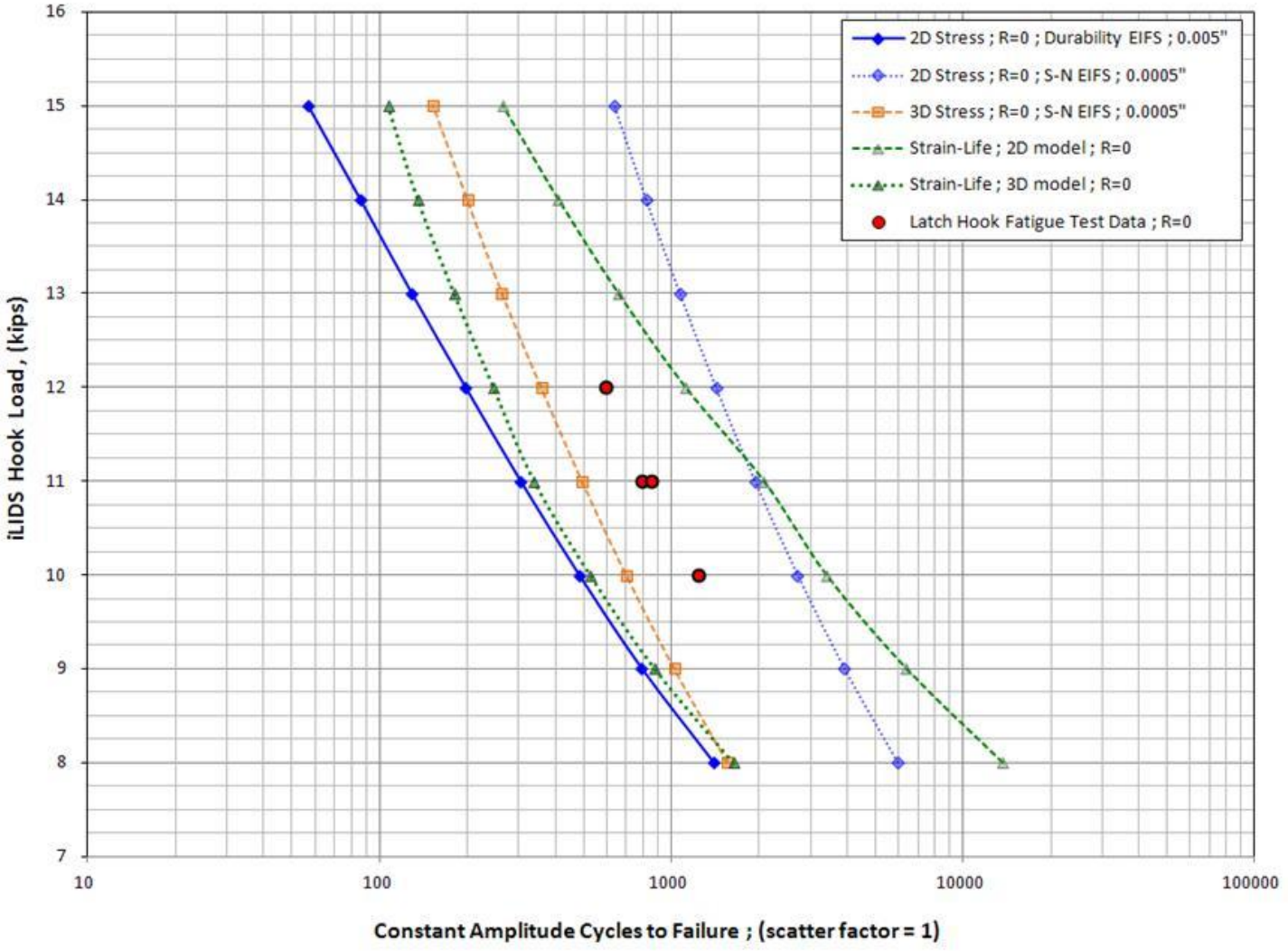

Latch Hook Mission Capability – Room Temp / Lab Air

The latch hook loading spectrum and resulting mission capability predictions are provided below.

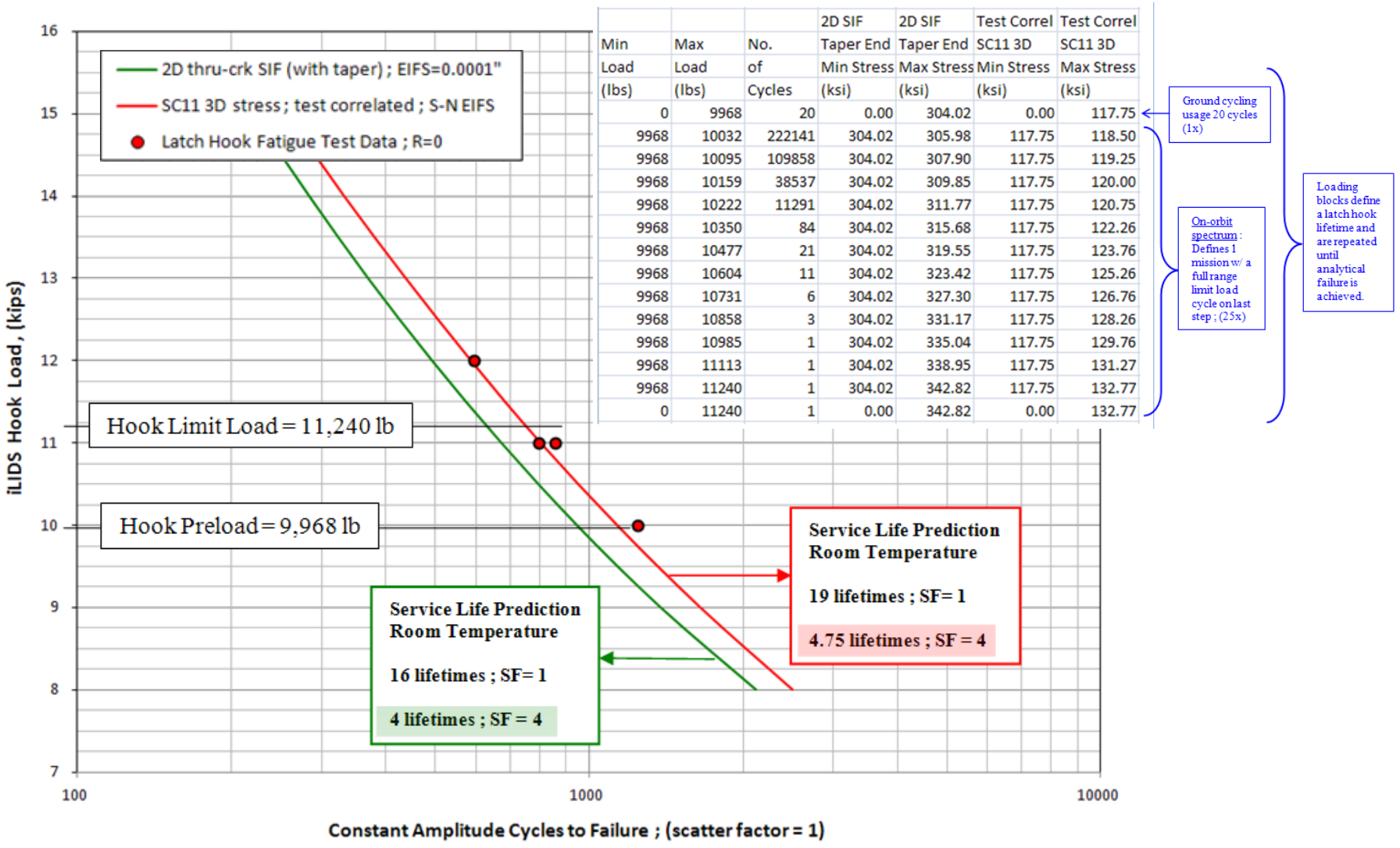

Min Load (lbs)	Max Load (lbs)	No. of Cycles	2D SIF Taper End Min Stress (ksi)	2D SIF Taper End Max Stress (ksi)	Test Correl SC11 3D Min Stress (ksi)	Test Correl SC11 3D Max Stress (ksi)
0	9968	20	0.00	304.02	0.00	117.75
9968	10032	222141	304.02	305.98	117.75	118.50
9968	10095	109858	304.02	307.90	117.75	119.25
9968	10159	38537	304.02	309.85	117.75	120.00
9968	10222	11291	304.02	311.77	117.75	120.75
9968	10350	84	304.02	315.68	117.75	122.26
9968	10477	21	304.02	319.55	117.75	123.76
9968	10604	11	304.02	323.42	117.75	125.26
9968	10731	6	304.02	327.30	117.75	126.76
9968	10858	3	304.02	331.17	117.75	128.26
9968	10985	1	304.02	335.04	117.75	129.76
9968	11113	1	304.02	338.95	117.75	131.27
9968	11240	1	304.02	342.82	117.75	132.77
0	11240	1	0.00	342.82	0.00	132.77

Ground cycling usage 20 cycles (1x)

On-orbit spectrum : Defines 1 mission w/ a full range limit load cycle on last step ; (25x)

Loading blocks define a latch hook lifetime and are repeated until analytical failure is achieved.

Failure Analysis of Latch Hooks

A schematic representation of a mode-I (tensile opening) fatigue failure is provided below. The presence of multiple fatigue crack initiation sites on different planes will result in the formation of ratchet marks as the cracks coalesce. Once the stable fatigue crack becomes unstable and the fast fracture advances across the remaining ligament the plane stress condition at a free-surface will result in failure along a 45° shear plane (slant fracture) and the resulting inclined failure region is called a shear lip.

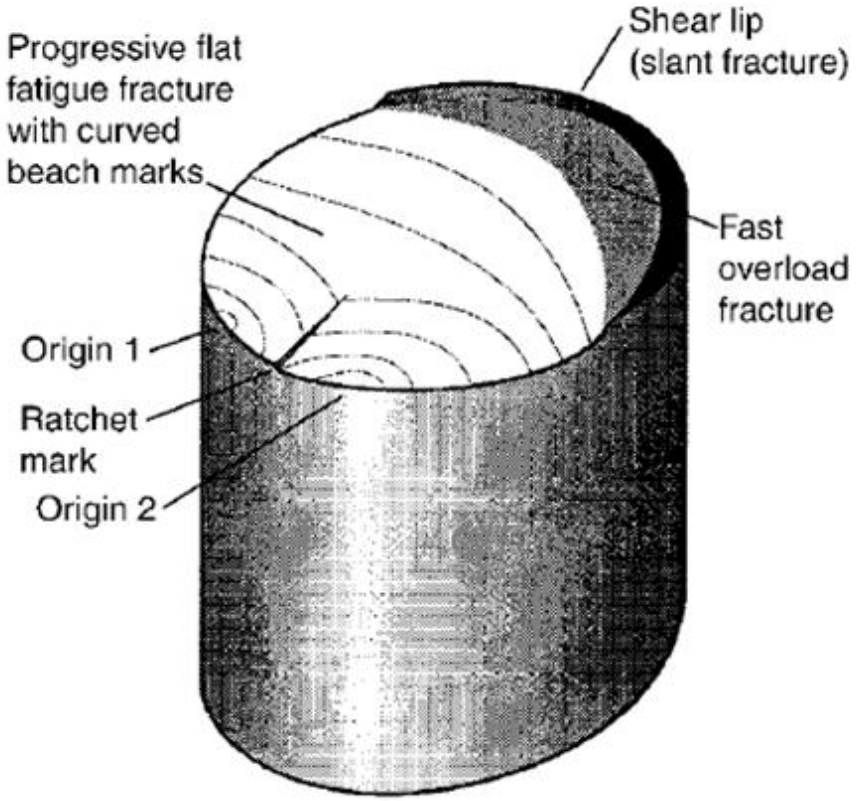

Failure Analysis of Latch Hook Fatigue Failures

Low magnification photos of the 2A hook are provided below. The numerous ratchet marks between the shear lips on the fracture initiation plane is indicative of multiple fatigue initiation sites within this region. The distribution of the fatigue damage about the centerline of the hook is consistent with the analytical results that demonstrate peak stress/strain response at the mid-plane that decreases in the direction of the hook outer surfaces.

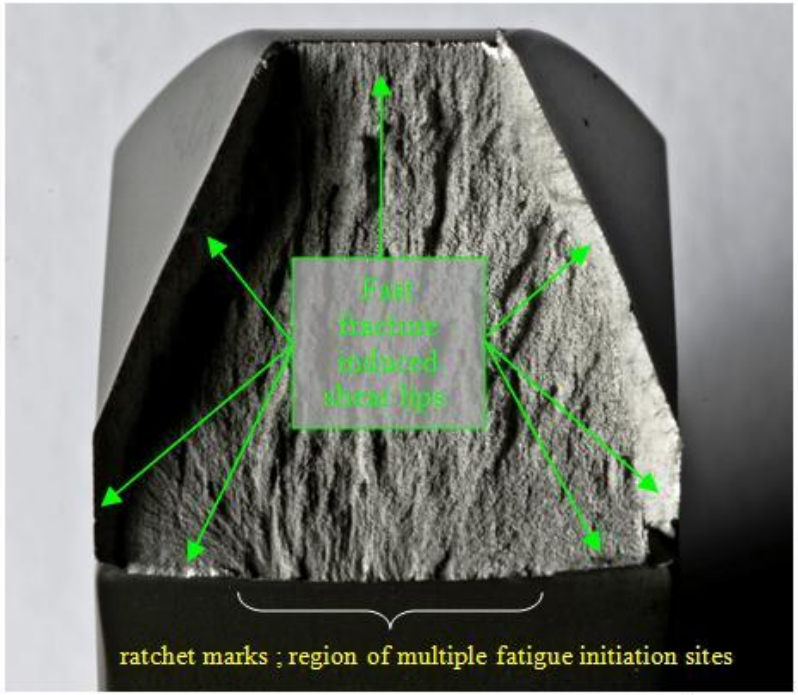

2A: 11 kip fatigue fracture surface

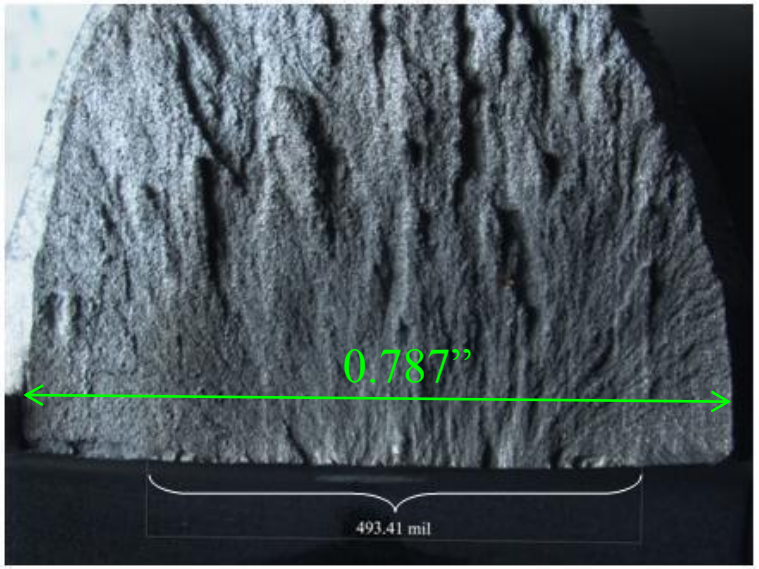

2A: ratchet mark zone ; crack initiation plane

Failure Analysis of Latch Hooks – (cont)

Scanning electron microscope (SEM) images of the 2A fracture surface adjacent to the shear lips and near the centerline of the section are provided below; striations (microscopic tear ridges resulting from cyclic loading induced crack front advancement) were detected all along the crack initiation front.

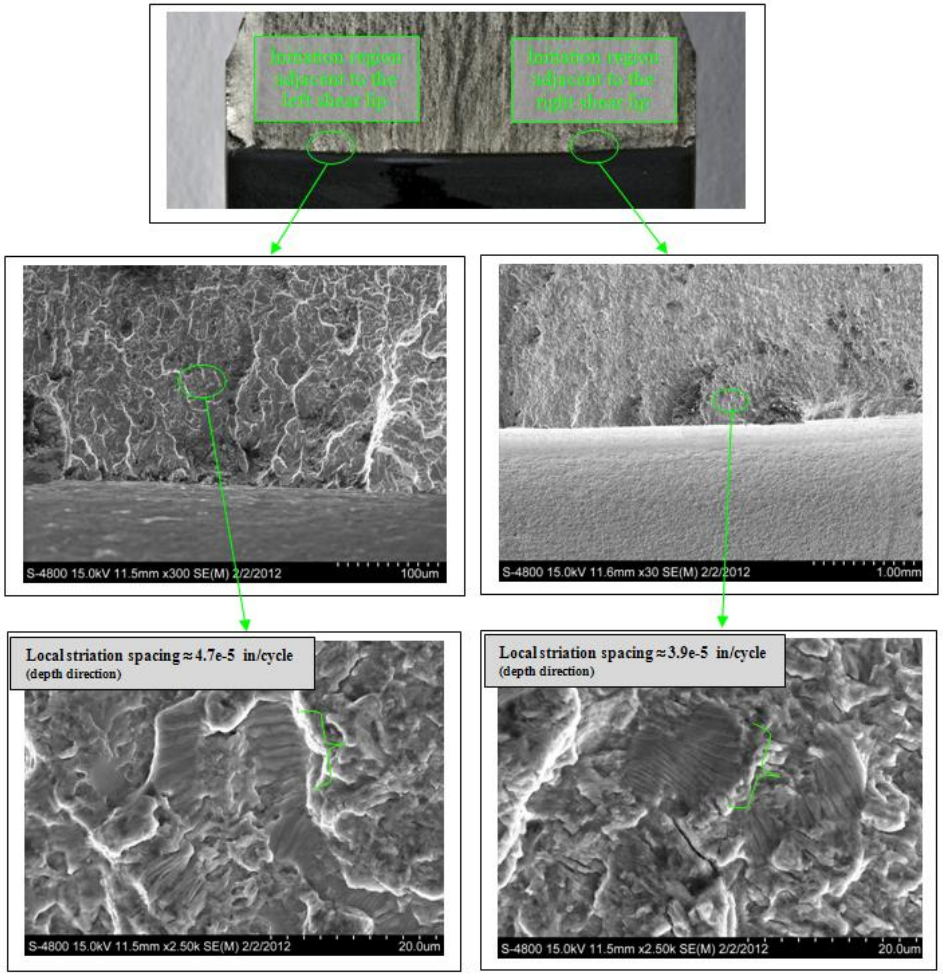

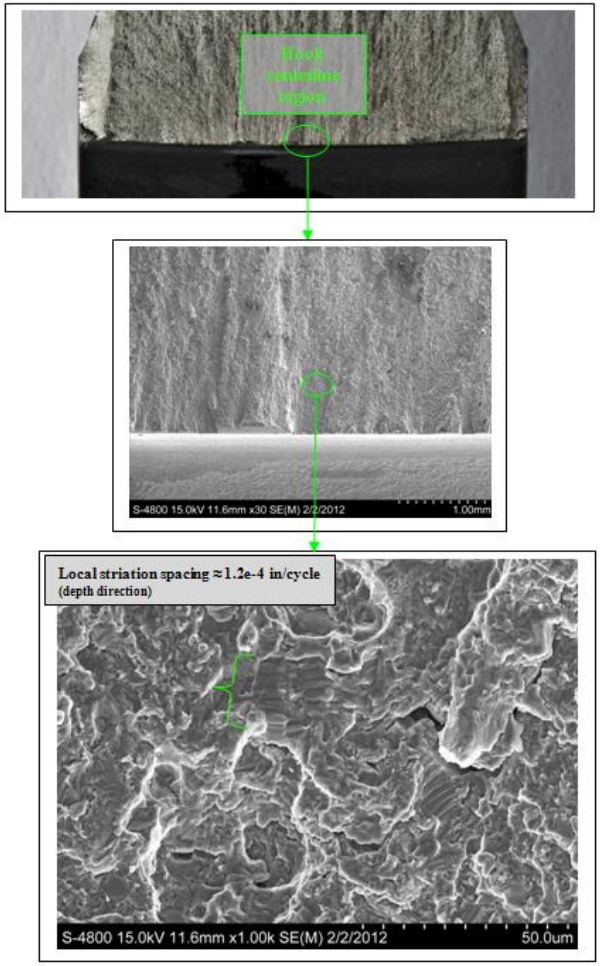

Why did LEFM Work for a Low-Cycle Fatigue Application?

The following is from J.D. Landes, Fracture Toughness, Comprehensive Structural Integrity.

7.02.2.2 Regimes of Fracture-toughness Testing

The behavior of a material during a fracture-toughness test can be specified by three sets of opposing conditions: *fracture behavior* of the material, the *deformation behavior* of the material, and the *constraint of the geometry*. Understanding the difference between these regimes can aid in the successful conduct of the fracture-toughness test. The essential features of these three sets of conditions and the differences between them are discussed in the following sections.

7.02.2.2.2 Deformation behavior

All deformation behavior for metallic materials starts as linear elastic. It can become nonlinear when the material begins to yield over a large region of the specimen. This nonlinear loading behavior results when the fracture toughness is high enough relative to the yield strength of the material, so that significant portions of the specimen yield before the fracture measurement region is reached. Nonlinearity of the force and displacement behavior can also be caused by crack extension. It is the nonlinear behavior due to significant plasticity in the specimen that requires a change from the linear-elastic parameter, K, to a nonlinear parameter, CTOD or

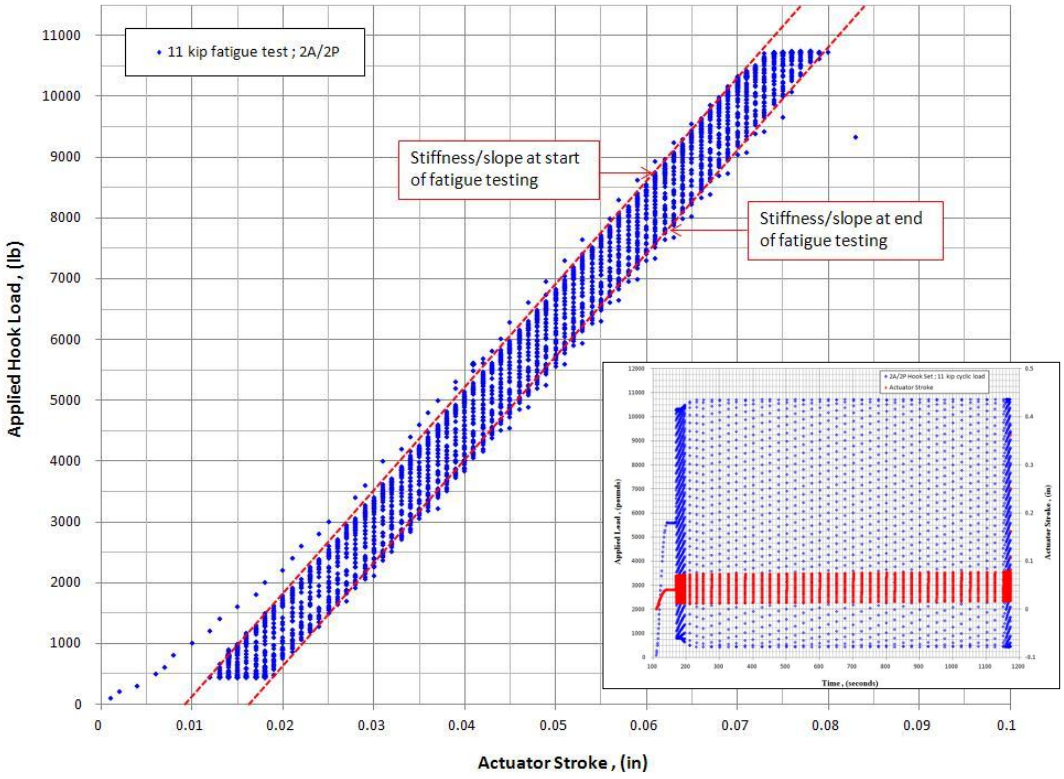

The fatigue test load-displacement trace demonstrates a minimal change in slope with accumulated fatigue damage (in both hooks) up to the point of failure. Thus the global structural stiffness of the engaged hooks is largely linear elastic throughout the fatigue crack initiation, fatigue crack propagation, and unstable propagation/failure process.

Why did LEFM Work for a Low-Cycle Fatigue Application? (cont)

In a comparison of elastic-plastic versus elastic analyses Newman demonstrates good agreement with test data over a large range of stresses prior to the elastic analysis becoming non-conservative at the higher stress levels.

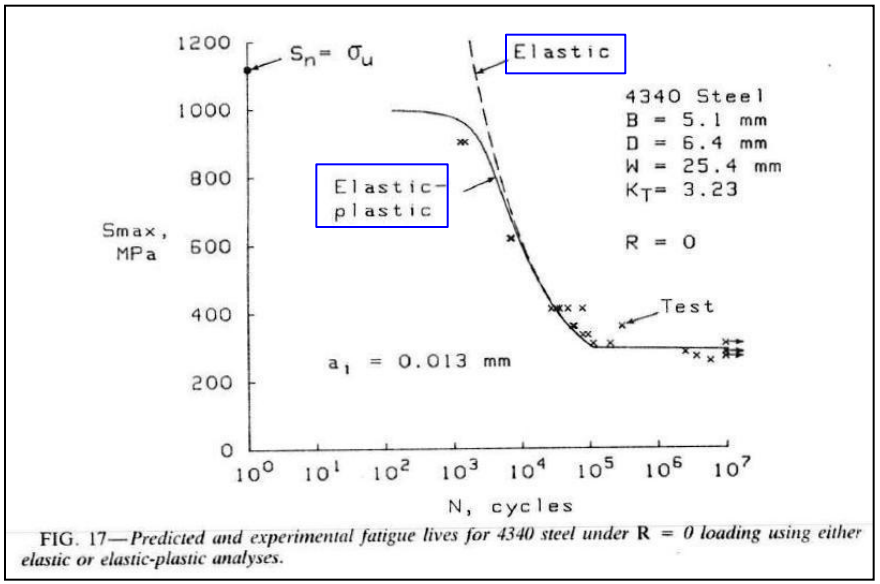

FIG. 17—*Predicted and experimental fatigue lives for 4340 steel under* R = *0 loading using either elastic or elastic-plastic analyses.*

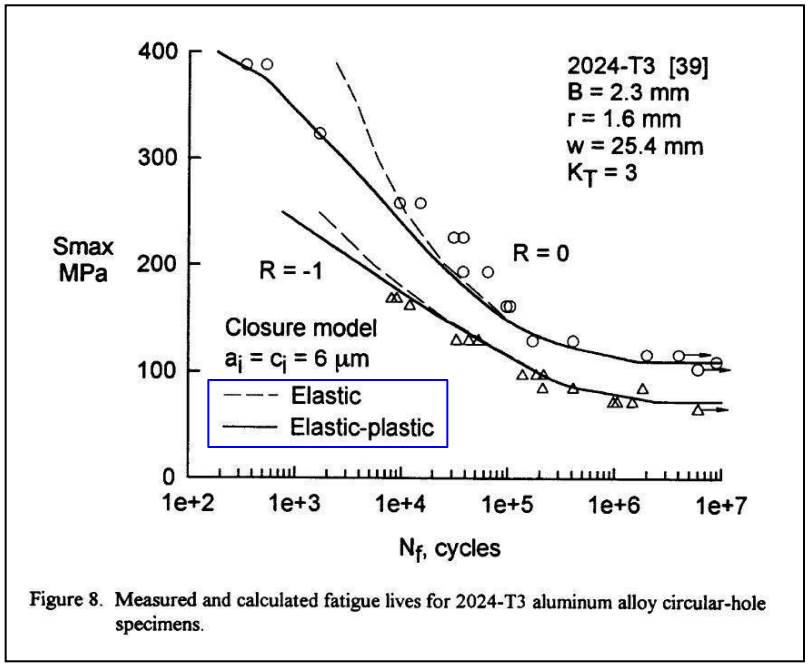

Figure 8. Measured and calculated fatigue lives for 2024-T3 aluminum alloy circular-hole specimens.

needed. To account for plasticity, a portion of the Dugdale cyclic-plastic-zone length (ω) has been added to the crack length, c. The cyclic-plastic-zone-corrected effective stress-intensity factor [10] is

$$(\Delta K_p)_{eff} = (S_{max} - S'_o)\sqrt{(\pi d)}\ F(d/w) \qquad (2)$$

where $d = c + \omega/4$ and F is the cyclic-plastic-zone corrected boundary-correction factor. Herein, the cyclic-plastic-zone corrected effective stress-intensity factor range will be used in the fatigue-life predictions unless otherwise noted.

The End..

Questions???

THANK YOU FOR ATTENDING…